Cape Peninsula
University of Technology

ELECTROCHEMICAL POLYCHLORINATED BIPHENYLS IMMUNOSENSOR BASED ON FUNCTIONALIZED POLYANILINE NANOCOMPOSITE

by

MALEFETSANE PATRICK KHESUOE
(BSc: Chemical Technology, NUL)

Thesis submitted in fulfilment of the requirements for the degree

Master of Technology: Chemistry

In the Faculty of Applied Sciences

At the Cape Peninsula University of Technology

Supervisor: Prof. MC Matoetoe

Cape Town campus
August 2015

CPUT copyright information

The thesis may not be published either in part (in scholarly, scientific or technical journals), or as a whole (as a monograph), unless permission has been obtained from the University

DECLARATION

I, **Malefetsane Patrick Khesuoe**, declare that the contents of this thesis represent my own unaided work, and that the thesis has not previously been submitted for academic examination towards any qualification. Furthermore, it represents my own opinions and not necessarily those of the Cape Peninsula University of Technology.

Signed Date

ABSTRACT

Immunosensors are analytical devices comprising antibody (*Ab*) molecules intimately integrated with electronic physicochemical transducers. *Abs* are responsible for specific recognition of an analyte so called antigen (*Ag*) while transducers are responsible for the conversion of chemical changes brought about by *Ab-Ag* interactions into measurable and processable signal. Amongst the many analytical tools, immunosensors have shown outstanding performance in applications in fields such as clinical diagnostics, agricultural purposes and environmental monitoring. They have come in place of the many conventional analytical methods which showed a number of disadvantages; high cost and longer time of operation, and requirement of highly knowledgeable personnel. On the other hand, immunosensors have shown potential to overcome these constraints. Their advantages include possibilities of portability, miniaturization, and simplified procedures. Of the possible fields of immunosensor applications, this study focussed on the environmental aspect. The safety of the environment is good for the well-being even though there are still some environmental threats that exist. Polychlorinated biphenyls (PCBs) have reportedly been found to be some of the potential substances to pose such threats due to their toxic and persistent behaviour.

In this study, we have developed an electrochemical immunosensor as an analytical tool for the analysis and monitoring of PCBs. The development was based on the use of silver nanoparticles-doped polyaniline (PANI/Ag NPs) for modification of an electrode as a process for fabrication of the transducer. The PANI/Ag NPs composite was deposited on the glassy carbon (GC) and platinum (Pt) electrodes by oxidative electropolymerization of aniline in the presence of Ag NPs in 1 M HCl using cyclic voltammetry (CV) by ramping the potential from -0.1 to 1.4 V at 50 mV/s. The composite was then characterized and evaluated as a potential material for electrochemical transduction. Evaluation was on electroactivity, which is the main property of interest for materials used in the fabrication of electrochemical devices. The PANI composites were characterized using spectroscopic (FTIR), microscopic (TEM) and electrochemical CV techniques. Results confirmed the formation of PANI in its emeraldine form and the presence of Ag NPs. Characteristic functional groups and peaks of PANI were observed in FTIR and CV respectively. TEM micrograms showed one dimensional nanofibric tubes and crystalline-like structure of the composite. The incorporation of Ag NPs was indicated by the transition from the amorphous (PANI) to crystalline (PANI/Ag NPs) structure accompanied by increase in size as well as smoothness of the tubes. EDS-TEM counts increase of the chlorine (Cl) peaks is due to the closeness of these peaks to those of Ag, thus confirming incorporation of Ag NPs.

Noticeable increase in electrochemical activities was observed in Ag NPs containing polymer for both Pt and GC based transducers. The GC based transducer showed superior electrochemical activities and stability, as a result, it was used in the immunosensor fabrication. The traducer was then integrated with the *Ab* through immobilization using covalent attachment approach by glutaraldehyde (GA) linkage to form the immunosensor. The success of the immobilization of *Ab* on the transducer demonstrated a good biocompatibility of the transducer with *Ab* as shown by CVs of each step in the immunosensor fabrication. The fabrication steps were optimized for immobilization; coating strategy, content of GA, incubation times for GA and *Ab*. Immersion, 1% GA, incubation times of 30 min and 2 hrs for GA and *Ab* respectively, were optimum conditions. The developed sensor was coupled with the electrochemical square wave voltammetric (SWV) detection for analysis of PCB 28. The current as the signal response, increased linearly with the increasing concentration of the PCB. The method linear range is 0.2 - 1.2 ng/mL. The LOD and LOQ are 0.269 ng/mL and 0.898 ng/mL respectively. The method was characterized by good and acceptable repeatability and specificity which were both below the highest acceptable level (5%) of error and interference respectively. This therefore represents a useful tool for environmental analysis and monitoring of PCBs.

ACKNOWLEDGEMENTS

I wish to express first and foremost my acknowledgments to God for His favour, grace, love and strength during the pursuit of this study. When I am weak then You are strong. I am eternally grateful.

I wish to extend my special thanks to my supervisor Prof. M.C. Matoetoe, first for granting me the opportunity to conduct research with you on this project. I am deeply indebted to you for your patience, guidance, assistance and encouragements during the study and writing of this work. This thesis would have remained a dream had it not been for your constructive and continuous evaluation of the work. I consider it a great honour and privilege to have worked with you. Thanks a great deal for your enlightenment, may God richly bless you.

My deepest appreciation and thanks to my mother Masalome R. Khesuoe for your gracious support and motivation throughout this project.

I share the credit of my work also with my brother Kabelo A. Khesuoe and his family; you have always been there in hard times.

To my precious sisters: Mamothibeli A., Maneo M., Keneuoe P., Rethabile S. and Liteboho P.; many thanks for your sincere love, you are each such a gift from God.

I gratefully acknowledge my colleague and friend, Oluoch F. Okumu for willingly assisting, motivating and encouraging me, your support I highly appreciate.

I cannot close this chapter without making reference to my friends; Lebohang G. Macheli, Lebusetsa L. Taleli and Mlandvo A. Dlamini for the encouragements and advices you rendered to me during times of difficulties.

Last, but not least, I gratefully acknowledge the government of Lesotho (NMDS) and appreciate the financial support for my studies.

DEDICATION

I dedicate this work to my family: my mother, my brother and my sisters who have always stood by me and dealt with all my absence from many family occasions with a smile. I applaud their commitment and support in the pursuit of this work.

My mother Masalome R. Khesuoe, I would not have gone this far if it was not by your support, motivation and prayers, may God Almighty keep you and bless you for being a mother and father to me.

My brother Kabelo A. Khesuoe, I so much appreciate your limitless love and support in all the situations.

My dear sisters; Mamothibeli, Maneo, Keneuoe, Rethabile and Liteboho, I thank God to have given me sisters like you. Your love I appreciate and acknowledge.

LIST OF PUBLICATIONS AND CONFERENCES ATTENDED

Publications

1. Malefetsane Khesuoe, Mangaka Matoetoe, Fredrick Okumu. Potential of silver nanoparticles functionalized polyaniline as an electrochemical transducer. (Journal of Nano Research, 2015, submitted).

Conferences

1. Malefetsane Khesuoe, Mangaka Matoetoe, Fredrick Okumu. Electrochemical analysis of PCBs using silver nanoparticles - polyaniline modified glassy carbon electrode. Oral presentation at ANALITIKA 2014 conference, Parys, Free State, South Africa, 7-11 September 2014.

2. Malefetsane Khesuoe, Mangaka Matoetoe, Fredrick Okumu. Interrogation of Ag NPs - doped polyaniline's potential for use as an electrochemical transducer. Poster presentation at MAPET 2015, 3rd Symposium on electrochemistry, Cape Town, South Africa, 26-28 May 2015.

TABLE OF CONTENTS

Contents

TABLE OF FIGURES

LIST OF TABLES

THESIS OUTLINE

This outlines the chapters in the thesis and short summary on what each chapter covers in attempt to fulfil the aims and objectives of the study, which is aimed at developing an electrochemical immunosensor based on functionalised polyaniline nanocomposite for the detection of PCBs.

Chapter one is the introduction covering the research background which indicates the challenges the environment faces with reference to PCBs. It further introduces the contents of this work with respect to immunosensor. The main problem that intrigued the undertaking of this research is discussed and the questions that need to be addressed in relation to the problem. The aims and objectives to be carried out to address the problem are also listed.

Chapter two of this thesis is the literature review which gives an insight and understanding of the study based on the previous findings and studies. It extends to the methods previoustly used for PCBs analysis. It also details the research trends that led to the development of immunosensors and the different important aspects necessary for their development. This iclude the materials, technologies and methods that play roles for this activity.

Chapter three involves the first step in preparation for immunosensor assembly. It deals with iterrogation of the materials used in the fabrication of immunosensor. It emcopasses the materials, chemical, techniques, methods and intruments needed for the process, and lastly the results obtained and their implications.

Chapter four in addition to chapter three, completes the experimental work and in like manner, reports the findings. It involves the ground development of the immunosensor and and possible application on analysis of PCBs.

Chapter five includes the conclusions and recommendations of the study.

1. INTRODUCTION

The chapter covers the general background on possible environmental threats with PCBs being the major concern. It also discusses the properties of these substances that give rise to their harmful effects. This is followed by the restrictions faced with the conventional methods for the analysis and monitoring of this substances in the environment. It further brings to attention the concept of immunosensors and their applications as the alternative analytical tools for PCBs.

1.1 Background

Wanekaya *et al.*, (2008) indicated environmental security as one of the fundamentals required for our well-being. Among several environmental threats existing, organic contaminants have shown greatest concern. The most frequently monitored environmental organic pollutants include PCBs, pesticides, phthalates, polycyclic aromatic hydrocarbons (PAHs) and alkylated PAHs due to their toxic, persistent and diffusive behaviour. These compounds could be found in surface waters, animal tissue and soil as disposed from municipal and industrial waste streams, agricultural activities and some non-point of source pollutions (NPS) (Net *et al.*, 2014). Researchers had studied the contamination levels of the above mentioned organic pollutants using the conventional methods.

PCBs, among the persistent organic pollutants (POPs), are the most known common environmental contaminants of concern. They are said to have potential harmful effects to the biota due to their previous wide usage and persistence. The previous practice on regulatory environmental monitoring and evaluation of PCBs was done by total PCB quantitation. The practice appeared to be erroneous due to lack of correlation between standards and real samples and could not have information pertaining to the potential biological implications for particular PCB mixture (Brown *et al.*, 1985; Schwartz *et al.*, 1987).

PCB congeners with 5 - 7 (penta-, hexa- and hepta-) chlorine atoms per molecule are perceived as the most bio-accumulative and contain about 54 % (112) of the 209 possible PCBs. They were synthesized in large quantities in several Aroclor mixtures, implicating their possible prevalence in the environment (Alford-Stevens, 1986). These Aroclors are believed to contain congeners that induce mixed function oxidase (MFO) (Goldstein, 1979; Parkinson *et al.*, 1981). Less (1 - 4) and highly (8 - 10) chlorinated congeners have less or no reported harmful biological effects due to limited bio-accumulation, low bio-availability and no toxicity

(Bunyan & Page, 1978). This is because less chlorinated configurations are easily metabolized hence, they can be eliminated once consumed and congeners with higher chlorination are in general, scarcely available (Bush *et al.*, 1985). This therefore, means that for routine regulatory monitoring, it would be unnecessary to carry analysis for all the 209 congeners. On this basis, it is essential to identify appropriated PCB congeners for which regulatory analytical method should be developed.

Over 50 of the 209 PCB congeners are suspected to be inducers of MFO activities in mammalian liver. MFO is a category of enzyme systems that catalyze redox bio-transformation of compounds involving aromatic rings. MFOs stimulated by PCBs fall in three characterizing classes, namely: phenobarbital type (PB - type), 3 - methylcholanthrene - type (3 - MC - type) and the one containing characteristics of both types (mixed - type). Stimulation of MFOs by PCBs can sometimes result in bio-activation of intermediates which are toxic from originally non-toxic parent substances (Parke, 1985). 3 - MC inducible enzymatic reactions were stated to have potential to contribute to toxicity by bio-activation.

Toxicity of PCBs can be influenced by their molecular structures in relation to their molecular configuration in space and force distributions. PCBs are believed to be isosteres (have the same number of atoms and valance electrons) of 2, 3, 7, 8-tetrachlorodibenzo-p-dioxin (2, 3, 7, 8-TCDD) which is known as the most potent environmental toxicant and it is considered a comparative standard for other organic toxicants like PCBs (Kociba & Cabey, 1985; Safe, 1987). Dioxins as commonly called (or polychlorinated dibenzodionxins (PCDDs)) are a group of polychlorinated aromatic compounds that form a planar volume as a box or rectangle and are potential environmental pollutants (McKinney & Singh, 1981). Safe *et al.*, (1985) declared that PCB congeners with para (4, 4') and at least two meta (3, 3', 5, 5') positions substituted with chlorine atoms with no ortho (2, 2', 6, 6') substitutions are the most toxic. This is believed to be due to less limited rotational freedom because increased ortho substitutions effect steric hindrance to the rotational movement.

PCBs that exhibit coplanar configurative structures, despite non-ortho substitutions, have been shown to pose toxic effects on marine mammals and humans. They are the 3-MC-type inducers and are said to be potent of posing threats even at higher magnitudes than 2, 3, 7, 8 TCDD itself. PCBs bearing coplanarity were found to be congeners 77, 81, 126 and 169 (Sawyer & Safe, 1985; Safe, 1987; Tanabe *et al.*, 1987). Mixed type inducer PCBs are analogues of the 3-MC-type still with coplanarity but singly ortho-chlorinated. Such congeners are 105, 114, 118, 123, 156, 157, 167 and 189 and they have PB- and 3-MC-type inducing properties and are potential toxicants of concern (Mcfarland & Clarke, 1989).

Di-ortho coplanar PCB congeners of the mixed-type are 128, 137, 138, 153, 158, 166, 168, 170, 180,190, 191, 194 and 205. Their potency as environmental threats is less compared to the non-ortho and mono-ortho coplanar molecules. Congeners 138 and 153 form the basic components of technical formation of PCBs and demonstrate the highest potential as inducers and toxicants among the di-ortho coplanar PCBs (Safe *et al.*, 1985). It is evident that amongst the 3 types of inducers, 3-MC-type and mixed-type inducers have the highest potency for toxicity in mammals, birds, fish and invertebrates.

In addition, the effect of molecular structure of congeners was also recently demonstrated by the study conducted by Louis and co-workers. Louis *et al.*, (2014) studied and reported the dynamics of mobilization of PCB 153 with respect to PCB 28 and PCB 118. They revealed the lipophilic character of PCBs that makes them to preferably be stored in the adipose tissue once bio-accumulated. The study showed inefficient mobilization of PCB 153 from adipocytes to the culture medium as compared to PCBs 28 and 118. This demonstrates that congeners' structures determine their rate of release from the adipocytes. According to these researchers, previous studies showed that the rate at which congeners are released is regularized by their physico-chemical properties which depend on the number and position of chlorine atoms on the biphenyl (La Merrill *et al.*, 2013). One characteristic of PCB 153 that makes it lipophilic is its exhibition of large electron-deficient zone which makes it be released more slowly than the other two which have rather a reduced electron-deficient zone.

A more priority classification has been made for PCBs posing or having great potential environmental threats based on: 1) toxicity potency, 2) occurrence frequency in the environmental samples and 3) relative abundance in animal tissues. The classification is derived based on MFO induction as it has already been indicated that 3-MC-type and mixed-type inducers are the most potential toxicants compared to PB-type inducers (Parkinson *et al.*, 1980; Parkinson *et al.*, 1981; McKinney & Singh, 1981; Safe *et al.*, 1985). The information was obtained from the then compiled PCB congener database collected from reported scientific literature (Mcfarland & Clarke, 1989). Environmental samples herein refer to organisms, sediments or water etc. from the field. Out of the 209 PCB configurations, 36 were regarded the most relevant for use in the regulatory evaluation of the environment and were classified into four priority groups as shown in table 1 below:

Table 1.1: Priority groups of PCBs

Groups				
1		2	3	4
A	B	87	18	37
77	105	99	44	81
126	118	101	49	114
169	128	153	52	119
	138	180	70	123
	156	183	74	57
	170	194	151	158
			177	167
			187	168
			201	189

(Mcfarland & Clarke, 1989)

Mcfarland & Clarke, (1989) suggested that it is quite important and better to make toxicologically appropriate evaluation and monitoring of environment contaminated with PCBs through analysis of specific PCBs in the four groups than as total PCBs or equivalent Aroclors. This gives meaningful focus as logical assessment of only congeners prevailing in the environment, bio-accumulative and potently toxic, can be made. In this regard, it is clear with reference to recent research on PCBs that there is a need for their evaluation and monitoring for the well-being of the environment. This work is focusing on indicator PCB 28 with the hope of development and validation of the relevant analytical method for evaluation and monitoring of these substances.

1.2 Research problem

Among other environmental threats, PCBs still remain a challenge because of their detectable elevated levels in the environment (Kucklick *et al.*, 2011). Therefore, in addition to lowering and/or removing the amounts of their toxic discharges into the environment, there still remains a need to develop techniques and methods that can detect and monitor these environmental pollutants in a cheap, sensitive and selective manner to enable effective remediation. The persistence (Bender & Sadik, 1998) and health effects (Bench, 1999) of PCBs due to their previous widespread usage are of great environmental threat and concern. In addition, Ricci *et al.*, (2007) pointed out that there is high demand for rapid,

sensitive and accurate methods for detection of both biological and chemical contaminants. The demand increase arises because the traditional methods for the biological contaminants require large periods of time to reach completion despite their sensitivity and inexpensiveness. The detection methods for the chemical contaminants on the other hand, use expensive and complicated instrumentation with the same specificity and accuracy. These hinder processors to act with corrective measures immediately when contaminants are detected (Doyle, 1993).

Therefore, development of portable, rapid, sensitive and selective immunosensor technologies which are capable to overcome the discussed analytical constraints (Laschi & Mascini, 2002; Kreuzer *et al.*, 2002) is of crucial interest. These are less expensive and can also be widely available for PCBs screening and other pollutants of priority. Immunosensor technologies are known for their high performance and generation of high sample throughputs with significant decrease in time needed to carry out the analysis (Bender & Sadik, 1998). These field analytical techniques are specifically suitable for continuous, rapid and in-situ on-site screening of environmental pollutants. Several immunochemical methods have been developed for the measurement of antibody-antigen (*Ab-Ag*) reactions and still remain the subject of a number of research efforts. These notably include electrochemical detection methods such as amperometry or voltammetry (McNeil *et al.*, 1995) and potentiometry (Monroe, 1990; Pranitis *et al.*, 1992). Other detections such as optical and piezoelectric methodologies have also been documented (Korotkaya, 2014).

A number of well-known analytical techniques and methods that have been developed and employed for the analysis of PCBs include laboratory non-portable bench based analysis such as gas chromatography (GC) with electron capture detector (ECD), mass selective detector (MSD) and mass spectrometry (MS). These are accurate, sensitive and reliable but they are often tedious, use expensive instruments and are costly to run for large scale continuous PCB screening purposes and require use of large volumes of expensive and toxic solvents (Kimbrough *et al.*, 1994; Ferrario *et al.*, 1997). Therefore, it is important not to ignore development of cost effective, easy to run, equally sensitive, selective and accurate detection techniques. This research's focus is based on the development of label-free reagentless electrochemical immunosensor based on two widely recognized scientific technological disciplines; polymer- and nano-sciences. It is anticipated that such immunosensor will have the ability to eliminate large experimental time frames and high expertise - required labelling procedures. In view of the analytical constraints elaborated above, the following research questions were formulated.

1.3 Research questions

Fabrication of an immunosensor consists of a transducer and biological material immobilized on the transducer. Therefore, the question is whether the Ag NPs-doped PANI material is ideal for the fabrication of electrochemical transducer by electrode modification. How compatible is AgNPs-doped PANI and the biomolecule (*Ab*)? Thirdly, what is the feasibility and extent of the application of the developed analytical method on the analysis of PCBs? Last is an attempt to determine the optimum conditions suitable for the successful efficient usage of developed PCBs method. What are the application parameters of the method? Reliability, reproducibility and validation of the method will also be undertaken. With these questions in mind, the following objectives were envisaged.

1.4 Aim and objectives of the research

The research major aim is the development of an immunosensor that will have most relevant applications in the field of PCBs monitoring and detection as an alternative method to the costly, time consuming and high expertise requiring methods.
This can be achieved through the following objectives:

1. To synthesize and characterize PANI/ Ag NPs
2. Evaluate PANI/ Ag NPs as an immobilizing material,
3. Optimize the conditions suitable for the immobilization of antibodies
4. Evaluate the antibody compatibility with the transducer,
5. Develop an electrochemical immunosensor,
6. Optimize the conditions suitable for the detection of PCB using the immunosensor, and
7. Validate the immunosensor

1.5 References

Alford-Stevens, A.L. 1986. Analyzing PCBs. *Environmental Science & Technology*, 20(12): 1194–1199.

Bender, S. & Sadik, O.A. 1998. Direct electrochemical immunosensor for lychlorinated biphenyls. *Environmental Science and Technology*, 32(6): 788–797.

Brown, J.F.J., Wagner, R.E., Bedard, D.L., Brennan, M.J., Carnahan, J.C. & May, R.J. 1985. PCB transformations in upper Hudson sediments. *Northeastern Environmental Science*, 3(3-4): 166–178.

Bunyan, P.J. & Page, J.M.J. 1978. Polychlorinated biphenyls: the effect of structure on the induction of quail hepatic microsomal enzymes. *Toxicology and Applied Pharmacology*, 43: 507–518.

Bush, B., Simpson, K.W., Shane, L. & Koblintz, R.R. 1985. PCB congener analysis of water and caddisfly larvae (Insecta:Trichoptera) in the upper Hudson river by glass capillary chromatography. *Bulletin of environmental contamination and toxicology*, 34(1): 96–105.

Doyle, M.P. 1993. Reducing foodborne disease-what are the priorities? *Nutrition Science Policy*, 51(11): 345–347.

Ferrario, J., Byrne, C. & Dupuy, A.E.J. 1997. Background contamination by coplanar polychlorinated biphenyls (PCBs) in trace level high resolution gas chromatography/high resolution mass spectrometry (HRGC/HRMS) analytical procedures. *Chemosphere*, 34(11): 2451–2465.

Goldstein, J.A. 1979. The structure-activity relationships of halogeneated biphenys as enzyme inducers. *Annals of the New York Academy of Sciences*, 320(1): 164–178.

Kimbrough, D.E., Chin, R. & Wakakuwa, J. 1994. Wide-spread and systematic errors in the analysis of soils for polychlorinated biphenyls, Part 1: a review of inter-laboratory studies. *The Analyst*, 119(6): 1277–1281.

Kociba, R. & Cabey, O. 1985. Comparative toxicity and bioligic activity of chlorinated dibenzo-p-dioxins and furans raltive to 2,3,7,8-tetrachlorodibenzo-p-dioxin (TCDD). *Chemosphere*, 14(6/7): 649–660.

Korotkaya, E.V. 2014. Biosensors: design, classification, and applications in the food industry. *Foods and Raw Materials*, 2(2): 161–171.

Kreuzer, M.P., Pravda, M., O'Sullivan, C.K. & Guilbault, G.G. 2002. Novel electrochemical immunosensors for seafood toxin analysis. *Toxicon*, 40(9): 1267–1274.

Kucklick, J., Schwacke, L., Wells, R., Hohn, A., Guichard, A., Yordy, J., Hansen, L., Zolman, E., Wilson, R., Litz, J., Nowacek, D., Rowles, T., Pugh, R., Balmer, B., Sinclair, C. & Rosel, P. 2011. Bottlenose dolphins as indicators of persistent organic pollutants in the western North Atlantic Ocean and northern Gulf of Mexico. *Environmental science & technology*, 45(10): 4270–4277.

Laschi, S. & Mascini, M. 2002. Disposable electrochemical immunosensor for environmental applications. *Annales de Chimie*, 92(4): 425–433.

Louis, C., Tinant, G., Mignolet, E., Thome, J. & Debier, C. 2014. PCB-153 shows different dynamics of mobilisation from differentiated rat adipocytes during lipolysis in comparison with PCB-28 and PCB-118. *PLoS ONE*, 9(9): e106495.doi:10.1371/journal.pone.0106495, [16 September 2014].

Mcfarland, V.A. & Clarke, J.U. 1989. Environmental occurrence, abundance, and potential toxicity of polychlorinated biphenyl congeners : Considerations for a congener-specific analysis. *Environmental Health Perspectives*, 81: 225–239.

McKinney, J.D. & Singh, P. 1981. Structure-activity relationships in halogenated biphenyls: unifying hypothesis for structural specificity. *Chemico-Biological Interactions*, 33(2-3): 271–285.

McNeil, C.J., Athey, D., Ball, M., Ho, W., Krause, S., Armstrong, R.D., Wright, J. Des & Rawson, K. 1995. Electrochemical sensors based on impedance measurement of enzyme-catalyzed polymer dissolution: theory and applications. *Analytical Chemistry*, 67(27): 3928–3935.

La Merrill, M., Emond, C., Kim, M.J., Antignac, J.P., Le Bizec, B., Clément, K., Birnbaum, L.S. & Barouki, R. 2013. Toxicological function of adipose tissue: Focus on persistent organic pollutants. *Environmental Health Perspectives*, 121(2): 162–169.

Monroe, D. 1990. Amperometric immunoassay. *Critical Reviews in Clinical Laboratory Sciences*, 28(1): 1–18.

Net, S., Dumoulin, D., El-Osmani, R., Rabodonirina, S. & Ouddane, B. 2014. Case study of PAHs , Me-PAHs , PCBs , phthalates and pesticides contamination in the Somme river water, France. *International Journal of Environmental Research*, 8(4): 1159–1170.

Parke, D.V. 1985. The role of cytochrome P-450 in the metabolism of pollutants. *Marine Environmental Research*, 17(2-4): 97–100.

Parkinson, A., Robertson, L., Safe, L. & Safe, S. 1981. Polychlorinated biphenyls as inducers of hepatic microsomal enzymes: effects of di-ortho substitution. *Chemico-Biological Interactions*, 35(1): 1–12.

Parkinson, A., Robertson, L., Safe, L. & Safe, S. 1980. Polychlorinated biphenyls as inducers of hepatic microsomal enzymes: structure-activity rules. *Chemico-Biological Interactions*, 30(3): 271–285.

Pranitis, D.M., Telting-diaz, M., Meyerhoff, M.E. & R.R.S. 1992. Potentiometric ion-, gas-, and bio-selective membrane electrodes. *Critical Reviews in Analytical Chemistry*, 23(3): 163–186.

Ricci, F., Volpe, G., Micheli, L. & Palleschi, G. 2007. A review on novel developments and applications of immunosensors in food analysis. *Analytica Chimica Acta*, 605: 111–129.

Safe, S. 1987. Determination of 2,3,7,8-TCDD toxic equivalent factors (TEFs): support for the use of the in vitro AHH induction assay. *Chemosphere*, 16(4): 791–802.

Safe, S., Bandiera, S., Sawyer, T., Robertson, L., Safe, L., Parkinson, A., Thomas, P.E., Ryan, D.E., Reik, L.M., Levin, W., Denomme, M.A. & Fujita, T. 1985. PCBs: structure-function relationships and mechanism of action. *Environmental health perspectives*, 60: 47–56.

Sawyer, T.W. & Safe, S. 1985. In vitro AHH induction by polychlorinated biphenyl and dibenzofuran mixtures: additive effects. *Chemosphere*, 14(1): 79–84.

Schwartz, T.R., Stalling, D.L. & Rice, C.L. 1987. Are polychlorinated biphenyl residues adequately described by aroclor mixture equivalents ? Isomer-specific principal components analysis of such residues in fish and turtles. *Environmental Science and Technology*, 21(1): 72–76.

Tanabe, S., Kannan, N., Subramanian, A., Watanabe, S. & Tatsukawa, R. 1987. Highly toxic coplanar PCBs: occurrence, source, persistency and toxic implications to wildlife and humans. *Environmental pollution*, 47(2): 147–163.

Wanekaya, A.K., Chen, W. & Mulchandani, A. 2008. Recent biosensing developments in environmental security. *Journal of environmental monitoring*, 10: 703–712.

2. LITERATURE REVIEW

2.1 Introduction

This chapter first looks into the general overview on PCBs as threat to the environment in relation to their properties that contributed/contribute to their continually observed adverse effects on the ecosphere since the commencement of their manufacturing. It also pays attention on the conventional analytical methods for PCBs and their limitations. The chapter further unfolds the details on immunosensors as the recent analytical methods under development for the analysis and monitoring of PCBs. The discussion herein also includes the details on the components of immunosensor namely, transducer and antibody. These are the pillars of basis for the selection of detection and immobilization techniques during the development of immunosensor. Detection and immobilization are the most crucial steps in the assembly of an immunosensor therefore, the techniques necessary to carry them are selected with care as further indicated during the progressions in this chapter.

2.2 Polychlorinated biphenyls (PCBs)

PCBs are a family of man-made organic compounds with 2 to 10 chlorine atoms attached to the biphenyl, which is a molecule composed of 2 benzene rings (U.S. EPA, 1976). In concentrated pure forms, they are odorless and tasteless oily liquids or mildly aromatic solids with high degree of inertness, often found in mixtures with other organic chemicals (ATSDR, 2000). They are inflammable, electrically resistant hence, good insulators, and maintain their stability under heat or pressure. They are very stable compounds; being resistant to oxidation, reduction, addition, elimination and electrophilic substitution and do not decompose readily (Boate *et al.*, 2004). They are also resistant to acids and alkalis (Afghan & Chau, 1989; Barbalace, 2003). The high thermal and chemical resistance of PCBs is the very one property attributed to their usefulness and harmfulness to the environment because they are not readily broken down when treated with heat or chemicals. This stability allows them to stay for long in the environment once emitted hence, they easily bioaccumulate.

These hazardous chemicals were never in existence naturally until their release into the environment by manufacturers and consumers commenced in the 1900's. They were first manufactured by an American company, Monsanto in 1929 and quickly gained industrial recognition (Barbalace, 2003). PCBs constitute a group of 209 individual chlorinated biphenyl rings singly called congeners. Individual congeners have specific names according to either IUPAC nomenclature (which indicates the numbering, positions and number of chlorine atoms in the biphenyl rings) or Ballschmiter and Zell (BZ) shorthand naming (which is done by arranging congeners in order from mono- to deca-chlorobiphenyl, then assigning a number sequentially from 1 - 209). This can be exemplified by congener number 180 which is PCB 180 by shorthand and 2, 2', 3, 4, 4', 5, 5'- heptachlorobiphenyl by IUPAC (Mills III *et al.*, 2007).

Typically, they were manufactured in mixtures of 60 to 90 different congeners. The mixtures are named based on the manufacturer and the well-known mixtures are **Aroclors** as the brand name for Monsanto PCBs. Aroclors are named using four digit code designations with the first two digits being 12 for the 12 carbons of the biphenyl rings in the structure while the second 2 digits indicate the average percentage weight of chlorine in the mixture. For aroclor PCBs the names include aroclors 1242, 1254, 1221, etc. (U.S. EPA, 1976; Barbalace, 2003). PCBs, because of their general inertness and thermal stability, gained a widespread of applications as dielectric fluids and insulators for transformers and capacitors, heat transfer fluids, coolants and lubricants. They were even recommended by fire code for their role in preventing fires and explosions (Afghan & Chau, 1989; Barbalace, 2003).

According to Rantanen, (1992), direct or indirect release of PCBs into the environment was as a result of improper disposal practices, accidents and leakages from industrial facilities in some applications. The PCBs residues are said to have been identified in air, freshwater, marine sediments, fish, wildlife, human adipose tissue, serum and milk (Kim & Cooper, 1999; Focant *et al.*, 2002). Their contamination in meat (pork and chicken) is said to exceed the tolerance level set by the European Commission (Bernard *et al.*, 1999). Due to their toxicity and stability, they are classified among the 16 chemicals as POPs (Bench, 1999). Individuals are exposed to PCBs through breathing in contaminated air, consuming contaminated food and by skin contact with old electrical equipment that contain PCBs (Ross, 2004). PCBs readily penetrate skin, polyvinyl chloride (PVC) and latex (natural rubber) (ANZECC, 1997). Once they accumulate in the body, they are said to interfere with the hormones, damage the liver and cause cancer. Despite the fact that the use of PCBs was banned in many industrialized countries, a considerable fraction of these compounds is still cycling in the ecosphere (Silberhorn *et al.*, 1990). This is because many transformers

contaminated with PCBs are still in use due to their long life-span of service (Date *et al.*, 2014). This implicates the high chances of environmental pollution with PCBs, and potential risks to health and ecosystems (Fránek *et al.*, 1997). The monitoring of PCBs in environmental samples is therefore essential for the identification and control of the contaminated areas.

2.2.1 Analytical methods

The conventional methods of PCBs analysis have been employed in the analysis of oil, soil, food and water. The first oldest complex laboratory-based and widely used instrumental techniques are gas chromatography (GC) coupled with a detecting system such as electron capture detector (ECD), high resolution mass spectrometry (HRMS) or low resolution mass spectrometry (LRMS) and liquid chromatography (LC) (Gordon *et al.*, 1982; Erickson, 1997; Sawatsubashi *et al.*, 2008). These techniques have high sensitivity, selectivity and accuracy but their development is expensive especially for large scale analysis and they are also costly to run, often complex to use, time-consuming and they utilize large volumes of expensive and toxic solvents (Bender & Sadik, 1998). They typically require sample preparation before chromatographic separation (Ferrario *et al.*, 1997).

Another problem with conventional analysis procedures is that they require instrumentation that is not applicable for on-site analysis (Laschi *et al.*, 2000). The PCB compounds are quantified by comparing the detector response to the response obtained from a standard of known concentration. The second method is a chemical-colorimetric test kit that simply tells whether or not the sample contains greater than 50 ppm PCB. The third is an electrochemical method that provides a quantitative result by testing for the total chlorine. Both the second and the third methods test for PCBs by analyzing for the total chlorine. However, the presence of chlorine does not guarantee the presence of PCB as other sources of chlorine may influence the test, so these two methods have limited specificity (Finch, 2006).

On the other hand, Rogers and Williams, (1995) reported the colorimetric kits, enzyme immunoassays (EIAs) and biosensors as some of the less expensive yet most available analytical techniques for PCBs and other priority pollutants. These techniques are said to require less time to be performed and among them, biosensors in general and immunosensors in particular, are reportedly the most suitable field analytical techniques for fast, continuous and on-site analysis of the environmental pollutants. They are potent in defeating the shortcomings presented by their conventional counterparts.

2.3 Immunosensor

Biosensors are defined as analytical devices incorporating a biological material, a biologically derived material, or biomimic, like enzymes, antibodies, nucleic acids and cells or deoxyribonucleic acid (DNA) intimately associated with or integrated within an electronic physicochemical transducer or transducing microsystem (González-Martínez *et al.*, 1999; Dhand, *et al.*, 2011). Biosensors can be categorized according to the biological recognition element (immuno, enzymatic, DNA and whole-cell biosensors) or the signal transduction method (optical, mass-based, electrochemical, and thermal biosensors) (Turner, 2000; Wanekaya *et al.*, 2008). Biosensors, through integration of the biological sensing species into a transducer, they convert the analyte concentration into electrical signal.

An immunosensor in this case is a biosensor that comprises antibody (*Ab*) fragments as bimolecular recognition species, for specific analyte so called antigen (*Ag*), a transducing component and a signal processor. A transducer converts the chemical changes evolving from the specific interaction between the *Ab* and *Ag* into measurable and processable electric or optical signal. For environmental control and monitoring, immunosensors can provide fast and specific data for contaminated sites. They have wide usage also in clinical diagnostics, bioprocess monitoring and, food and agricultural product processing (Piro *et al.*, 2013).

The prominent aspects of immunosensors that promote their usability include their high specificity and sensitivity which permit detection of broad spectrum of analytes even in complex sample matrices with minimal requirements for sample preparation or pre-treatment (Draisci *et al.*, 1998; Moscone *et al.*, 1999; Panfili *et al.*, 2000). The specificity of the *Ab* to target *Ag* promotes immunoassays in simplifying the complex analytical techniques (Lambert *et al.*, 1997). They offer other advantages over the conventional analytical methods such as the possibility of portability, simplicity to use, working on-site and compatibility to data processing technologies.

Furthermore, immunosensors offer the possibility of determining not only specific chemicals, but also their biological effects, such as toxicity or endocrine-disrupting effects. Toxicity and endocrine-disrupting effects of a substance are sample information of great interest (Rodriguez-Mozaz *et al.*, 2004). Fig. 2.1 represents the scheme for immunosensor development and some of the successfully developed electrochemical immunosensors for PCBs and other analytes are presented in Table 2.1.

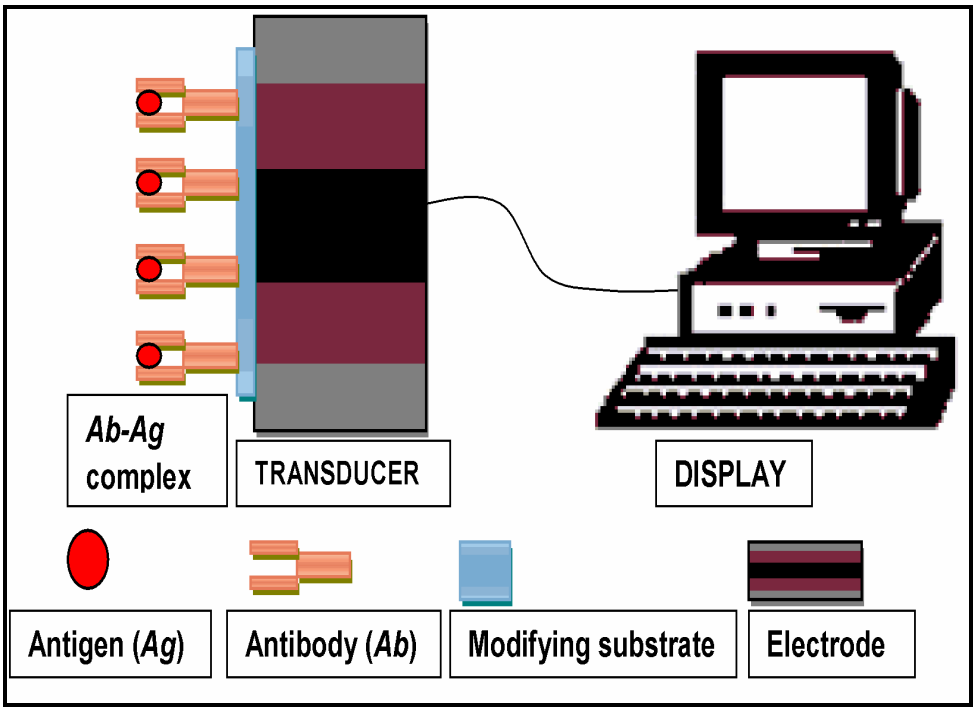

Figure 2. 1: Schematic immunosensor development

Immunoassay analytical techniques are based on the specific and selective reaction between *Abs* and corresponding *Ags* to form affinity complexes (Ghindilis *et al.*, 1998). These techniques are applicable in clinical chemistry, medical diagnostics, environmental monitoring and food quality control (Roberts & Durst, 1995). The extent of the affinity reaction can be assessed using different assay schemes;

a) *Direct assay*- Here the *Ab-Ag* complex's signal is determined directly from the transducer and the concentration of the analyte is directly proportional to the output measurement, e.g. faradaic current depending on the detection technique used.

b) *Direct competitive assay*- This assay can follow two approaches: the first one is whereby the *Ag* is conjugated with an enzyme label and this conjugated antigen (*Ag**) of known concentration competes directly with the sample analyte (free sample *Ag*) for the immobilized *Ab* binding sites. The activity of the enzyme is measured as the enzyme catalyses the reduction of the substrate or mediator in the presence of another cosubstrate. The enzyme activity is inversely proportional to the concentration of the analyte.

Table 2. 1: Successfully developed electrochemical immunosensor for various analytical detections

Immunosensor	Transduction & immobilization	Recognizing biomolecule	Analyte	Matrix	Reference
Direct electrochemical	Glassy carbon electrode, polypyrrole, entrapment in polypyrrole films	Antibodies (Anti-PCB antiserum, pool AC-3	PCBs (stds Aroclor 1016, 1242, 1248, 1254, 1260 & 1268)	Water	(Bender & Sadik, 1998)
Electrochemical	Screen printed carbon electrode, direct adsorption on SPE	sheep polyclonal antibodies (IgG), HRP-labelled antibodies (direct & indirect competition)	PCBs (std PCB 15, Aroclor 1242 & 1248)		(Laschi *et al.*, 2000)
Electrochemical	SPCE, direct adsorption on SPE	sheep IgG	PCBs Alkaline phosphatase-labelled PCB (AP-PCB 28)-direct competition (std PCB 28,101,118)	Food	(Laschi *et al.*, 2003)
Electrochemical	SPCE, magnetic beads, direct adsorption on MBs	Antibodies (IgG anti-PCB 28, IgG anti-PCB 77)	PCBs; PCB 28 - AP, PCB 77- AP: direct competition (std PCB 77 & 126, Aroclor 1242, 1248 & 1016)	Marine sediments	(Centi *et al.*, 2006)
Disposable reagentless electrochemical	SPCE, AuNPs, biopolymer/sol-Gel	HRP-labelled antibodies, carcinoemryonic antigen (CEA)-antibodies	Tumor markers	Clinical serum samples	(Wu *et al.*, 2006)
Electrochemical direct competition	SPGE	ELISA, HRP, monoclonal anti-fumonisins antibodies	Fumonisins micotoxins	Food: corn samples	(Kadir & Tothill, 2010)
Electrochemical impedance	Screen printed gold electrode, direct adsorption	specific antibody	infection biomarkers		(Ciani *et al.*, 2012)
Fluorescent sandwich	Gold sensor disk/ self-assembled monolayers	Polyclonal goat anti-COX-2 antibodies, rabbit anti COX-2 polyclonal secondary antibody conjugated AP	Cyclooxygennase-2 (COX-2) pain biomarkers	Simulated blood	(Noah *et al.*, 2011)
Electrochemical	gold electrode , direct adsorption	gliadin antigen molecules	antigliadin antibodies		(Rosales-Rivera *et al.*, 2011)
Electrochemical		human serum antibodies	Japanese encephalitis virus (JEV)		(Tran *et al.*, 2012)
Electrochemical impedance	Gold electrode, alkanethiol SAM	myoglobin antibodies	Myoglobin	Blood serum	(Gunda *et al.*, 2012)

Electrochemical	Glassy carbon electrode, carbon nanotubes, adsorption	rabbit polyclonal antibody, AP-anti-IgG for direct competition	neuron specific enolase (NSE)	Clinical serum samples	(Yu *et al.*, 2012)
Electrochemical voltammetric	Screen printed carbon electrode, carbon nanotubes, adsorption		human anti-glian antibodies (AGA); AGA IgA and AGA IgG	real serum samples	(Neves *et al.*, 2012)
Electrochemical sandwiched	GCE, graphene, gold nanoparticles, adsoption	rabbit anti-human IgG and Ferrocene derivative labelled- goat antihuman IgG	human IgG	Bovine serum albumin	(Wang *et al.*, 2013)
Electrochemical sandwiched	SPCE, adsoption	Mouse polyclonal antibodies (anti-*acillussubtilis,* anti- *Escherichia coli*), rabbit polyclonal anti *Francisellatularensis* Antibodies, HRP as label.	Microorganisms (*B. atrophaeus*, *E. coli, Salmonella Typhimurium, Francisellatularensis*)	Air	(Skládal *et al.*, 2013)
Label-free photoelectrochemical	CdTe quantum dots/CdS Co-sensitized TiO_2 Nanotube, adsorption	Rabbit polyclonal antibody	Octachlorostyrene	Water	(Cai *et al.*, 2013)
Electrochemical	AuNPs, PANI/ multiwall carbon nanotubes/ chitosan, entrapment	Anti-chlorpyrifos monoclonal antibodies	Chlorpyrifos	Cabbage, parchoi, lettuce, leek	(Sun *et al.*, 2013)
Displacement and competitive	AuNPs, ELISA microwell plate ,adsorption	Bisphenol A antibodies, avidin-HRP	Bisphenol A		(Lee *et al.*, 2013)
Electrochemical	Silicon/glutaraldehyde substrate, protein G-AuNPs, covalent linking	IgG (Rat)			(Li *et al.*, 2013)
Label-free electrochemical	Gold-silicon carbide, GCE, adsoption	Anti hCG antibody	Human chorionic gonadotrophin (hCG)		(Yang *et al.*, 2014)
Electrochemical (direct)	ZnO nanorods/ gold coated glass, adsorption	D-dimer antibody	D-dimer		(Ibupoto *et al.*, 2014)

The activity is obtained through measuring the signal produced by the cosubstrate (Del Carlo & Mascini, 1996). The second one has immobilized *Ags* in competition with free *Ags* for labelled free antibodies (*Ab**) (Bonwick & Smith, 2004).

c) *Indirect competitive assay*- Here the conjugated *Ag* is first immobilized onto the electrode surface as the basis for the immobilization process. Then the primary *Ab* is reacted with the sample and the small amount of the mixture is added onto the immobilized *Ag* for the competition between the immobilized *Ag* and the sample for the *Ab*. The secondary enzyme labelled *Ab* is then used to evaluate the extent of the affinity between the *Ab* and the *Ags* (Laschi *et al.*, 2000).

d) *Sandwich assay*- The *Ab* here is immobilized on the electrode substrate and put into contact with a solution containing the analyte (*Ag*), and lastly the *Ab** is then added resulting in the *Ag* sandwiched between the two antibodies (*Ab* and *Ab**).

The most popular immunoassays were enzyme immunoassay (EIA) and enzyme linked immunosorbent assay (ELISA) which were commercialized as EIA and ELISA test kits which gained popularity in 1970s and 1980s (Engvall, 1980; Lequin, 2005). These were based on the principle of an enzyme used as the reporter label. Recent applications of the enzymes as labels do not involve the test kits for the competition reactions because of the use of electrodes as the solid phase (transducer) instead of the ELISA microplates. Moreover, these microtiter plates demand time and skilled personnel to operate and are inefficient for: carrying several analyses at the same time, continuous detection and transduction purposes.

In the past researches, inorganic signal amplification tags such as quantum dots (Yu *et al.*, 2009) or catalytic gold nanoparticles (de la Escosura-Muñiz *et al.*, 2010; de la Escosura-Muñiz & Merkoçi, 2011) have been used in place of the enzyme labels. They were believed to improve the assay sensitivity and correlate well with the standard tests. However, these enzymatic and inorganic labels are a great source of high costs and increased analysis time due to the need of conjugated antibodies, addition of substrates, use of different several reactions and washing steps. Piro *et al.*, (2013) on the other hand, showed that it would be more important and interesting for the signal transduction and detection to be performed with no labelling of the biomolecules using redox tags or any addition of the redox reagent to the analysis solution.

2.3.1 Transduction methods

A transducer is a device used to convert a physical quantity to its corresponding electrical signal. It is a prominent component of an immunosensor normally designed to sense or respond to a particular measurand. It basically has two main components, namely; sensing and transduction elements. The first element senses and responds to the physical quantity or the rate of change of the physical quantity. The output of the sensing element is passed on to the second element which is responsible for converting the non-electrical signal into proportional electrical signal. In some cases, this element performs both sensing and transduction with no external or additional sensing element. There are four basic transduction methods, namely; electrochemical, optical, piezoelectric and thermal techniques (Korotkaya, 2014).

Electrochemical transducers are further classified into potentiometric, voltammetric, conductometric and impedimetric with the resultant detectable signals being potential drop between working and reference electrodes, current change from oxidation or reduction of electroactive substance, electrical conductivity as a result of immunological reaction and variation of impedance respectively. In optical transducers the reaction changes are converted into absorption, fluorescence, luminescence, reflectance, refractive index, optical path or surface plasmon resonance. Piezoelectric transducers such as quartz crystal microbalances and microcantilevers measure the mass changes that take place after the formation of *Ab-Ag* complex. The quite uncommon thermal transducers measure the amount of heat with a sensitive thermistor as a way to obtain the concentration of the analyte (Moina & Ybarra, 2012; Korotkaya, 2014).

According to Moina and Ybarra, (2012), statistically, the three popular transduction techniques have been used to develop immunosensors but electrochemical ones lead the trend in research publications. Optical and piezoelectric, despite their high sensitivity, demand highly sophisticated instrumentations and induce compromised integration with sensitive biological molecules. Their detections are often fragile (Prodromidis, 2010; Moina & Ybarra, 2012). These inconveniences led to the use of robust, cost effective, low power consuming, simple, fast, affordable, sensitive, compatible and portable electrochemical detections that can be used at site (Prodromidis, 2010). Immunosensors coupled with electrochemistry can offer and guarantee sensitivity, flexible label-free and reagentless detection methods with less interferences and low detection limits (Del Carlo *et al.*, 1997; Piro *et al.*, 2013).

Electrochemical techniques involve use of solid electrodes made from inert materials such as carbon, platinum or gold, whose surfaces act as both the support for the immobilization of the recognition element and the transducing device. In electroanalytical measurements the surface of electrode is a powerful tool as it acts as a sensor and/or support for immobilization of sensing biomolecules in biosensors (Ciucu, 2014). Due to some complexities associated with some of the electrochemical analyses depending on the materials involved and analyst's desires for higher output, the electrode can have limited applicability. For example, many biologically and environmentally important compounds do not respond within a potential window of bare solid electrode or they influence over-potential therefore, direct electrochemical detection will require large potentials for these compounds. This can result in increased background currents that liberate undesirable detection limits.

Direct detection with the bare electrode also can pose a risk of passivation, poisoning and/or deactivation of the electrode surface due to possible unwanted adsorption of macromolecules or reaction products thereby sacrificing the stability of the response, the activity and sensitivity of electrode (Baldwin & Thomsen, 1991). To overcome these potential constraints, in recent practices the chemical nature of the surface of electrode is manipulated and modified with suitable substances that protect the electrode and maintain or enhance its activity for improvement of quantitative analysis. These are exemplified by nanomaterials such as carbon nanotubes, gold nanoparticles, graphene, and magnetic beads (MB) (Liu *et al.*, 2011; Serafín *et al.*, 2011).and conducting electroactive polymers (CEPs). These materials can be used as individual components or can be hybridized together or with other materials.

It is worth noting that the process of immobilization (discussed in section 2.3.2.1 below) integrates the *Ab* with the transduction component, meaning the transduction system in this case performs double role as both the immobilization platform and transducing component therefore, this section of the review is inclusive of biocompatibility and integration possibilities of the transducer with the *Ab*.

For example, magnetic beads (MBs) in particular, can be easily functionalized with various groups such as steptavidin (Moreno-Guzmán *et al.*, 2011), tosyl groups and amino groups (Zacco *et al.*, 2007; Lermo *et al.*, 2009; de la Escosura-Muñiz & Merkoçi, 2011) to enhance fast and specific immobilization of the biomolecule. These improve the sensitivity of the assay and reduce the reaction time and there is also possibility to use small volumes of the solution on the working electrode. The electrode in this case acts as part of transducer hence there is neither passivation nor electrochemical interferences expected. The use of

nanoparticles and magnetic beads results in an improved electrochemical performances (Agüí *et al.*, 2008; Qureshi *et al.*, 2009). These materials moreover, improve the surface area for the adsorption of large number of biomolecules because of their small size.

The challenge with the use of these materials is that the electrode surface modifications are often long processes that are even difficult to implement industrially. They are usually quite expensive, thus cost assessment should be well made when using them (Ricci *et al.*, 2012). The other problem associated with MBs, in particular, is the fact that the recognition element is not in direct contact with the electrode surface at the end of the immunological chain and this may pose some limitations to the sensitivity of the assay (Zacco *et al.*, 2007; Lermo *et al.*, 2009; Liébana *et al.*, 2009). Electrode surface modifications could rather be performed CEPs.

Wei and Ivaska, (2006) acknowledged there are a number of advantages and new possibilities offered by the electrochemical immunosensors based on conducting polymers for the detection of biologically significant compounds. CEPs are a class of organic materials that can easily be synthesized chemically or electrochemically from their monomers. The electrodes which act as transducers for the *Ab-Ag* interaction signal are modified with the CEP matrix for the immobilization of *Abs*. The use of CEPs in immunosensor development exhibits several advantages; CEPs act as immobilization matrices since they are generally insoluble, making them easy to carry and immobilize the bioactive species.

CEPs have gained considerable momentum in research because they are applicable in a number of new growing technologies such as recognising molecules (stimuli) approaching the polymer surface unlike other materials (Müller & Lange, 1986; Carey *et al.*, 1987; Gardner & Bartlet, 1995; Carey *et al.*, 1986). They are capable of generating rapid, analytically useful signals (Sadik & Van Emon, 1996) as they can convert the biological information into electrical signal, acting as electrochemical transducers. Their applicability as prominent materials for fabricating chemical and biological sensors relies on their exhibition of highly reversible redox behaviour with distinctive chemical memory. Sensors fabricated from conducting polymers reveal more advantages over other sensors because of the availability of a wide range of polymers which are readily synthesized and they can be operated at room temperature (Koul *et al.*, 2001).

Hoa *et al.*, (1992) conceptualized these polymers acting as both the immobilization matrices and the physicochemical transducers that convert the chemical signal into the electrical signal. Hartmann, (2005) reported that the use of conducting materials as mediators and functional biointerfaces enhances the direct electron transfer. Additionally, Cosnier, (1999) and Murphy, (2006) independently and on different occasions indicated that using and taking an advantage of the conducting host polymer, the direct electrical communication can be obtained between the immobilized biomaterial and the surface of the electrode which subsequently enhances the immunological reaction that can be electrochemically detected. They are smart materials which exhibit transduction abilities with no supplementary redox labels conjugated on the biomolecule or put in solution (Cosnier, 1999; Sargent & Sadik, 1999; Gerard *et al.*, 2002; Cosnier, 2003). Polymers can be fabricated into exquisite structures using a wide range of techniques and they are generally inexpensive (Yu *et al.*, 2014). Some of the CEPs include polypyrrole, polyaniline, polythiopene and polyacetylene (Shinde & Kher, 2014).

Among these polymers, polyaniline (PANI) and polypyrrole (Ppy) have been extensively utilized for immobilization due to their relatively stable electrical conductivity and Ppy in particular, can be electro-synthesized under biocompatible conditions (Bidan, 1992; Mousty *et al.*, 2001; Uang & Chou, 2002). Contrarily, sensors fabricated based on Ppy reportedly have higher susceptibility to degradation. Even the potential method to remediate this problem, the covalent attachment of the linking components on the monomer, is technically complex and does not guarantee the polymerization of the modified monomer (Davis *et al.*, 1995). On the other hand, Ahuja and co-workers indicated there have been a number of reports that have previously been published on the immobilization of biomolecules into PANI films (Ahuja *et al.*, 2007).

2.3.1.1 Polyaniline (PANI)

PANI, as a versatile electroactive and conducting polymer, has shown advantages in applications of electrode modification by electropolymerization. It acts as an effective mediator for electron transfer and a suitable matrix for immobilization since it exhibits two redox couples (Luo & Do, 2004). It is thermally (Wang *et al.*, 1995), electrochemically (Chiang & MacDiarmid, 1986) and environmentally (Pruneanu *et al.*, 1999; Chandrakanthi & Careem, 2000; Park *et al.*, 2004) stable. It is easily deposited directly on the sensor electrode and it has high surface area. It has various controllable and variable properties such as thickness, electrical, chemical and structural flexibility (Kang *et al.*, 2004; Dhand *et*

al., 2011). PANI, among other polymers, is the most promising polymer because of low cost of monomer and simplicity to synthesize (Grennan *et al.*, 2003; Kwon *et al.*, 2010).

However, PANI conductivity is pH sensitive which explains why its synthesis is carried out in acidic medium (Wallace *et al.*, 2009). This acidic pH dependence narrows the industrial utilization of the polymer in applications that do not favour the acidic medium such as immunological reactions which favour slightly acidic to neutral conditions, in as much as it has been successfully used in sensor fabrication (Xie *et al.*, 2002; Nicolas-Debarnot & Poncin-Epaillard, 2003; English *et al.*, 2006). To defeat these challenges and achieve electroanalytical applications of PANI in sensors, the polymer is hybridized with materials that can enhance or maintain the polymer conductivity. Previous studies showed that the incorporation of noble metal nanoparticles into a polymer matrix results in composite with outstanding physical and chemical properties (Park *et al.*, 2004; Kinyanjui *et al.*, 2006; Neelgund *et al.*, 2008) and could boost the electrical, dielectric and optical properties of the polymer (Sarma *et al.*, 2002; Xue *et al.*, 2006; Yakuphanoglu *et al.*, 2006).

In this regard, the preference is given to silver nanoparticles (Ag NPs) because silver is said to have the highest electrical and thermal conductivities among all the metals (Sun & Xia, 2002). This implies that its incorporation into PANI could result in materials with improved electrical properties and surface area (Choudhury, 2009). The incorporation of Ag NPs into PANI has been reported previously (Jing *et al.*, 2007; Choudhury, 2009; Crespilho *et al.*, 2009; Reda & Al-ghannam, 2012; Khan *et al.*, 2013; Dhibar & Das, 2014) even though the composites were intended for sensors not necessarily immunosensors.

2.3.2 Antibodies

Abs are extraordinary selective and versatile reagents provided by nature. These biological species are proteins produced in animals by an immunological response to the presence of foreign substances, *Ags*, and have specific affinity for these *Ags* (Luppa *et al.*, 2001; Bojorge Ramírez *et al.*, 2009). There are five primary classes of *Abs* (or immunoglobulins, Ig) which differ by the type of heavy chain in the molecule. The different chains are gamma (G), mu (M), alpha (A), epsilon (E) and delta (D) and the resulting *Abs* are IgG, IgM, IgA, IgE and IgD respectively. These distinctions in heavy chains make the *Abs* to have different immune responses. The distinctive structure of each *Ab* allows it to specifically attach to an *Ag* in a lock and key configuration (Kumagai & Tsumoto, 2001; Bojorge Ramírez *et al.*, 2009). This results in the destruction or elimination of *Ag.* It is only IgG that is used in immunosensors (Piro *et al.*, 2013). It accounts for 70-75 % of the total immunoglobulin pool in human serum.

Based on its relative abundance and outstanding specificity towards antigens, it is said to be the principle *Ab* that has great application in immunological research and clinical diagnostics and it is the most extensively investigated (Kumagai & Tsumoto, 2001).

2.3.2.1 Antibody immobilization methods

Immobilization of a biomolecule on a matrix is the restriction of the biomolecule to gross over but rather keep it in a relatively defined region of space to enhance its stability and reusability (Dhand *et al.*, 2011). The immobilization of a biomolecule to the surface of a transducer plays an important role as the first prominent step in construction of an immunosensor for its specificity, sensitivity and reproducibility (Sai *et al.*, 2006; Ahuja *et al.*, 2007). This is based on the fact that immunosensors usually measure the signals resulting from the specific immunoreactions between analytes and the *Abs* immobilized. This step can also influence the way the *Ab* and the *Ag* interact and it also contributes to the modification of the sensing surface itself. Immobilization step should therefore, be performed with the heed taken that the recognition species does not passivate the sensing surface and in a way such that the activity of the recognition species is not prohibited.

The choice of the technique used for connecting the biological component to the transducer is important because the biomolecule stability, longevity and sensitivity largely depend on the configuration of the antibody layer (Ahuja *et al.*, 2007). Different approaches have therefore, been evaluated and applied to successfully immobilize the antibody on the polymer-modified electrode substrate. These are adsorption, covalent attachment and electrochemical immobilization. Adsorptive immobilization results in biomolecule adsorbed in the interface of the transducer and solution by Coulomb, van de Waals, hydrophobic, polar, ionic or hydrogen interactions. It is the simplest method because no substantial pre-treatment of substrate or special chemicals needed. It is very good for mass production of biosensors.

However, adsorption does not afford a high concentration of a biological component and it results in recognition elements that are very sensitive to pH, temperature, ionic strength, and mediator concentration variations. These can affect the binding forces thereby increasing chances of loss of activity by the *Ab* or *Ag*. Biomolecule is at the risk of getting leached out into solution during measurement since is immobilized on the outer layer of the polymer. This threatens the lifetime stability of the sensor. This method is limited to research where the sensor is not intended for long term use. Forces acting between the biomolecule and substrate are mainly low-energy interaction that repeated washing can destabilize the

attachment therefore, this approach is not appropriate in repeated analytical measurements. (Bender & Sadik, 1998; Ahuja *et al.*, 2007; Korotkaya, 2014; Yu *et al.*, 2014).

Covalent attachment is achieved by formation of covalent bond between the *Ab* and transducer. It is the most widespread immobilization method and it ensures strong biomaterial-support binding. Covalent linking coupled with the porous morphology of the polymer film results in high biomaterial loading and prevents biomaterial loss. It produces sensors with a long service life and good stability even under adverse conditions and provides high degree of surface coverage. It occurs only on the outer surface of the polymer, thus, permitting optimization of conditions for each step of the reaction. For example, initial polymer formation can be performed under organic solvents, high potential values, and highly reactive generated monomer radicals; the conditions that can be troublesome for the biomolecules.

Then, the covalent linkage of the biomolecule to the polymer composite can easily be carried out in aqueous buffer solutions that can maintain the activity and recognition properties of the biomaterial. In most cases the attachment is made by use of the cross-linking materials to ensure strong linkage. Cross-linking results in sensors with short response times. It significantly increases biomolecule loading onto the transducer and enhances direct electron transfer resulting in high biological activity. Cross-linking reportedly renders the sensor surface hydrophobic, the characteristic that maintains the native or near-native structure of the biomolecule. Unfortunately, cross-linking, in particular, partly denatures the biomolecule and results in poor stability because the biomolecule is exposed directly into the bulk solution, and covalent linkage, in general, results in irreversible binding (Cosnier, 1999; Ahuja *et al.*, 2007; Korotkaya, 2014; Yu *et al.*, 2014).

Electrochemical immobilization involves entrapment of the biomaterials in the layers of electrochemically synthesized polymer. It is accomplished by ramping the potential of the working electrode soaked in an aqueous solution constituting electro-polymerizable monomer and the biomaterial thus, incorporating the biomaterial into the growing polymer films. The conducting polymer matrices form porous networks with high potential to allow reagents to freely reach the electrode surface The recognition element is entrapped electrostatically in the polymer matrix and it is this polymer matrix that introduces the reagent into the immunological chain to play its important role in the detection system of the immunosensor (Cosnier, 1999; de la Escosura-Muñiz & Merkoçi, 2011; Liu *et al.*, 2011; Xie *et al.*, 2011). This method enhances reproducibility and controlled film thickness from which the other methods suffer even though they have been extensively used. It is a one fast step

process and ensures a mutual stabilization of both the polymer and biomolecule. It is a reagentless approach easily applicable to a wide range of biomolecules. It ensures good proximity of the active site of biomolecule and conducting surface of the transducer with controllable deposition of the biomolecule to a defined position on the transducer. Electropolymerization can be accomplished from small volumes of electrolyte, thus markedly reducing the amount of biomolecule to be entrapped.

On the other hand, electrochemical immobilization also has its own drawbacks. It requires high concentrations of the monomer and biomaterials and high monomer concentration can affect activity of biomolecule. Biomolecule stability is sacrificed at low pH since acidic pH is suitable for polymerization but stability is much higher at around neutral pH. Entrapment may change the chemical and biological properties of biomolecule due to reduced degrees of freedom and possible interactions with the inner surface of polymer films and the biomolecule has limited access to the bulk solution of the analyte (Cosnier, 1999; Ahuja *et al.*, 2007; Yu *et al.*, 2014).

2.3.3 Electrochemical transduction and detection techniques

Three of the voltammetric electrochemical techniques frequently applied in transduction and detection are differential pulse voltammetry (DPV), square wave voltammetry (SWV) and electrochemical impedance spectroscopy (EIS).

2.3.3.1 Differential pulse voltammetry

Analytical sensitivity of classical voltammetric methods is usually good at about 5×10^{-05} mol/dm^3. This however, is lowered by the currents due to double layer effects or other non-faradaic sources at the lowest concentrations. To improve and maintain the sensitivity therefore, differential pulse voltammetry is an option. In DPV, a linear potential is ramped at the rate of v to the working electrode with the succession of pulses. The current is monitored twice with the first sample taken just when the pulse starts before rise in potential and the second one is taken at the end of the pulse before it goes back to the baseline. The output is then the difference in current, ΔI. This ΔI is zero unless there is analyte reduction at the working electrode. The magnitude of ΔI increases swiftly when the potential approaches to $E_{1/2}$, so differential voltammogram has the peak at $E_{1/2}$ which is the identity of the substance in solution. With this technique, it is the area under the peak which is proportional to the concentration. DPV is more advantageous in that many analytes can be analyzed from a

single voltammogram when the analytical peaks are well resolved. Differential current, hence the voltammetric peak results in improved sensitivity.

2.3.3.2 Square wave voltammetry

Square wave voltammetry is the most sensitive alternative to the mentioned techniques. Its functionality is based on the application of a potential waveform to the working electrode. Then the current is measured in pairs for each wave period (cycle), i.e. in the forward direction ($I_{forward}$) and the reverse direction ($I_{reverse}$). The difference between these currents, $I_{difference}$ is the analytical signal whose peak height is directly proportional to the analyte concentration. SWV advantages are based on that $I_{difference}$ is greater than either $I_{forward}$ or $I_{reverse}$, so it is easy to read the height of the voltammetric peak, thereby increasing the accuracy. Secondly, the contributions by the capacitive effects to the overall current are minimized. In SWV high scan rates can be achieved without compromising the peak resolution.

2.3.3.3 Electrochemical impedance spectroscopy (EIS)

Another alternative electrochemical approach is the measurement of impedance. With the dynamic electroanalyses mentioned before, the potential was either constant or ramped at constant rate, $v\left(v = \frac{dE}{dt}\right)$. With EIS, a sinusoidally varying potential is applied across an electrochemical cell (sample) inducing an alternating current (AC) as a response. The AC equivalence of Ohm's law (V = IR) is given by:

$$\bar{V} = \bar{I}Z \qquad (2.1)$$

Where V = potential, I = current, R = resistance of a resistor and Z = impedance, a resistance that varies in cyclical manner with time. Over-bars imply that the quantities are varying with time.

What actually happens with impedance measurement is that a frequency dependent resistance (overall/complete impedance), Z* of a cell or sample is measured over a typical frequency broad range of 10^6 - 10^{-2} Hz using frequency analyser, phase-gain analyser or signal-response analyser depending on the exact mode of the measurement. The analyser applies a very small voltage, $\bar{V}$ possibly superimposed on a pre-set voltage, across the

sample/cell. $\bar{V}$ varies with time because it is regulated sinusoidally and the analyser measures the current, $\bar{I}$ with respect to time and therefore, calculates Z* and **time lag**, θ experienced between voltage and current. The frequency analyzer then changes the frequency at which the voltage oscillates and Z* is recalculated now with respect to frequency for as many as up to 50 various frequencies from higher frequency to the lower one. From the values of Z* and θ, the two components of Z*; real component Z' and imaginary component Z'' are determined hence, generation of Nyquist plot. Z*, Z' and Z'' are related by:

$$Z^* = Z' - jZ'' \qquad (2.2)$$

Where $j = \sqrt{-1}$, hence Z* is said to be “complex” impedance.

A plot of Z'' (y) vs. Z' (x) is called Nyquist plot or simply an impedance plot as shown in Fig. 2.2 (Monk, 2001).

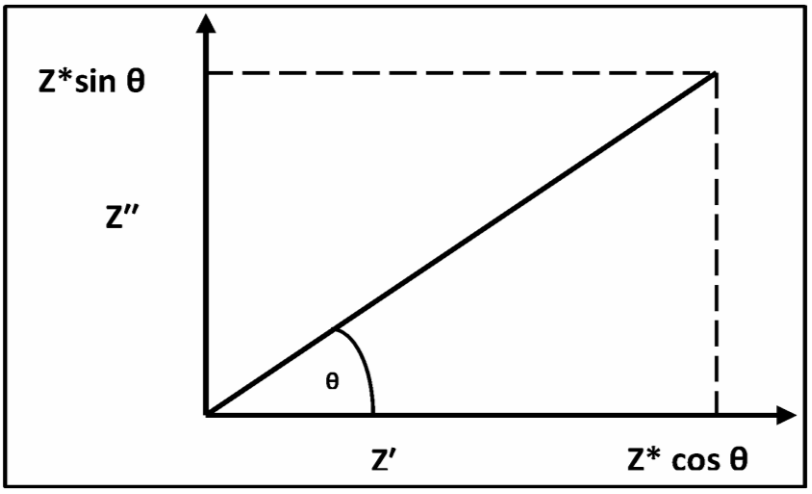

Figure 2.2: Nyquist plot of the imaginary impedance Z'' vs. real impedance Z' showing how Z* and θ are defined

2.3.4 Characterization techniques

It is important to monitor the formation of an immunosensor at each step of its fabrication by determining useful informative properties of the composite. Such properties are electrochemical, morphological and optical which are respectively studied by cyclic voltammetry (CV) and EIS, transmission electron microscopy (TEM), scanning electron microscopy (SEM) and powder X-ray diffraction (PXRD) and, Fourier transform infra-red (FTIR) spectroscopy and Ultra Violet visible (UV-Vis) spectroscopy.

2.3.4.1 Cyclic voltammetry

CV is one voltammetric technique during which the potential of the working electrode is ramped at the scan rate of v from an initial potential, E_i with linear sweep at the end of which the direction of the scan is reversed switching the potential again back to E_i. For a reversible redox process, oxidation occurs if the scan goes positive from E_i during the forward direction and reduction occurs during the reverse direction and vice versa. There are normally peaks observed during oxidation (anodic peaks) and reduction (cathodic peaks) which are characteristic of the material. The number of peaks depends on the type of material undergoing redox transformations. In CV the magnitude of the peak current is proportional to the analyte concentration. CV helps to study the electroactivity of the material in terms of conductivity and electroreversibility.

2.3.4.2 FTIR spectroscopy

Infra-red region from the electromagnetic spectrum covers a range from 0.78 to 1000 µm (wavelength). FTIR spectra is normally measured in wavenumbers, cm^{-1} (wavenumber = 1/wavelength, cm). The most useful IR region is from 4000 to 400 cm^{-1} which is the middle infra-red. IR radiation does not have adequate energy to cause electronic transitions like UV, but its absorption is limited to compounds with small variation in energy in the possible rotational and vibrational levels. A molecule absorbs IR radiation if the frequency of radiation matches the frequency of vibration (for example) resulting in change to the amplitude of molecular vibration. Molecular rotational transitions are of little use to the spectroscopist. With molecular vibrations, it is considered that the positions of atoms in a molecule are not fixed but they are free to undergo either stretching (symmetric or asymmetric) or bending vibrations.

IR spectroscopy is an extremely effective tool and method that is used to determine the presence or absence of a number of molecular functional groups which undergo vibrational transitions. The spectra of IR for organic compounds have two areas, viz: the **functional group** region within 4000 - 1500 cm^{-1} and the **fingerprinting** region within 1500 - 400 cm^{-1}. Peaks in the former region characterize specific types of bonds hence; they can be used to predict the presence of particular functional groups. The peaks in the latter region are due to complex distortions of the molecule. These may characterize the molecular symmetry or combination bands due to simultaneous deformations of multiple bonds. The application of IR spectroscopy is motivated by the fact that it can be used to monitor the extent of chemical

reactions in situ and analyze chemical structures by determination of functional groups in a compound or polymer (Ingle & Crouch, 1988).

2.3.4.3 UV-Vis spectroscopy

UV-Vis region covers 200 - 800 cm wavelength of the electromagnetic spectrum. The energy associated with this region is in the form of electronic transitions from ground state to excited high energy state. The absorption of UV-Vis radiation corresponds to the excitation of the outer electrons, which are either bonding forming sigma (σ) or pi (π) bonds, or non - bonding lone pair electrons (n). Absorption of UV-Vis radiation in molecules is restricted to certain functional groups containing valance electrons of low excitation energy. The three main types of electronic transitions are:

1. Transitions involving σ, π and n electrons
2. Transitions involving charge transfer electrons
3. Transitions involving d and f electrons

The first type is the most common in organic molecules while the second is shown by many inorganic species. The third one is not so common. The possible electronic transitions involving σ, π and n electrons are shown in Fig. 2.3. UV-Vis radiation is absorbed by many molecules and it is ideal for characterizing the optical and electronic properties of various materials such as films, powders, monolithic solids and liquids (Ingle & Crouch, 1988).

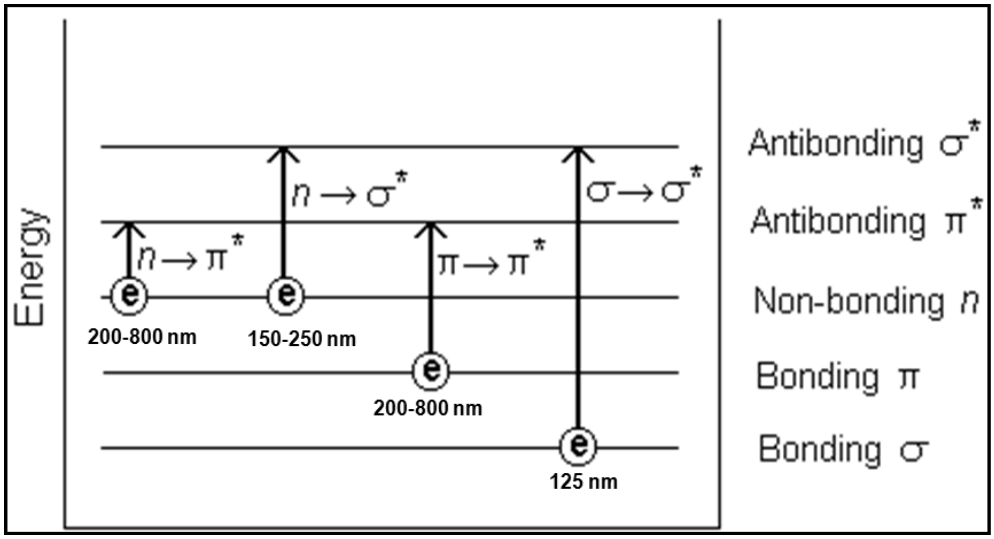

Figure 2.3: Electronic transitions involving σ, π and n electrons

2.3.4.4 Electron microscopy: SEM and TEM

Electron microscopy is a type of microscopy with a different approach of using electrons instead of light as in light microscopy, with possible magnification of ~ 2 000 000. The electrons are generated from electron gun and accelerated to the sample. Upon interaction with the sample, electrons are either backscattered (SEM) or transmitted through the sample (TEM) to the detector with a step-wise formation of the image. SEM gives the topographic (roughness/smoothness) and compositional morphology when the sample is scanned at a focussed point. TEM illuminates the whole sample to give the structural and compositional morphology (Radetic, 2011). The topography of a material can affect its performance especially the materials used in electrochemistry where thin smooth deposits are favourable for improved electroactivity. Structure and composition studies confirm the formation of the intended material.

2.4 References

Afghan, B.K. & Chau, A.S.Y. 1989. *Analysis of trace organics in the aquatic environment.* Boca Raton, Fla: CRC Press.

Agency for Toxic Substances and Disease Registry (ATSDR). 2000. *Toxicological profile for polychlorinated biphenyls (PCBs).* U.S. Department of health and human services, Atlanta, Georgia.

Agüí, L., Yáñez-Sedeño, P. & Pingarrón, J.M. 2008. Role of carbon nanotubes in electroanalytical chemistry. A review. *Analytica Chimica Acta*, 622: 11–47.

Ahuja, T., Mir, I.A., Kumar, D. & Rajesh. 2007. Biomolecular immobilization on conducting polymers for biosensing applications. *Biomaterials*, 28: 791–805.

Baldwin, R.P. & Thomsen, K.N. 1991. Chemically modified electrodes in liquid chromatography detection. A review. *Talanta*, 38(1): 1–16.

Barbalace, R.C. 2003. The Chemistry of polychlorinated biphenyls. *Environmental Chemistry.com. http://EnvironmentalChemistry.com/yogi/chemistry/pcb.html,* [02 June 2015].

Bench, D.W. 1999. PCBs, mining, and water pollution. Paper presented the WM'99 conference, Tucson, Arizona, USA. February 28 – March 4,1999.

Bender, S. & Sadik, O.A. 1998. Direct electrochemical immunosensor for polychlorinated biphenyls. *Environmental Science and Technology*, 32(6): 788–797.

Bernard, A., Hermans, C., Broeckaert, F., De Poorter, G., De Cock, A. & Houins, G. 1999. Food contamination by PCBs and dioxins. *Nature*, 401: 231–232.

Bidan, G. 1992. Electroconducting conjugated polymers: new sensitive matrices to build up chemical or electrochemical sensors. A review. *Sensors and Actuators B: Chemical*, 6(1-3): 45–56.

Boate, A., Deleersnyder, G., Howarth, J., Mirabelli, A. & Peck, L. 2004. Chemistry of PCBs. http://wvlc.uwaterloo.ca/biology447/modules/intro/assignments/Introduction2a.htm, [20 August 2013].

Bojorge Ramírez, N., Salgado, A.M. & Valdman, B. 2009. The evolution and developments of immunosensors for health and environmental monitoring: problems and perspectives. *Brazilian Journal of Chemical Engineering*, 26(2): 227–249.

Bonwick, G.A. & Smith, C.J. 2004. Immunoassays: their history, development and current place in food science and technology. *International Journal of Food Science and Technology*, 39: 817–827.

Cai, J., Sheng, P., Zhou, L., Shi, L., Wang, N. & Cai, Q. 2013. Label-free photoelectrochemical immunosensor based on CdTe/CdS co-sensitized TiO_2 nanotube array structure for octachlorostyrene detection. *Biosensors and Bioelectronics*, 50: 66–71.

Carey, W.P., Beebe, K.R. & Kowalski, B.R. 1987. Multicomponent analysis using an array of piezoelectric crystal sensors. *Analytical Chemistry*, 59(8): 1529–1534.

Carey, W.P., Beebe, K.R., Kowalski, B.R., Illman, D.L. & Hirschfeld, T. 1986. Selection of adsorbates for chemical sensor arrays by pattern recognition. *Analytical Chemistry*, 58(14): 149–153.

Del Carlo, M., Lionti, I., Taccini, M., Cagnini, A. & Mascini, M. 1997. Disposable screen-printed electrodes for the immunochemical detection of polychlorinated biphenyls. *Analytica Chimica Acta*, 342: 189–197.

Centi, S., Rozum, B., Laschi, S., Palchetti, I. & Mascini, M. 2006. Disposable electrochemical magnetic beads-based immunosensors for monitoring polychlorinated biphenyl (PCBs) pollutants. *Chemia Analityczna (Warsaw)*, 51: 963–975.

Chandrakanthi, N. & Careem, M.A. 2000. Thermal stability of polyaniline. *Polymer Bulletin*, 44: 101–108.

Chiang, J.C. & MacDiarmid, A.G. 1986. Polyaniline: protonic acid doping of the emeraldine form to the metallic regime. *Synthetic Metals*, 13(1-3): 193–205.

Choudhury, A. 2009. Polyaniline/silver nanocomposites: dielectric properties and ethanol vapour sensitivity. *Sensors and Actuators B: Chemical*, 138(1): 318–325.

Ciani, I., Schulze, H., Corrigan, D.K., Henihan, G., Giraud, G., Terry, J.G., Walton, A.J., Pethig, R., Ghazal, P., Crain, J., Campbell, C.J., Bachmann, T.T. & Mount, A.R. 2012. Development of immunosensors for direct detection of three wound infection biomarkers at point of care using electrochemical impedance spectroscopy. *Biosensors and Bioelectronics*, 31(1): 413–418.

Ciucu, A.A. 2014. Chemically modified electrodes in biosensing. *Biosensors & Bioelectronics*, 5(3): 154. doi: 10.4172/2155-6210.1000154, [13 January 2015].

Cosnier, S. 1999. Biomolecule immobilization on electrode surfaces by entrapment or attachment to electrochemically polymerized films. A review. *Biosensors and Bioelectronics*, 14: 443–456.

Cosnier, S. 2003. Biosensors based on electropolymerized films: new trends. *Analytical and Bioanalytical Chemistry*, 377: 507–520.

Crespilho, F.N., Iost, R.M., Travain, S.A., Oliveira Jr., O.N. & Zucolotto, V. 2009. Enzyme immobilization on Ag nanoparticles/polyaniline nanocomposites. *Biosensors & bioelectronics*, 24(10): 3073–3077.

Date, Y., Aota, A., Sasaki, K., Namiki, Y., Matsumoto, N., Watanabe, Y., Ohmura, N. & Matsue, T. 2014. Label-free impedimetric immunoassay for trace levels of polychlorinated biphenyls in insulating oil. *Analytical Chemistry*, 86: 2989–2996.

Davis, J., Vaughan, H.D. & Cardosi, M.F. 1995. Elements of biosensor construction. *Enzyme and Microbial Technology*, 17(12): 1030–1035.

Dhand, C., Das, M., Datta, M. & Malhotra, B.D. 2011. Recent advances in polyaniline based biosensors. *Biosensors and Bioelectronics*, 26(6): 2811–2821.

Dhibar, S. & Das, C.K. 2014. Silver nanoparticles decorated polyaniline/multiwalled carbon nanotubes nanocomposite for high-performance supercapacitor electrode. *Industrial & Engineering Chemistry Research, 53: 3495-3508.*

Draisci, R., Volpe, G., Lucentini, L., Cecilia, A, Federico, R. & Palleschi, G. 1998. Determination of biogenic amines with an electrochemical biosensor and its application to salted anchovies. *Food Chemistry*, 62(2): 225–232.

English, J.T., Deore, B.A. & Freund, M.S. 2006. Biogenic amine vapour detection using poly(anilineboronic acid) films. *Sensors and Actuators, B: Chemical*, 115(2): 666–671.

Engvall, E. 1980. Enzyme immunoassay ELISA and EMIT. *Methods in Enzymology*, 70: 419–439.

Erickson, M.D. 1997. *Analytical chemistry of PCBs*. Lewis publishers, 2nd Ed. Boca Raton: CRC Press.

Ferrario, J., Byrne, C. & Dupuy, A.E.J. 1997. Background contamination by coplanar polychlorinated biphenyls (PCBs) in trace level high resolution gas chromatography/high resolution mass spectrometry (HRGC/HRMS) analytical procedures. *Chemosphere*, 34(11): 2451–2465.

Finch, S. 2006. A comparison of current PCB analytical techniques. Proceedings of the *3 rd international conference for the remediation of PCB contamination – a Pennwell Conference, Dexsil Corporation,* One Hamden Park Drive, Hamden.

Focant, J.F., Eppe, G., Pirard, C., Massart, A.C., André, J.E. & De Pauw, E. 2002. Levels and congener distributions of PCDDs, PCDFs and non-ortho PCBs in Belgian foodstuffs - assessment of dietary intake. *Chemosphere*, 48: 167–179.

Fránek, M., Pouzar, V. & Kolář, V. 1997. Enzyme-immunoassays for polychlorinated biphenyls: structural aspects of hapten-antibody binding. *Analytica Chimica Acta*, 347(97): 163–176.

Gardner, J.W. & Bartlet, P.N. 1995. Application of conducting polymer technology in microsystems. *Sensors and Actuators A*, 51: 57–66.

Gerard, M., Chaubey, A. & Malhotra, B.D. 2002. Application of conducting polymers to biosensors. *Biosensors and Bioelectronics*, 17: 345–359.

Ghindilis, A.L., Atanasov, P., Wilkinst, M. & Wilkins, E. 1998. Immunosensors : electrochemical sensing and other engineering approaches. *Biosensors & Bioelectronics*, 13(1): 113–131.

González-Martínez, M.A., Puchades, R. & Maquieira, A. 1999. On-line immunoanalysis for environmental pollutants: from batch assays to automated sensors. *TrAC - Trends in Analytical Chemistry*, 18(3): 204–218.

Gordon, R.J., Szlta, J. & Faeder, E.J. 1982. Determination of polychlorinated biphenyls in transformer oils by capillary gas chromatography. *Analytical Chemistry*, 54(3): 478–481.

Grennan, K., Strachan, G., Porter, A.J., Killard, A.J. & Smyth, M.R. 2003. Atrazine analysis using an amperometric immunosensor based on single-chain antibody fragments and regeneration-free multi-calibrant measurement. *Analytica Chimica Acta*, 500: 287–298.

Gunda, N.S.K., Singh, M., Roy, S.S. & Mitra, S.K. 2012. Developing electrochemical impedance immunosensor for the detection of myoglobin. *The 14th International Meeting on Chemical Sensors (IMCS)*: 181–184.

Hartmann, M. 2005. Ordered mesoporous materials for bioadsorption and biocatalysis. *Chemistry of Materials*, 17: 4577–4593.

Hoa, D.T., Kumar, T.N.S., Punekar, N.S., Srinivasa, R.S., Lal, R. & Contractor, A.Q. 1992. A biosensor based on conducting polymers. *Analytical Chemistry*, 64(7): 2645–2646.

Ibupoto, Z.H., Mitrou, N., Nikoleli, G.P., Nikolelis, D.P., Willander, M. & Psaroudakis, N. 2014. The development of highly sensitive and selective immunosensor based on antibody immobilized ZnO nanorods for the detection of D-dimer. *Electroanalysis*, 26: 292–298.

Ingle, J.D. & Crouch, S.R. 1988. *Spectrochemical analysis*. Upper Saddle River, New Jersey: Prentice Hall, Inc. 07458, pp. 327 - 337.

Jing, S., Xing, S., Yu, L., Wu, Y. & Zhao, C. 2007. Synthesis and characterization of Ag/polyaniline core-shell nanocomposites based on silver nanoparticles colloid. *Materials Letters*, 61(13): 2794–2797.

Kadir, M.K.A. & Tothill, I.E. 2010. Development of an electrochemical immunosensor for fumonisins detection in foods. *Toxins*, 2: 382–398.

Kang, Y., Kim, S.K. & Lee, C. 2004. Doping of polyaniline by thermal acid-base exchange reaction. *Materials Science and Engineering C*, 24: 39–41.

Khan, M.J., Husain, Q. & Ansari, S.A. 2013. Polyaniline-assisted silver nanoparticles: a novel support for the immobilization of α-amylase. *Applied microbiology and biotechnology*, 97(4): 1513–22.

Kim, Y. & Cooper, K.R. 1999. Toxicity of 2,3,7,8-tetrachlorodibenzo-p-dioxin (TCDD) and polychlorinated biphenyls (PCBs) in the embryos and newly hatched larvae of the Japanese Medaka (Oryzias Latipes). *Chemosphere*, 39(3): 527–538.

Kinyanjui, J.M., Wijeratne, N.R., Hanks, J. & Hatchett, D.W. 2006. Chemical and electrochemical synthesis of polyaniline/platinum composites. *Electrochimica Acta*, 51(14): 2825–2835.

Korotkaya, E.V. 2014. Biosensors: design, classification, and applications in the food industry. *Foods and Raw Materials*, 2(2): 161–171.

Koul, S., Chandra, R. & Dhawan, S.K. 2001. Conducting polyaniline composite: a reusable sensor material for aqueous ammonia. *Sensors and Actuators, B: Chemical*, 75: 151–159.

Kumagai, I. & Tsumoto, K. 2010. Antigen-antibody binding. *Encyclopedia Of Life Sciences*. John Wiley & Sons Ltd, Chichester. http://www.els.net, doi:10.1002/9780470015902.a0001117.pub2, [26 June 2013].

Kwon, S.J., Seo, M., Yang, H., Kim, S.Y. & Kwak, J. 2010. Application of polyaniline to an enzyme-amplified electrochemical immunosensor as an electroactive report molecule. *Bulletin of the Korean Chemical Society*, 31(11): 3103–3108.

De la Escosura-Muñiz, A., Maltez-da Costa, M., Sánchez-Espinel, C., Díaz-Freitas, B., Fernández-Suarez, J., González-Fernández, Á. & Merkoçi, A. 2010. Gold nanoparticle-based electrochemical magnetoimmunosensor for rapid detection of anti-hepatitis B virus antibodies in human serum. *Biosensors and Bioelectronics*, 26: 1710–1714.

De la Escosura-Muñiz, A. & Merkoçi, A. 2011. A nanochannel/nanoparticle-based filtering and sensing platform for direct detection of a cancer biomarker in blood. *Small*, 7(5): 675–682.

Lambert, N., Fan, T.S. & Pilette, J. 1997. Analysis of PCBs in waste oil by enzyme immunoassay. *The Science of the Total Environment*, 196: 57–61.

Laschi, S., Franek, M. & Mascini, M. 2000. Screen-printed electrochemical immunosensors for PCB detection. *Electroanalysis*, 12(16): 1293–1298.

Laschi, S., Mascini, M., Scortichini, G., Franek, M. & Mascini, M. 2003. Polychlorinated biphenyls (PCBs) detection in food samples using an electrochemical immunosensor. *Journal of Agricultural and Food Chemistry*, 52(7): 1816–1822.

Lee, N.A., Lu, Y., Peterson, J.R., Luais, E. & Gooding, J.J. 2013. Characterisation of bisphenol-a functionalised gold nanoparticles binding to antibodies for immunosensor development. *Meeting Future Food Demands : Security & Sustainability, Conference Proceedings Oral Presentations - Part 1, 13th ASEAN Food, Conference, Singapore, 9-11 September 2013*.

Lequin, R.M. 2005. Enzyme immunoassay (EIA)/enzyme-linked immunosorbent assay (ELISA). *Clinical Chemistry*, 51(12): 2415–2418.

Lermo, A., Fabiano, S., Hernández, S., Galve, R., Marco, M.P., Alegret, S. & Pividori, M.I. 2009. Immunoassay for folic acid detection in vitamin-fortified milk based on electrochemical magneto sensors. *Biosensors and Bioelectronics*, 24: 2057–2063.

Liébana, S., Lermo, A., Campoy, S., Cortés, M.P., Alegret, S. & Pividori, M.I. 2009. Rapid detection of Salmonella in milk by electrochemical magneto-immunosensing. *Biosensors and Bioelectronics*, 25: 510–513.

Lin, K., Lim, W.K., Yee, N.S., Di, S.X. & Bin, L. 2013. Immunosensor characterization using impedance spectroscopy. *Journal of Biosensors & Bioelectronics*, 04(4): http://dx.doi.org/10.4172/2155–6210.1000138 [03 October 2013].

Liu, S., Lin, Q., Zhang, X., He, X., Xing, X., Lian, W. & Huang, J. 2011. Electrochemical immunosensor for salbutamol detection based on CS-Fe_3O_4-PAMAM-GNPs nanocomposites and HRP-MWCNTs-Ab bioconjugates for signal amplification. *Sensors and Actuators, B: Chemical*, 156(1): 71–78.

Luo, Y.C. & Do, J.S. 2004. Urea biosensor based on PANi(urease)-Nafion/Au composite electrode. *Biosensors and Bioelectronics*, 20: 15–23.

Luppa, P.B., Sokoll, L.J. & Chan, D.W. 2001. Immunosensors-principles and applications to clinical chemistry. *Clinica chimica acta*, 314(1-2): 1–26.

Mills III, S.A., Thal, D.I. & Barney, J. 2007. A summary of the 209 PCB congener nomenclature. *Chemosphere*, 68(9): 1603–1612.

Moina, C. & Ybarra, G. 2012. Fundamentals and applications of immunosensors. In: Chiu, N.H.L., Christopoulos, T.K. *Advances in Immunoassay Technology*, InTech, Janeza Trdine 9, 51000 Rijeka, Croatia.

Monk, P.M. 2001. *Fundamentals of electroanalytical chemistry*. Chichester, New York: John Wiley & Sons Ltd.

Moreno-Guzmán, M., González-Cortés, A., Yáñez-Sedeño, P. & Pingarrón, J.M. 2011. A disposable electrochemical immunosensor for prolactin involving affinity reaction on streptavidin-functionalized magnetic particles. *Analytica Chimica Acta*, 692: 125–130.

Moscone, D., Bernardo, R.A, Marconi, E., Amine, A. & Palleschi, G. 1999. Rapid determination of lactulose in milk by microdialysis and biosensors. *The Analyst*, 124: 325–329.

Mousty, C., Galland, B. & Cosnier, S. 2001. Electrogeneration of a hydrophilic cross-linked polypyrrole film for enzyme electrode fabrication. Application to the amperometric detection of glucose. *Electroanalysis*, 13(3): 186–190.

Müller, R. & Lange, E. 1986. Multidimensional sensor for gas analysis. *Sensors and Actuators*, 9: 39–48.

Murphy, L. 2006. Biosensors and bioelectrochemistry. *Current Opinion in Chemical Biology*, 10: 177–184.

Neelgund, G., Hrehorova, E., Joyce, M. & Bliznyuk, V. 2008. Synthesis and characterization of polyaniline derivative and silver nanoparticle composites. *Polymer international*, 57: 1083–1089.

Neves, M.M.P.S., González-García, M.B., Santos-Silva, A. & Costa-García, A. 2012. Voltammetric immunosensor for the diagnosis of celiac disease based on the quantification of anti-gliadin antibodies. *Sensors and Actuators, B: Chemical*, 163: 253–259.

New Zealand Environmental and Conservation Council (ANZECC). 1997. *Identification of PCB-containing capacitors*.

Nicolas-Debarnot, D. & Poncin-Epaillard, F. 2003. Polyaniline as a new sensitive layer for gas sensors. *Analytica Chimica Acta*, 475(1-2): 1–15.

Noah, N.M., Mwilu, S.K., Sadik, O.A., Fatah, A.A. & Arcilesi, R.D. 2011. Immunosensors for quantifying cyclooxygenase 2 pain biomarkers. *Clinica Chimica Acta*, 412(15-16): 1391–1398.

Panfili, G., Manzi, P., Compagnone, D., Scarciglia, L. & Palleschi, G. 2000. Rapid assay of choline in foods using microwave hydrolysis and a choline biosensor. *Journal of Agricultural and Food Chemistry*, 48: 3403–3407.

Park, J.E., Park, S.G., Koukitu, A., Hatozaki, O. & Oyama, N. 2004. Electrochemical and chemical interactions between polyaniline and palladium nanoparticles. *Synthetic Metals*, 141: 265–269.

Park, S.Y., Cho, M.S. & Choi, H.J. 2004. Synthesis and electrical characteristics of polyaniline nanoparticles and their polymeric composite. *Current Applied Physics*, 4: 581–583.

Piro, B., Reisberg, S., Anquetin, G., Duc, H.T. & Pham, M.C. 2013. Quinone-based polymers for label-free and reagentless electrochemical immunosensors: application to proteins, antibodies and pesticides detection. *Biosensors*, 3(1): 58–76.

Prodromidis, M.I. 2010. Impedimetric immunosensors-A review. *Electrochimica Acta*, 55(14): 4227–4233.

Pruneanu, S., Veress, E., Marian, I. & Oniciu, L. 1999. Characterization of polyaniline by cyclic voltammetry and UV-Vis absorption spectroscopy. *Journal of Materials Science*, 34: 2733–2739.

Qureshi, A., Kang, W.P., Davidson, J.L. & Gurbuz, Y. 2009. Review on carbon-derived, solid-state, micro and nano sensors for electrochemical sensing applications. *Diamond and Related Materials*, 18(12): 1401–1420.

Radetic, T. 2011. Fundamentals of scanning electron microscopy and energy dispersive X-ray analysis in SEM and TEM. NFMC Spring School on Electron Microscopy. www.nanotechftm.tmf.bg.ac.rs/images/...school/tamara%20radetic.pdf, [06 May 2014].

Rantanen, J. 1992. Industrial and environmental emergencies; lessons learned. *Organohalogen Compounds*, 10: 291–294.

Reda, S.M. & Al-ghannam, S.M. 2012. Synthesis and electrical properties of polyaniline composite with silver nanoparticles. *Advances in Materials Physics and Chemistry*, 2: 75–81.

Ricci, F., Adornetto, G. & Palleschi, G. 2012. A review of experimental aspects of electrochemical immunosensors. *Electrochimica Acta*, 84: 74–83.

Roberts, M.A. & Durst, R.A. 1995. Investigation of liposome-based immunomigration sensors for the detection of polychlorinated biphenyls. *Analytical chemistry*, 67(3): 482–491.

Rodriguez-Mozaz, S., Marco, M.P., De Alda, M.J.L. & Barceló, D. 2004. Biosensors for environmental applications: future development trends. *Pure and Applied Chemistry*, 76(4): 723–752.

Rogers, K.R. & Williams, L.R. 1995. Biosensors for environmental monitoring: a regulatory perspective. *Trends in Analytical Chemistry*, 14(7): 289–294.

Rosales-Rivera, L.C., Acero-Sánchez, J.L., Lozano-Sánchez, P., Katakis, I. & O'Sullivan, C.K. 2011. Electrochemical immunosensor detection of antigliadin antibodies from real human serum. *Biosensors and Bioelectronics*, 26(11): 4471–4476.

Ross, G. 2004. The public health implications of polychlorinated biphenyls (PCBs) in the environment. *Ecotoxicology and Environmental Safety*, 59: 275–291.

Sadik, O.A. & Van Emon, J.M. 1996. Applications of electrochemical immunosensors to environmental monitoring. *Biosensors & bioelectronics*, 11(8): i–xi.

Sai, V.V.R., Mahajan, S., Contractor, A.Q. & Mukherji, S. 2006. Immobilization of antibodies on polyaniline films and its application in a piezoelectric immunosensor. *Analytical Chemistry*, 78(24): 8368–8373.

Sargent, A. & Sadik, O.A. 1999. Monitoring antibody–antigen reactions at conducting polymer-based immunosensors using impedance spectroscopy. *Electrochimica Acta*, 44: 4667–4675.

Sarma, T.K., Chowdhury, D., Paul, A. & Chattopadhyay, A. 2002. Synthesis of Au nanoparticle-conductive polyaniline composite using H_2O_2 as oxidising as well as reducing agent. *Chemical communications (Cambridge, England)*, (111): 1048–1049.

Sawatsubashi, T., Tsukahara, C., Baba, K., Ohi, E., Shinoda, A. & Miura, N. 2008. Development of new-type rapid analysis technology of polychlorinated biphenyls by using liquid chromatographic clean-up material (polyvinyl alcohol gel). *Journal of Chromatography A*, 1177: 138–149.

Serafín, V., Eguílaz, M., Agüí, L., Yáñez-Sedeño, P. & Pingarrón, J.M. 2011. An electrochemical immunosensor for testosterone using gold nanoparticles - carbon nanotubes composite electrodes. *Electroanalysis*, 23: 169–176.

Shinde, S.S. & Kher, J.A. 2014. A review on polyaniline and its noble metal composites. *International Journal of Innovative Research in Science, Engineering and Technology*, 3(9): 16570–16576.

Silberhorn, E.M., Howard, P.G. & Robertson, L.W. 1990. Critical Reviews in: Carcinogenicity of polyhalogenated biphenyls: PCBs and PBBs. *Critical Reviews in Toxicology*, 20(6): 440–496.

Skládal, P., Kovář, D., Krajíček, V., Šišková, P., Přibyl, J. & Švábenská, E. 2013. Electrochemical immunosensors for detection of microorganisms. *International Journal of Electrochemical Science*, 8: 1635–1649.

Sun, X., Qiao, L. & Wang, X. 2013. A novel immunosensor based on Au nanoparticles and polyaniline/multiwall carbon nanotubes/chitosan nanocomposite film functionalized interface. *Nano-Micro Letters*, 5(3): 191–201.

Sun, Y. & Xia, Y. 2002. Large-scale synthesis of uniform silver nanowires through a soft, self-seeding, polyol process. *Advanced Materials*, 14(11): 833–837.

Tran, Q.H., Hanh Nguyen, T.H., Mai, A.T., Nguyen, T.T., Vu, Q.K. & Phan, T.N. 2012. Development of electrochemical immunosensors based on different serum antibody immobilization methods for detection of Japanese encephalitis virus. *Advances in Natural Sciences: Nanoscience and Nanotechnology*, 3: 015012. doi:10.1088/2043-6262/3/1/015012, [21 February 2015].

Turner, A.P.F. 2000. Biosensors-sense and sensitivity. *Science*, 290(5495): 1315–1317.

Uang, Y.M. & Chou, T.C. 2002. Criteria for designing a polypyrrole glucose biosensor by galvanostatic electropolymerization. *Electroanalysis*, 14(22): 1564–1570.

United States Environmental Protection Agency (EPA). 1976. *PCBs in the United States - industrial use and environmental distribution- Task I, Final report,* Washington D.C.

Wallace, G.G., Spinks, G.M., Kane-Maguire, P., L.A. & Teasdale, P.R. 2009. *Conductive electroactive polymers: intelligent polymer systems*. Boca Raton, Florida, U.S.A: CRC Press (Taylor & Francis Group).

Wanekaya, A.K., Chen, W. & Mulchandani, A. 2008. Recent biosensing developments in environmental security. *Journal of environmental monitoring*, 10(April): 703–712.

Wang, G., Gang, X., Zhou, X., Zhang, G., Huang, H., Zhang, X. & Wang, L. 2013. Electrochemical immunosensor with graphene/gold nanoparticles platform and ferrocene derivatives label. *Talanta*, 103: 75–80.

Wang, X.H., Geng, Y.H., Wang, L.X., Jing, X.B. & Wang, F.S. 1995. Thermal behaviors of doped polyaniline. *Synthetic Metals*, 69: 265–266.

Wei, D. & Ivaska, A. 2006. Electrochemical biosensors based on polyaniline. *Chemical Analysis (Warsaw)*, 51: 839–852.

Wu, J., Tang, J., Dai, Z., Yan, F., Ju, H. & El Murr, N. 2006. A disposable electrochemical immunosensor for flow injection immunoassay of carcinoembryonic antigen. *Biosensors & bioelectronics*, 22(1): 102–108.

Xie, D., Jiang, Y., Pan, W., Li, D., Wu, Z. & Li, Y. 2002. Fabrication and characterization of polyaniline-based gas sensor by ultra-thin film technology. *Sensors and Actuators B: Chemical*, 81(2-3): 158–164.

Xie, Y., Chen, A., Du, D. & Lin, Y. 2011. Graphene-based immunosensor for electrochemical quantification of phosphorylated p53 (S15). *Analytica Chimica Acta*, 699(1): 44–48.

Xue, W., Qiu, H., Fang, K., Li, J., Zhao, J. & Li, M. 2006. Electrical and magnetic properties of the composite pellets containing DBSA-doped polyaniline and Fe nanoparticles. *Synthetic Metals*, 156: 833–837.

Yakuphanoglu, F., Basaran, E., Senkal, B. & Sezer, E. 2006. Electrical and optical properties of an organic semiconductor based on polyaniline prepared by emulsion polymerization and fabrication of Ag/polyaniline/n-Si Schottky diode. *Journal of Physical Chemistry B*, 110: 16908–16913.

Yang, L., Zhao, H., Fan, S., Deng, S., Lv, Q., Lin, J. & Li, C.P. 2014. Label-free electrochemical immunosensor based on gold-silicon carbide nanocomposites for sensitive detection of human chorionic gonadotrophin. *Biosensors & bioelectronics*, 57: 199–206.

Yu, H.W., Lee, J., Kim, S., Nguyen, G.H. & Kim, I.S. 2009. Electrochemical immunoassay using quantum dot/antibody probe for identification of cyanobacterial hepatotoxin microcystin-LR. *Analytical and Bioanalytical Chemistry*, 394: 2173–2181.

Yu, Q., Wang, Q., Li, B., Lin, Q. & Duan, Y. 2014. Technological development of antibody immobilization for optical immunoassays: progress and prospects. *Critical Reviews in Analytical Chemistry*, 45(1): 62–75.

Yu, T., Cheng, W., Li, Q., Luo, C., Yan, L., Zhang, D., Yin, Y., Ding, S. & Ju, H. 2012. Electrochemical immunosensor for competitive detection of neuron specific enolase using functional carbon nanotubes and gold nanoprobe. *Talanta*, 93: 433–438.

Zacco, E., Adrian, J., Galve, R., Marco, M.P., Alegret, S. & Pividori, M.I. 2007. Electrochemical magneto immunosensing of antibiotic residues in milk. *Biosensors and Bioelectronics*, 22: 2184–2191.

3. FABRICATION OF Ag NPs-DOPED PANI TRANSDUCER BY ELECTRODE MODIFICATION AND ITS CHARACTERIZATION

3.1 Introduction

This chapter deals with fabrication and characterization of the electrochemical transducer. For these purposes, both Pt and GC electrodes were considered as substrates. The electrodes comparison in terms of electropolymerization, electrochemical performance and evaluation of the significance of presence of Ag NPs in PANI were undertaken. For further comparison, fabrication and characterization were also done for PANI polymerized in the absence of Ag NPs. The transducer is a component on which an *Ab* is immobilized to make an immunosensor for the analysis of PCBs. Per its definition, it is designed to respond to and convert the specific interaction and formation of the complex between the *Abs* and PCBs into measurable electrical signal.

Chemical modification of electrodes has triggered an interesting consideration in analytical chemistry especially in electrochemical detection of organic compounds and sensor development. Intentional chemical modifications of electrode surface bring about more favourable interactions between an analyte and the surface of electrode by altering the thermodynamic and kinetic properties of the reactants, intermediates or products engaged in redox changes. Such resultant electrodes possess interesting properties that can lay a good foundation for new applications in sensors (Brown & Gray, 2010). These modifications further, ease the process of immobilizing other useful materials such as *Abs* on the electrode surface.

The techniques used to modify electrode surfaces are covalent attachment, spin/drop coating and electropolymerization. Covalent modifications result in strong irreversible covalent attachment that can restrict the reusability of the electrode while the coating results in unstable and easily detached molecules from the electrode surface. Electropolymerization remains the most suitable option for several reasons such as ease and possibility of electrode reproducibility and polymer formation within a short period of time (Brown & Gray, 2010). This technique provides unparalleled strategy of reproducible immobilization of electrochemically active materials onto the electrode surface (Brown *et al.*, 2002). It is a process of generating polymer film layers on interdigital structures.

The three basic methods possible to carry out this process are potentiostatic (constant potential), galvanostatic (constant current) and pulse signal electrolyses. The first method involves keeping the voltage constant between the working and reference electrodes by potentiostat. The three-electrode configuration is required for this process. The potential of the working electrode is ramped between two fixed limits with respect to the reference electrode potential. The polymer layers are created within this voltage range. The thickness of the polymer layer for this method is controlled by the magnitude of the voltage and the time of immersion of electrodes in the solution. The second method consists of keeping the current constant between the working and auxiliary electrodes using a galvanostat. Only a simple two-electrode system is needed for galvanostatic electropolymerization. Here the film thickness is controlled by the current magnitude and the period of plunge of electrodes in the solution.

In the third method, the power supply is a square wave generator with possible set up of frequency, pulse ratio and output signal offset. The thickness of the polymer on the interdigital structure can be controlled by the magnitude of voltage, offset, pulse ratio, frequency of input signal, time of plunge and distance between electrodes. The potentiostatic and pulse signal methods offer satisfactory results for creating polymer layers. The disadvantage with the latter is that many parameters (such as voltage magnitude, frequency, pulse ratio, offset, time of plunge and distance of electrodes) have influence on the entire electropolymerization process unlike the former which is influenced by voltage magnitude and time of plunge of electrodes in the solution. The galvanostatic electropolymerization, on the other hand, does not demonstrate adequately satisfactory results due to the resultant porosity of the polymer layers, rough and uneven surface, and a very narrow current range within which electropolymerization process is controlled (Ling, 1998; Blecha *et al.*, 2007). The potentiostatic method is therefore, preferred for modification of the electrode through electropolymerization, which is achieved using CV. CV reportedly produces uniform and dense layers of PANI on inert electrodes despite many other electrochemical methods (Obaid *et al.*, 2014).

In this chapter, an electrochemical transducer was fabricated by modifying the surfaces of Pt and GC electrodes through electropolymerization of aniline in the absence and presence of Ag NPs. The PANI/Ag NPs modifications were aimed at improving the conductivity, electrochemical and biocompatibility properties of the electrodes. These modifications would further ease the process of immobilizing *Abs* on the transducer.

The fabricated transducers were characterized using spectroscopic, microscopic and electrochemical techniques to study and confirm their structural composition, morphological and electrochemical properties. Physical and electrochemical factors such as surface coverage, film thickness, conductivity and band gap are known to affect the transducer functionality as an electrical transport device and antibody immobilization support (Prodromidis *et al.*, 2000; Leonat *et al.*, 2013; Obaid *et al.*, 2014), therefore, it is vital to study them. For this study, the desirable behaviours of the proposed electrochemical transducer were electrical and electrochemical activity, sensitivity and antibody compatibility. These behaviours are directly influenced by the factors mentioned above.

Spectroscopic characterization involves the use of FTIR technique which provides information about the structural composition, i.e. functional groups of the modifying materials of the transducer. These groups are the identities and finger prints of such materials and are responsible for their characteristic chemical reactions. Determination of these groups is the confirmation of the formation of materials on the electrode surface hence, the measure of the success of electrochemical modification and fabrication. They also give information about the type of interactions and transformations, in terms of bonding, electron transfers or any other form, undergone during modifications which can have direct or indirect effect on the resultant performance of the fabricated transducer. Microscopic studies were done using TEM. It gives insight on the structural and compositional morphology of the modifying materials of the transducer. This goes for the appearance and arrangement of the constituents and the elemental composition. This also affirms the formation of the desired material.

The electrochemical characterization was done by CV technique to determine the physical and electrochemical properties of the Ag NPs and PANI based transducers. Physical properties include surface coverage, film thickness, band gap and stability while electrochemical properties are conductivity and electroreversibility. Surface coverage and film thickness were studied from the fabrication experiments while others were studied from CV experiments in monomer free electrolyte. Surface coverage is one crucial parameter to be taken into account during optimization and modification of electrodes. It is the amount of substrate (in moles) used as a modifier on the electrode surface per area of the electrode surface. The degree of surface coverage on the electrode can directly or indirectly affect the electron transfer kinetics between the adsorbed species and the structure of the underlying electrode, the stability of the sensor and the nature of the diffusion or kinetics limiting the current produced (Prodromidis *et al.*, 2000). This parameter and its significance have been ignored in several previous studies reporting electrode modifications.

In like manner, the thickness of the films deposited on the electrode surface during modification, directly affect the charge which is the measure of electron transfer associated with redox changes (Obaid *et al.*, 2014). In this case, the electron transfer kinetics depends on the amount of modifier deposited on the surface of an electrode and the distance from the surface of the electrode to the surface of the covering layer of the modifying substance. Film thickness also affects the stability of the adsorbed layers of the modifying substance in that beyond a certain limit of the thickness, the molecules of the adsorbed films tend to be weakly attached to the electrode lattice by the weak Van der Waals intermolecular forces with consequent continuous detachment from the multilayer structure (Prodromidis *et al.*, 2000). Stability is the measure of the longevity of life span and usability of the transducer with acceptable reproducibility.

The work reported by Valaski *et al.*, (2002), evidenced the dependence of the film layer morphology on the layer thickness. They showed that films exhibiting smooth morphology with ordered structures, demonstrate improved electrical behaviour due to increased charge carrier mobility. Film thickness also has a strong effect on the activity and stability of the biomolecule (Almeida *et al.*, 1993) which, for the development of an immunosensor, is integrated with the transducer depending on the method used for the biomolecule immobilization. This means that the control of surface coverage and film thickness can ensure good stability and electroactivity of the modified electrode or transducer.

Band gap (Eg) on the other side is the characteristic of a material conductivity. It is the separation between the conduction and valence bands in a molecule. PANI as an appropriate material for active semiconducting layer of a transducer, forms the basis for the place where charge (electrons) is generated, separated and transferred (Leonat *et al.*, 2013). It is therefore, ideal to determine its band gap. Electron transfer depends on the accessibility of the conduction band within a molecule which is determined by the knowledge of the energy levels; highest occupied molecular orbital (HOMO), lowest unoccupied molecular orbital (LUMO) and the band gap between the two levels (Admassie *et al.*, 2006; Leonat *et al.*, 2013). Band gap is not accessible for electrons and its value tells how badly or best the material conducts. Generally, the smaller the gap, the higher the conductivity of the material. One important standard characteristic for electrochemical technique that is used to estimate the HOMO, LUMO and Eg, is cyclic voltammetry (Kulkarni *et al.*, 2004; Andrade *et al.*, 2005). It is an analytical characterization technique appropriate for investigation of any process involving transfer of electrons (Li & Barron, 2010). To the best of our knowledge,

there have not been reports on electrochemical band gap for electrochemically synthesized PANI composites using CV.

Electroreversibility entails the extent at which the electrons involved / transferred in electrochemical process can be the same for the forward reaction and the reverse reaction. This can aid in deduction of whether electrochemical process is reversible, quasi-reversible or irreversible following the diagnostic criteria in table 3.1. Reversibility is an indication of how probable it is to study the behaviour of the transducer in both the forward and reverse directions of CV. In dynamic analytical measurements, such as voltammetric analysis, the systems are under diffusion control as the sole mode of mass transport (Monk, 2001). Diffusion is specifically important in electroanalyses since the conversion reaction only happens at the electrode surface. The current response of redox polymer films is dependent on the magnitudes of diffusion layer thickness and film layer thickness since they determine the extent of diffusion effects. Diffusion layer thickness depends on diffusion coefficient and the experimental time scale (Bott, 2001).

Table 3.1: Summary of electrochemical reactions mechanism diagnostic tests

Reversible	Quasi reversible	Irreversible
Anodic and cathodic peaks $\Delta E = \frac{0.00591}{n}$	Anodic and cathodic peaks broad and widely separated	Anodic or cathodic peaks with small size
Ratio of anodic and cathodic peak currents equals unity (I_{pa}/I_{pc} =1)	Anodic and cathodic peak currents are not always equal	Only one peak is observed
Peak current is directly proportional to square root of scan rate (I_p α $v^{1/2}$)	Peak current is directly proportional to square root of scan rate (I_p α $v^{1/2}$)	Peak current is directly proportional to square root of scan rate (I_p α $v^{1/2}$)
Peak potential, Ep is independent on scan rate, v	Peak potential is dependent on scan rate	Shift of potential with scan rate(dependent on scan rate)

Details of structural, morphological, physical and electrochemical properties of PANI/Ag NPs based electrodes are discussed. All the relevant electroactivities of these modified electrodes are determined and compared with those based on PANI alone. The following section (3.2) details the experimental.

3.2 Experimental

3.2.1 Materials and chemicals

Aniline (99 %, Sigma Aldrich) was pre-distilled and stored refrigerated before use, hydrochloric acid, HCl (32 %), distilled water used for preparation of aqueous solutions, alumina (Al_2O_3) powder (0.05, 0.3, 1.0 µm) (Buhler), ethanol (99 %, analytical grade), N, N - dimethyl formamide (DMF) (99.8 %, analytical grade), silver nanoparticles (Ag NPs) preformed, micro - cloth pad (Buhler) and analytical grade nitrogen gas.

3.2.2 Equipment and apparatus

Computer interfaced with AUTOLAB potentiostat 101 with Nova software was employed for all electrochemical measurements. A three compartment electrochemical cell with Pt (diameter = 1.6 mm) or GC (diameter = 3.0 mm) working electrode (WE), Pt wire auxiliary (counter) electrode (AE) and silver/silver chloride (Ag/AgCl, 3 M KCl) reference electrode (RE) were used for all electrochemical experiments. Ultrasonic cleaner was used for cleaning the WEs. FTIR studies were done using Perkin Elmer model Spectrum 100 series within 400-4000 cm^{-1}. HR-TEM (Tecnai, G2 F20 X-Twin MAT) was used for TEM analysis.

3.2.3 Preparation of electrodes

The WEs were polished with 1.0, 0.3 and 0.05 µm alumina slurries on a wetted polishing micro-cloth pad moving the electrode in a circular motion across the surface of the polishing pad followed by rinsing with distilled water. Rinsing was further done by sonication in ethanol, distilled water and finally in the operative solvent/electrolyte each for 5 minutes using ultrasonic cleaner. The Pt wire auxiliary electrode was cleaned by washing with DMF after polymerization and heating in open flame to remove the polymer. The reference electrode was cleaned with distilled water.

3.2.4 Electrode fabrication

This was achieved by oxidative electropolymerization of 0.1 M aniline in the absence and presence of Ag NPs on Pt and GC electrodes in aqueous solution of acid (1 M HCl) by running 10 cycles of CV scanning the potential from -100 to +1400 mV at 50 mV/s. Prior to the measurement, background CV was run in 1 M HCl. The solution was deoxygenated by running nitrogen gas through the solution for 10 minutes then allowed to gain quiescence for

about 10 seconds before every scan. This was done also for all other electrochemical experiments. A further oxidative sweep was initiated and halted at +400 V to ensure polyaniline was in its conductive emeraldine state at the end of electropolymerization. At the end of electropolymerization, the electrode was washed with excess 1 M HCl and distilled water to remove unpolymerized aniline then allowed to dry in a vacuum oven at room temperature.

3.2.5 Spectroscopic characterization

This was done by obtaining FTIR spectra of the modifying PANI based materials. The samples for FTIR analysis were used directly in powder form by placing on the scan plates and recording the spectra for PANI and PANI/Ag NPs samples at 4000-400 cm^{-1}.

3.2.6 Microscopic characterization

The study of morphologies of PANI and PANI/Ag NPs composite films was accomplished by microscopic imaging using TEM technique. The samples were obtained by the described electropolymerization procedures and were prepared for analysis by taking a small amount of the powder sample into a glass vial. Ethanol was then added to the sample and dispersed by sonication for 5 minutes. The mixture was micro pipetted onto micro plates made of copper and carbon which was mounted on to the microscope for imaging.

3.2.7 Electrochemical characterization of modified electrodes

Electrochemical properties of the fabricated electrode composites were determined and studied using CV voltammograms of the materials (electropolymerization (EP) and characterization in monomer-free (MF) 1M HCl). A summary of equations used in calculations of the parameters is tabulated in Table 3.2. For the MF experiments, CV measurements were run for each electrode (bare (Pt and GC), PANI based (Pt/PANI and GC/PANI) and PANI/Ag NPs based (Pt/PANI/Ag NPs and GC/PANI/Ag NPs) in a MF electrolyte solution scanning the potential from -100 to +1400 mV at 10 mV/s for conductivity studies. For electroreversibility, mass transport and electron transfer kinetics, which were studied from the effect of scan rate on peak current using Randles-Sevcik plots through Randles-Sevcik equation (Table 3.2), scan rates of 10 to 250 mV/s were used. The criteria for electroreversibility were based on the diagnostic tests in table 3.1.

Stability of the composites was studied by the measurement of current as a response of the modified electrodes at intervals of three days for a period of 15 days (3, 6, 9, 12 and 15 days). Each measurement was done in three replicates. Stability was also investigated by solubility studies of PANI and PANI/Ag NPs in some of the common solvents namely; DMF, dimethyl sulphoxide (DMSO), chloroform and tetrahydrofuran.

Table 3.2: Electrochemical parameters and equations utilized in calculations from cyclic voltammograms EP and MF

Parameter	Equation	Reference
Number of electrons (EP)	$W_{1/2PH} = \frac{3.53RT}{nF}$ (3.1)	(Brownson & Banks, 2014)
Surface coverage (mol/cm^2) (EP)	$Q = nFA\Gamma$ (3.2)	(Brown & Gray, 2010)
Film thickness (cm) (EP)	$d = \frac{QM_w}{nFA\rho}$ (3.3)	(Hassan *et al.*, 2012)
Band gap (eV) (MF)	$Eg = e(E_{red}^{onset} - E_{ox}^{onset})$ (3.4)	
Randles-Sevcik equation (MF)	$Ip = (2.69\ x\ 10^5)n^{3/2}AD^{1/2}Cv^{1/2}$ (3.5)	(Monk, 2001)
Sweep potential time (s) (ME)	$t = \frac{E_f - E_i}{v}$ (3.6)	(Brownson & Banks, 2014)
Diffusion layer thickness (MF)	$\delta = [2Dt]^{1/2}$ (3.7)	(Bott, 1996; Brownson & Banks, 2014)

3.3 Results and discussions

This section reports and gives the discussion in depth during electrochemical fabrication of the modified electrodes and their spectroscopic, morphological and electrochemical behaviours which confirm the fabrication and feasibility of their applicability in transduction and as support for *Ab* immobilization.

3.3.1 Oxidative electropolymerization of aniline

The stepwise mechanism of oxidative electropolymerization of aniline monomer to form PANI in HCl acid is outlined in Fig 3.1. It involves the initiation of radical formation, propagation and polymer formation. This aniline polymerization is believed to follow an

electrophilic substitution, whereby according to Sapurina and Shishov, (2012), at pH < 2.5, the process occurs by head-to-tail substitution. For this work, 1 M HCl solution was used as a supporting electrolyte which has pH < 2.5. In the initiation step, aniline monomer is first oxidised at E ≈ 1.0 V during the 1st cycle (Fig 3.2 and 3.3) as it has been observed previously.(Pharhad Hussain & Kumar, 2003; Cătrănescu *et al.*, 2012) This is the formation of aniline reactive cation radicals (Zotti *et al.*, 1988) which normally occurs at higher positive potentials than the redox potentials of PANI (Inzelt, 2008). This was explained by Genies and co-workers for electrophilic substitution of oxidative electropolymerization of aniline. They explained that when the platinum working electrode is clean, the potential is high and aniline is oxidized to nitrenium.

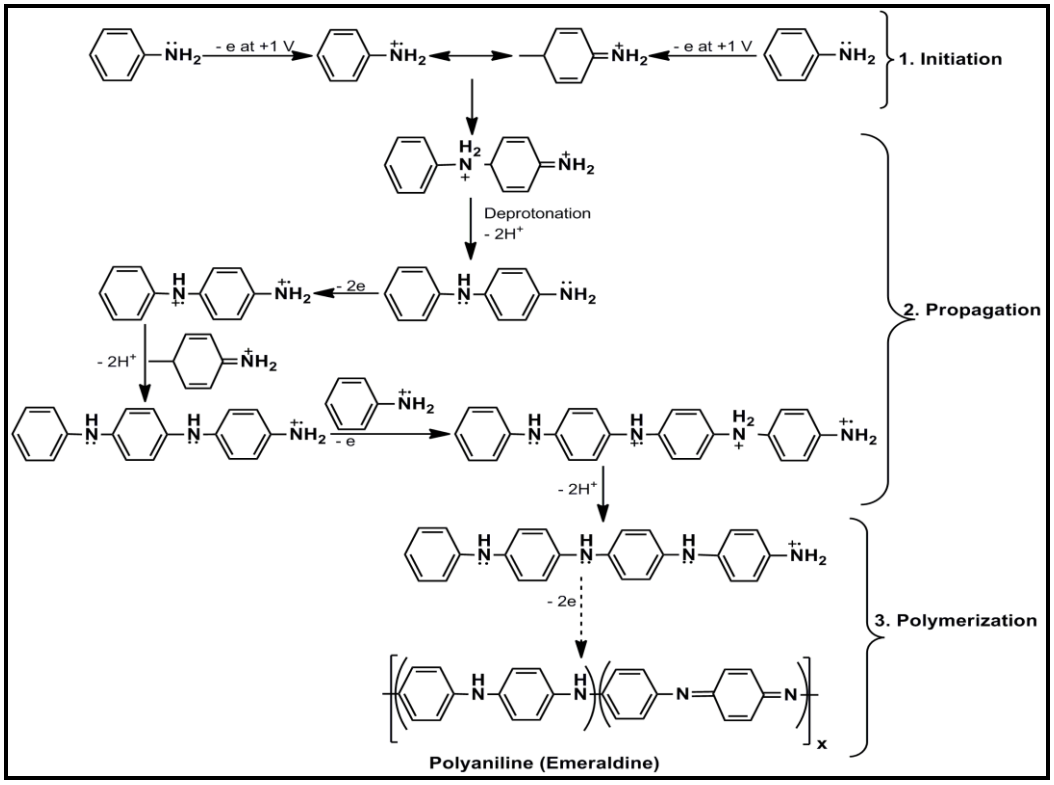

Figure 3.1: Mechanism of oxidative polymerization of aniline

After the formation of some polymer on the electrode, the applied potential in the interface of aniline solution and polymer on the electrode surface is low due to ohmic drop in the polymer film, and the aniline oxidation yields cation radical not nitrenium (Geniès *et al.*, 1988). The radicals attack the para positions of the either protonated, oxidized or even neutral aniline molecules to form aniline anilinium cations. These are further oxidized at the terminal amine group. It is this oxidized amine group that acts as an electrophile that replaces the hydrogen atom of the new aniline oxidized, protonated or neutral molecule at the para position. Once formed, the reactive radicals trigger the chain propagation and polymerization from 2nd up to

the 10th cyclic scan with increasing magnitudes in current. This happens with simultaneous deprotonation and results in formation of regular polyconjugated para-structured polymer chains of high conductivity. The increasing current magnitudes and high conductivity of polymer chains are due to formation of emeraldine salt form of PANI on the electrode surface. Shinde & Kher, (2014) mentioned that the resulting conducting PANI contains more than 95% of the para-substituted aniline fragments connected in head-to-tail structures resulting strictly from regular assembly of aniline units.

3.3.1.1 Formation of PANI

Cyclic polymerization voltammogram for PANI formation on Pt is depicted in Fig 3.2. The initiation peak is observed during the first scan at 1.02 V. This peak appears at higher potentials than those of the redox forms of PANI and is due to the initial oxidation of aniline monomer as explained in the mechanism above (Fig 3.1). Three pairs of peaks characterize the PANI formation voltammogram (three oxidation/ anodic peaks and three reduction/cathodic peaks): pa_1, pc_1; pa_2, pc_2 and pa_3, pc_3 as shown in Fig 3.2. On the anodic side, the first (pa_1) and third (pc_3) peaks are characterized by high currents with pa_1 being the highest. The middle and second peak (pa_2) is ill-defined with lower current. On the reverse side, the corresponding cathodic peaks have $pc_3 > pc_1 > pc_2$ order of intensity. The second peak seems to disappear with increasing scans. The same results were obtained when a GC electrode was used (voltammogram not shown), but the cathodic intensity order was $pc_3 > pc_2 > pc_1$.

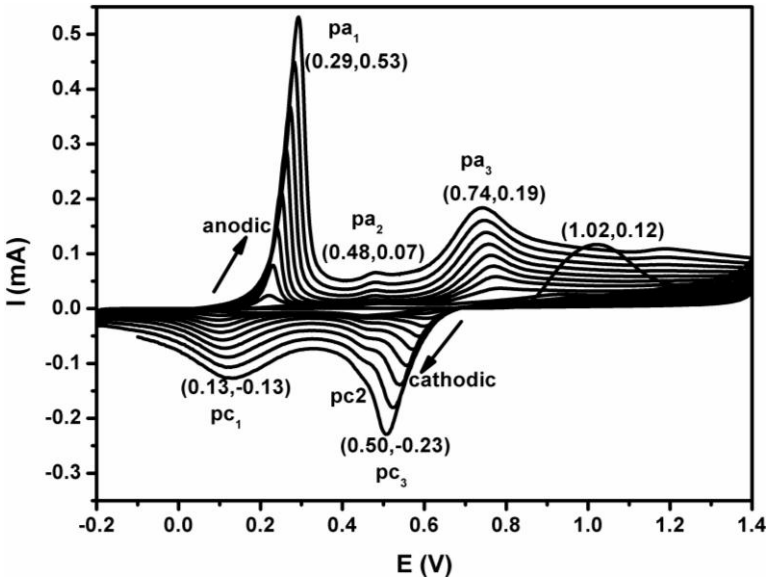

Figure 3. 2: Electropolymerization of aniline monomer in 1M HCl scanned at 50 mV/s on Pt

All polymerization CVs were characterized by potential shifts with successive scans. The first pair of peaks shifts slightly to the higher potentials with increasing scans, while the other two pairs show the opposite shift to the smaller potentials from their first appearance. The maximum shifts from the first 3rd scan to the 10th are 0.07, 0.02, -0.05 and -0.10 V for pa_1, pc_1, pa_3 and pc_3 respectively for both Pt and GC. For pa_2 no observable shift while pc_2 has -0.02 V from the 7th to 9th scans of their appearance for Pt. From their first appearances, peak currents increased with increasing scan. The current changes for Pt were as follows: 0.506, -0.11, 0.151, -0.197, 0.453 and -0.039 mA for pa_1, pc_1, pa_3, pc_3, pa_2, and pc_2 respectively. For GC they were respectively, 1.61, -0.44, 0.46, -0.48 0.58, and -0.97 mA.

In HCl, the three base forms of PANI, leucoemeraldine (LE), emeraldine (EM) and peningraniline (PG) are protonated and doped, forming the corresponding salts. Doping occurs by chloride, Cl^- counter ions which are simultaneously inserted into PANI films to neutralize the positive charge induced by H^+ ions as shown in Fig 3.3 route (1). This doping behaviour of the HCl supporting electrolyte is consistently influenced by the surface electron transfer process (Orata & Buttry, 1987). It is enhanced by the presence of the Cl^- ions which enter the polymer chain during oxidative polymerization and remain in the polymer chains partaking in the redox changes by accepting or contributing one electron (Pharhad Hussain & Kumar, 2003).

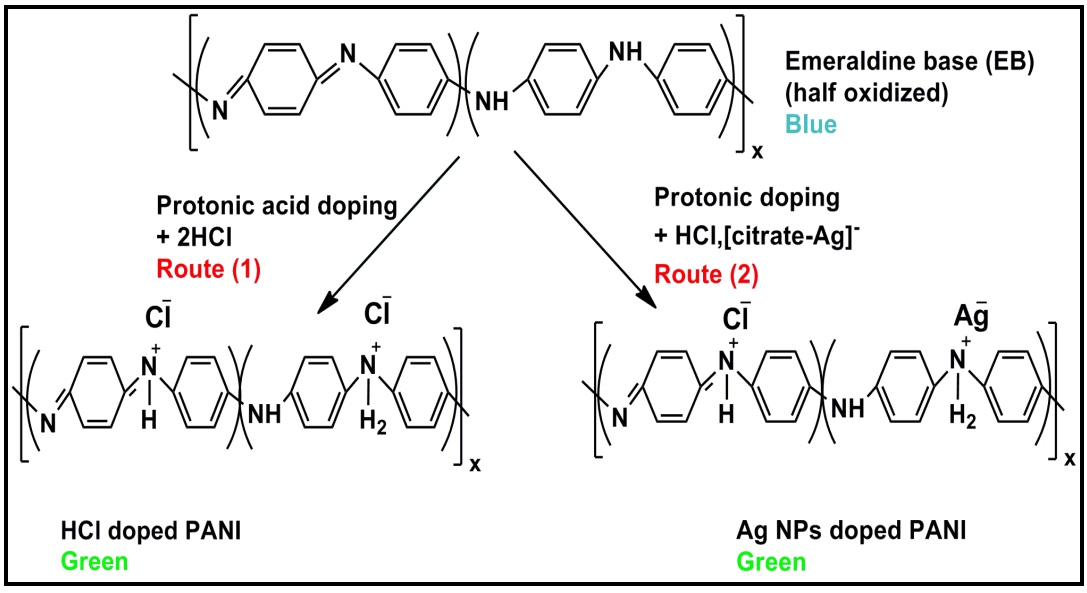

Figure 3. 3: Mechanism showing PANI doping by HCl and AgNPs

3.3.1.2 Formation of Ag NPs-doped PANI

Similar to formation of PANI, when polymerization is carried out in the presence of Ag NPs for formation of PANI/Ag NPs on Pt (Fig 3.4), subsequent PANI characteristic peaks, pa_1 and pc_3 first appeared during the third scan of electropolymerization while pa_2 appeared during the 7th scan. The voltammograms for the formation of Ag NPs-doped PANI (Pt/PANI/Ag NPs) are characterized by three pairs of peaks similar to those for Pt/PANI.

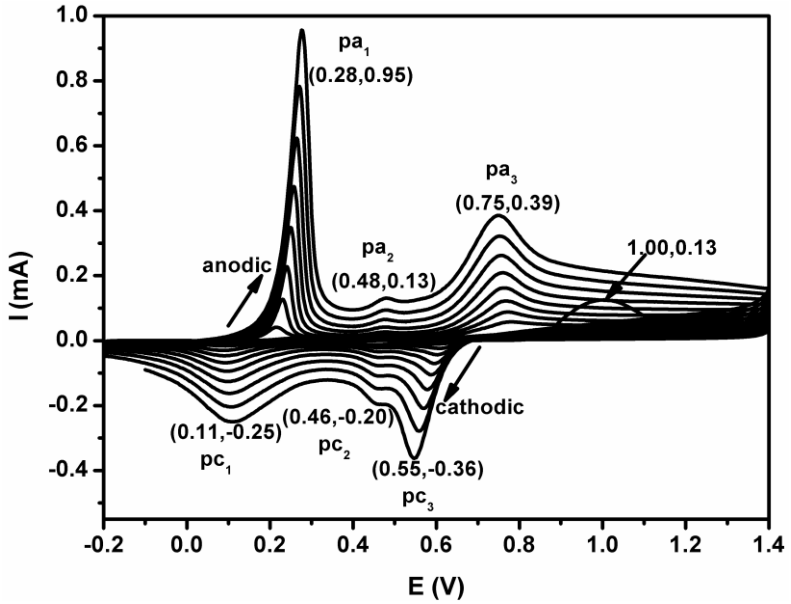

Figure 3. 4: Electropolymerization of aniline in the presence of Ag NPs in 1M HCl scanned at 50 mV/s on Pt

The peaks are similar in appearance and resolution, direction of position shifting and current increase with increasing scans. This can be attributed to the behavioural dominance of PANI in the composite. The potential shifts are: 0.06, 0.014, -0.03, -.008 V and the current shifts: 0.902, -0.216, 0.332 and 0.336 mA for pa_1 pc_1, pa_3 and pc_3 from the 3rd scan. For pa_2 and pc_2 there is no observable potential shift while the current shifts are respectively 0.082 and -0.111 mA from the 7th to 10th scan. Similar behaviour was observed with films on GC with some differences in shifts magnitudes. Potential shifts are: 0.09, 0.03, 0.025, -0.025, -0.025, -0.14 V and currents shifts are: 3.50, -1.46, 1.38, -1.85, 1.53, -2.25 mA. The increase in current with the cyclic voltammetric scan implies the formation and growth of the conducting layers of Ag NPs-doped PANI films on the electrode surface.

The Ag NPs used in this study had been synthesized using trisodium citrate, $Na_3C_6H_5O_7$, as a reducing agent. According to Van Dong *et al.*, (2012), the nanoparticles are stabilized against aggregation by adsorbing citrate ions on their surface thereby rendering the surface a negative charge. The then surface-negatively-charged Ag NPs were adsorbed to the protonated positively charged nitrogen atoms of the emeraldine PANI by electrostatic interactions. In this case, Ag NPs acted in similar manner to the Cl^- ions. The doping of PANI by Ag NPs is believed to occur simultaneously with doping by Cl^- ions and it is understood to follow route (2) in Fig. 3.3 above page 50.

3.3.1.3 Comparison of the formation of PANI and Ag NPs-doped PANI

The initiation peak for the formation of both PANI and Ag NPs-doped PANI has almost the same potential irrespective of the type of electrode while the current with respect to GC is higher than that with Pt (Fig. 3.5 (A) insert). The middle cathodic peak, pc_2 is not observed in Pt/PANI in the 10th scan but appears in the rest of the modified electrode composites. The peaks show some slight shift in the order: Pt/PANI → Pt/PANI/Ag NPs → GC/PANI → GC/PANI/Ag NPs with differences of ± 0.01 to 0.05 V, except the middle peak that has no observable shift.

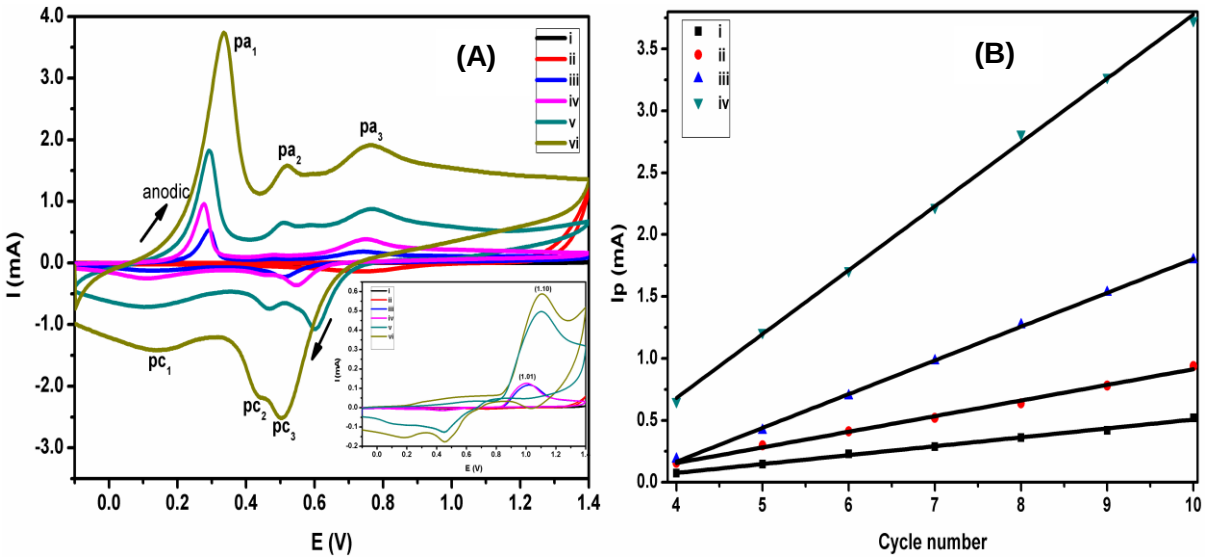

Figure 3.5: CVs for 10th (1st as insert) scans: (i) Pt, (ii) GC, (iii) Pt/PANI, (iv) Pt/PANI/Ag NPs, (v) GC/PANI, (vi) GC/PANI/Ag NPs (A), effect of cycle number on peak current (pa_1): (i) Pt/PANI, (ii) Pt/PANI/Ag NPs, (iii) GC/PANI, (iv) GC/PANI/Ag NPs (B)

The Ag NPs-doped PANI currents are some orders of magnitude larger than those of PANI per electrode in particular, and generally, those based on GC have much higher values as in the order above as Fig 3.5 (A) shows. Fig 3.5 (B) shows linear relationship between the peak current (Ipa_1) and the voltammetric cycle number for the modified Pt and GC electrodes.

This implies that the induction of the formation of PANI composite films on the electrodes follows the same mechanism. The current is the measure of the rate of electropolymerization and its increase with the cyclic voltammetric scan implies the formation and growth of the conducting layers of PANI films on the electrode surface. The variation of current in Pt and GC is predominately due to differences in their surface area; diameter of 1.6 and 3.0 mm for Pt and GC respectively. The linear plots have non-zero intercepts. This observation signifies that the initial electropolymerization process that initiates the diffusion of the monomer to the electrode surface is fast (Calvert *et al.*, 1983). The increased rate of electropolymerization also notes the right choice and importance of HCl as supporting electrolyte, which has limited ion pairing and is capable of promoting mass transport. In that effect, it enhances the mobility of cation radicals to the electrode surface for polymer formation.

In addition, the intercepts of the linear plots for PANI/Ag NPs modified electrodes are further from zero compared to those modified with bulk PANI. Also, the slopes of PANI/Ag NPs modified electrodes exceed those of PANI modified. It is again noted, in particular, that the intercepts and slopes with respect to GC based electrodes are more further away from zero and higher respectively than those with respect to Pt base electrodes. In these cases, it is clear that the conductivity of PANI, hence the transducer, is influenced by the presence of Ag NPs incorporated in the PANI films and by the type of electrode substrate. The presence of Ag NPs within PANI films resulted in increased rate of aniline polymerization and enhanced conductivity. Ag is said to have the highest electrical and thermal conductivities among all the metals (Sun & Xia, 2002). The Ag NPs act as the conductive bridges and junctions between the PANI chains resulting in significant increase in electrical conductivity of the polymer composites (Gangopadhyay & De, 2000; Del Castillo-Castro *et al.*, 2007). Therefore Ag NPs incorporation into PANI result in materials with improved electrical properties (Choudhury, 2009).

Based on the above investigations in relation to PANI and PANI/Ag NPs, PANI conductivity can be summarized as follows: Amongst the three salt forms of PANI, it is only the EM salt that conducts and carries the charge. The conductivity follows the electron hopping mechanism as Dhand *et al.*, (2011) highlighted. First, the two neighbouring nitrogen atoms of EM base, which are not bonded to hydrogens, are protonated to cation radicals and stabilize by forming a polaron such that the radicals are not adjacent. The radicals are electrically neutralized by accepting electrons jumping from the neighbouring neutral nitrogen atoms, which are left as holes or radicals again. This electron transfer movement hence, charge transfer, is the way the EM salt form of PANI conducts electricity.

This movement is not possible with LE and PG even in their salt forms because all their nitrogen atoms have the same electronic environments along the polymer chain. The incorporation of Ag NPs into the polymer resulted in improved PANI conductivity due to high concentration of delocalized electrons because of Ag.

3.3.2 FTIR spectroscopic characterization

The spectra for PANI and PANI/Ag NPs are shown in Fig 3.6. These characterize the PANI composites in terms of the functional groups that determine the structure of the polymer and suggest on the interaction between PANI and Ag NPs. The bands are labelled with the corresponding functional groups with EM for emeraldine and bracketed s and b for stretch and bending respectively. From the spectra, the bands are observed at the wavenumbers 3864, 2682, 2343, 2100, 1704, 1534, 1405 , 1235, 1071 and 924 for PANI and at 3857, 2671, 2343, 2100, 1704, 1528, 1371, 1224, 1065, and 924 cm^{-1} for PANI/Ag NPs. The broad band at 3864 cm^{-1} is assigned to N-H stretch which is near the region 3600 - 3300 cm^{-1} and is normally attributed to the overlap of N-H stretching vibrations. The bands at 2682 and 2343 cm^{-1} are due to NH_2^+ vibrations since the bands ranging between 3000 and 2200 cm^{-1} are generally assigned to the vibrations associated with NH_2^+ which is as a result of some of the NH groups being protonated by the acid to NH_2^+ as stated by Furukawa *et al.*, (1988). This confirms the protonation of PANI by HCl acid.

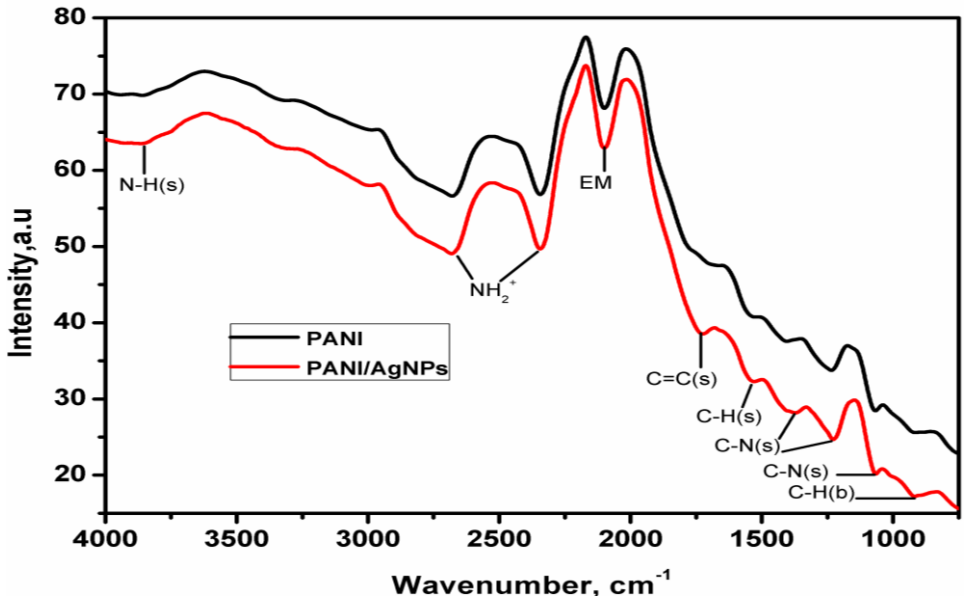

Figure 3.6: FTIR spectra for HCl-doped PANI and PANI/Ag NPs from 4000 to 750 cm^{-1}

The bands overlapping with those for NH_2^+ and additional one at 2100 cm^{-1} present the conduction due to free electrons in an acid doped PANI because according to Cao *et al.*, (1986), the spectral region around 3000 ~ 2000 cm^{-1} is ascribed to emeraldine salt form of PANI. PANI shows C=C stretch bands at 1704 cm^{-1} which usually occur within 1680 - 1640 cm^{-1} (Pharhad Hussain & Kumar, 2003). The band revealed at 1534 cm^{-1} represent C-H stretching in PANI since the absorption bands obtained in 1600 - 1500 cm^{-1} region correspond to C-H stretching in aromatic compounds (Vijayanand *et al.*, 2011). PANI shows C-N stretch bands at 1405 and 1235 cm^{-1}, which are normally within 1400 - 1200 cm^{-1} region of C-N stretch of aromatic amines (Ghadimi *et al.*, 2002; Pharhad Hussain & Kumar, 2003; Vijayanand *et al.*, 2011; Zhang *et al.*, 2012). The band at 1071 cm^{-1} arises due to C-N stretch that habitually occurs in the range 1250 - 1020 cm^{-1} for aliphatic amines and some of them overlap with those of C-N stretch of aromatic amines.

The band at 924 cm^{-1} is assigned to the =C-H bending which appears in the region 1000 - 650 cm^{-1} in alkenes. It is noticed from Fig 3.6 that the two spectra of PANI and PANI/Ag NPs are similar. This signifies that PANI structure is retained in the /PANI/Ag NPs electrode nanocomposite despite some slight shifts in some of the bands. The shift can be due to interfacial electronic interactions between PANI and Ag NPs. The shift favoured the lower wavenumber as seen with N-H, NH_2^+, C-H and C-N (both aromatic and aliphatic) from PANI to PANI/Ag NPs. This redshift could be attributed to the increase in mass of atoms due to the introduction of heavy silver atoms that leads to reduction in absorption frequency or wavenumber according to Hooke's law.

3.3.3 Morphological studies

The electrochemically synthesized PANI and PANI/Ag NPs materials' images were obtained from TEM microscope as shown in Fig 3.7 (A) and (C) for PANI, and (B) and (D) for PANI/Ag NPs. The micrographs (Fig 3.7 (A) and (B)) demonstrate the one dimensional nanofibric tubes characterizing the PANI composites. These have been previously described as the supramolecular structures of PANI and aniline oligomers. The emergence of nanotubes and nanofibres are said to normally accompany the formation of polymers from oligomers (Sapurina & Shishov, 2012). The images demonstrate a remarkable distinction in the morphology of PANI/Ag NPs compared to PANI. The latter is characterized by the amorphous morphology with no regular arrangements (Fig 3.7 (C)) while the former is characterized by the transition from amorphous to organized morphologies (Fig 3.7 (D)). This observation was also previously reported by Park and co-workers (Park *et al.*, 2004).

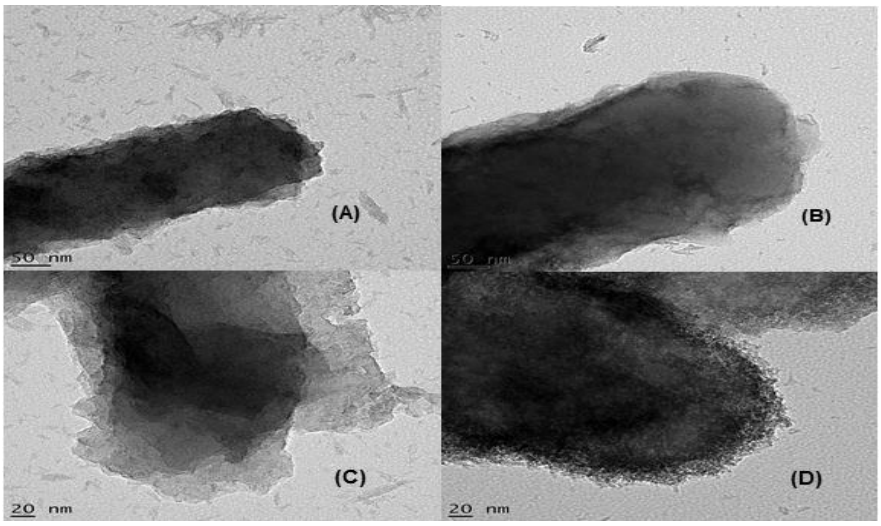

Figure 3.7: TEM images for PANI ((A) and (C)) and PANI/Ag NPs ((B) and (D))

The micrographs do not clearly show the silver particles embedded within the polymer, which are normally dispersed as spherical particles of the metallic silver in the polymer matrix (Neelgund *et al.*, 2008). From the EDS analysis (Fig 3.8 (B)), they appear in close proximity with Cl atoms. They are only highlighted in trace amounts evidenced by the increase in counts from 256 (Fig 3.8 (A)) to 277 (Fig 3.8 (B)). The co-existence of Ag NPs and Cl atoms could result in sacrificing some of the Ag due to obstruction by the chlorines. The presence of both Ag and Cl explains why doping by Ag NPs is believed to occur simultaneously with Cl^- doping. The EDS analyses clearly show the presence of carbon, nitrogen and chlorine atoms for both PANI and PANI/Ag NPs, which constitute the backbone of PANI and protonic acid doping effect on the polymer. This confirms the formation and acid doping of PANI. The presence of copper is contributed by the micro-plates used for sample preparation, which are coated with copper.

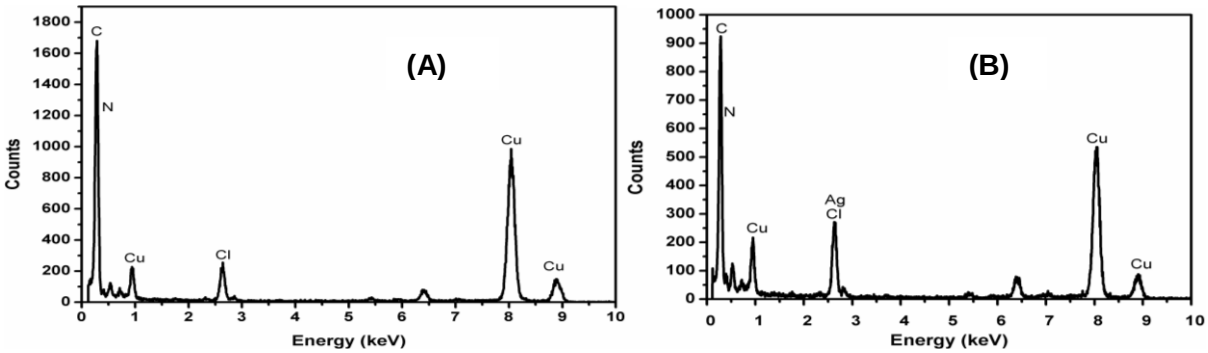

Figure 3.8: EDS analysis for PANI (A) and PANI/Ag NPs (B)

3.3.4 Electrochemical characterization

Electrochemical properties of the modified electrodes, Pt/PANI, Pt/PANI/Ag NPs, GC/PANI and GC/PANI/Ag NPs and the parameters of the modifying substrate affecting such properties were investigated as outlined in section 3.2.7 and are reported in this section. The details of the effects of surface coverage, film thickness and band gap on the electrochemical effectiveness of the electrodes and the effect of Ag NPs incorporation in PANI are provided. Surface coverage and film thickness were determined from EP voltammograms while band gap was determined from voltammograms obtained by MF electrolyte CV scans. The latter was also used to study electroreversibility and stability of the modified electrodes. The determined values for these parameters are summarized in Table 3.3.

Table 3.3: Films properties affecting electrochemical properties (n = 3)

Parameter	Pt		GC	
	PANI	**PAN /Ag NPs**	**PANI**	**PANI /Ag NPs**
Number of electrons (n)	2.00	2.00	2.00	2.00
Surface coverage (r) x 10^{-9} mol/cm^2	3.00	10.0	11.0	29.0
Charge (Q) x 10^{-6} C	6.28	20.9	160.0	401.0
Film thickness(d) x 10^{-8} cm	5.60	18.8	106.6	267.2
Band gap (eV)	0.78	0.61	0.81	0.61

3.3.4.1 Surface coverage, charge and film thickness

Relatively, these values are small, accounting for the smoothness of the PANI composite films on the electrodes. They are comparable to those obtained in the previous studies with ranges in 10^{-9} mol/cm^2 for surface coverage and 10^{-6} cm for film thickness for PANI modified electrodes (Hassan *et al.*, 2012; Orata *et al.*, 2014). This means that the fabricated electrodes are appropriate for applicability in further studies. Comparatively, incorporation of Ag NPs in the polymer resulted in increased surface coverage, charge and film thickness. This could be due to high conducting and catalytic ability of the nanoparticles that facilitate the propagation and polymerization of aniline molecules resulting in layer-by-layer PANI-Ag NPs arrangements. The relative standard deviations (RSD) from the calculated values range between 0.1 and 5%. These are reasonably small and account for reproducibility of electropolymerization of aniline which results in formation of PANI films on the electrode surface.

3.3.4.2 Band gap

The band gap values mean that these materials are semiconducting since both their values are between 0.1 and 3 eV, the band energy gap range for semiconductors (Molapo *et al.*, 2012; Shinde & Kher, 2014). The band gap for Ag NPs-doped PANI is lower than that of PANI. This means that the Ag NPs-doped PANI is more conducting than PANI alone as it was stated from the theory that the smaller the gap, the higher the conductivity of the material (Molapo *et al.*, 2012). It is valid therefore, to believe that Ag NPs played an important role in lowering the gap between HOMO and LUMO energy levels of PANI from around 0.80 to 0.61 eV thereby increasing conductivity irrespective of the electrode type used. This significantly emphasizes the important role of the incorporation of Ag NPs in PANI. The decrease in band gap can be associated with the interactions between PANI and Ag which have been evidenced by the changes in morphological states from amorphous to crystalline and FTIR bands shifts (sections 3.3.2 and 3.3.3 respectively). The study by Reda & Al-ghannam, (2012) suggested that optical absorption is influenced by the morphology of the material. Most reports that have been made on optical band gap of doped and undoped PANI show values above 1 (Kwon & Mckee, 2000; Joshi *et al.*, 2003; Abdulla & Abbo, 2012; Gopalakrishnan *et al.*, 2012; Harish *et al.*, 2012; Molapo *et al.*, 2012; Reda & Al-ghannam, 2012). On the other hand, Chauhan *et al.*, (2011) reported a value of 0.5 eV. All these values were for the polymer composites that were chemically synthesized. The reported values for electrochemical band gap for polymer composites herein reflect relatively reduced energy gaps as the equivalent optical band gaps would be lower than these electrochemical values according to Admassie *et al.*, (2006). They reported that electrochemical band gaps are slightly higher than their optical counterparts with the differences not exceeding ± 0.15 eV.

3.3.4.3 Study of electrochemical behaviour of electrodes

For this purpose, the voltammograms presented in Fig. 3.9 (A) were obtained by running CV for unmodified and modified Pt and GC electrodes in monomer-free 1 M HCl at 10 mV/s. These were used to thoroughly study and compare the electrochemical behaviour of the electrodes and finally the significance of chemical modifications on the Pt and GC electrodes' surfaces with PANI and Ag NPs-doped PANI films. From Fig. 3.9, the Pt bare voltammogram exhibits one anodic peak around 1.32 V and two cathodic peaks around 1.14 and 0.50 V. The anodic peak is due to the oxidation of Pt electrode to Pt oxide. The catholic peak at 1.14 V represents the reduction of Pt oxide while the less pronounced one at 0.50 V is ascribed to the reduction of hydrogen ions by Pt. The positions of Pt peaks are normally

said to be pH dependent. In acidic medium their positions shift towards higher potentials while in basic medium they shift toward lower potentials (Daubinger *et al.*, 2014). Their peaks appeared at around 1.0, 0.75 and 0.15 V respectively in H_2SO_4 at pH 1.0. This study used HCl, pH 0, thus a shift to the higher potentials is shown.

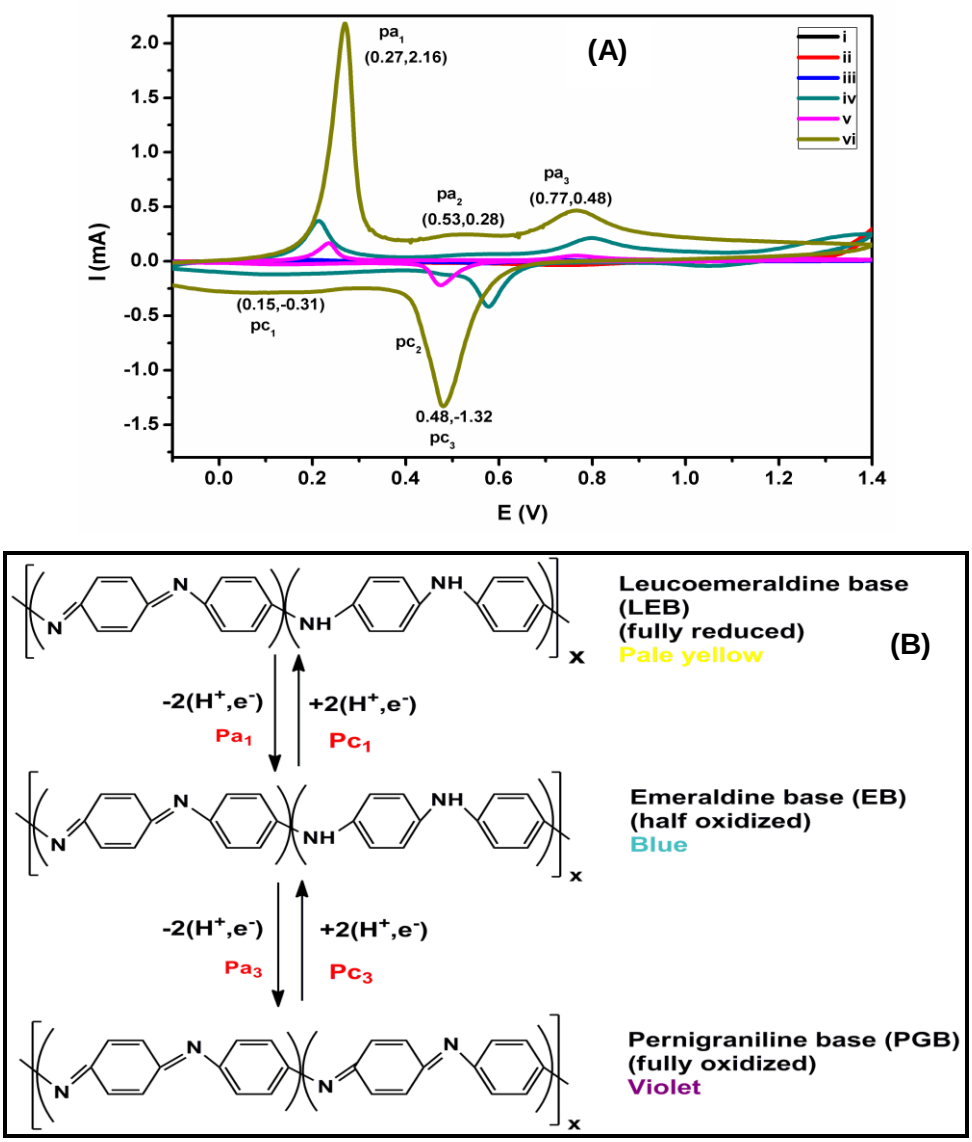

Figure 3.9: **CVs for PANI and PANI/Ag NPs films on Pt and GC in aniline-free 1 M HCl at 10 mV/s: (i) Pt, (ii) GC, (iii) Pt/PANI, (iv) Pt/PANI/Ag NPs, (v) GC/PANI, (vi) GC/PANI/Ag NPs (A), redox transformations of PANI (B)**

The cyclic voltammogram representing PANI modified Pt electrode exhibits characteristic pair of peaks similar to the electropolymerization cyclic voltammograms (Fig. 3.2). These peaks' current magnitudes order is as follows: $pc_3 > pa_1 > pa_3 > pc_1 > pc_2 > pa_2$, notably with the middle pair still ill-defined. The peaks are attributed to the transformations between the three forms of PANI, namely; fully reduced LE, half oxidized EM and fully oxidized PG as clearly demonstrated by the mechanism in Fig. 3.9 (B). The first anodic peak is normally

related to the transition from LE to EM (Motheo *et al.*, 1998). This transformation occurs by deprotonation and oxidation. Deprotonation involves removal of two hydrogen ions while oxidation involves removal of two electrons from LE. The two electrons involved have been calculated and presented in Table 3.3.

The middle (second) anodic peak is due to unwanted intermediate reactions such as the formation of phenazine chains due to crosslinking of PANI chains or reaction of aniline nitrenium cations at ortho positions resulting in a low conducting material (Geniès *et al.*, 1988; Sapurina & Shishov, 2012) or it is due to the oxidative degradation of PANI (Cătrănescu *et al.*, 2012). This ill-defined peak here appears more smaller than the first and the third peaks, the reason being that the formation of such intermediates or unwanted oxidation of PANI are not favoured in acidic medium (Sapurina & Shishov, 2012). In the work done by Tawde and the group, for example, this peak was initially not visible, but came about due to instability of the polymer in a prolonged usage and measurements (Tawde *et al.*, 2002). This validates our terms that it is unwanted.

The third peak is the formation of fully oxidized PG from half-oxidized EM. On the reverse case, the cathodic side, the peaks are associated with the reduction transformations from PG to the fully reduced LE, implying that the polymer is in its reduced form at the end of polymerization (Heinze *et al.*, 2010) if the scan is ended at the starting potential.

According to Genies and colleagues, the intermediates and PANI oxidative degradation exist at the expense of the EM as they explained that the intensities of the first and third peaks are inversely proportional to that of the second peak (Geniès *et al.*, 1988). Notably, in this work, the middle peak is less pronounced, giving more significance to the desired EM. This is supported by the trends of increasing current magnitudes observed above, that favour the existence of EM form of PANI as pa_1 and pa_3 are the highest in magnitude. This behaviour has also been observed in Fig 3.2 section 3.3.1. The voltammograms showed the favour in formation of the doped EM represented by transition in the anodic phase, LE-EM, and that in the cathodic phase, PG-EM. The formation of EM, results in high magnitudes in current because doped EM is the only conducting form of PANI.

In the presence of Ag NPs embedded in the polymer films, three anodic peaks and two cathodic peaks prevail for Pt (Fig 3.9 (A)). The first peak is the formation of EM and the second one the formation of PG and cathodic peaks correspond to them. The third anodic peak denotes the irreversible oxidation of Pt. This peak is not visible with Pt/PANI. The middle undesired peak representing the destructive oxidation of PANI is not visible in the

presence of Ag NPs. This could mean that the presence of Ag NPs stabilizes and strengthens the polymer against possible side reactions. The peaks have slight shifts in similar manner to the electropolymerization.

From bare Pt electrode to PANI modified Pt and further to Ag NPs-doped PANI modified Pt, there is significant enhancement of the conductivity evidenced by the increased currents. This indicates that modified Pt behaves differently from the bare electrode implicating the significance of PANI on Pt and more importantly, the effect of Ag NPs embedded in the PANI films resulting in more enhanced electroactivity. The electroactivity (conductivity) increases in the order: Pt < Pt/PANI < Pt/PANI/Ag NPs. On the bases of GC as the modification substrate, the CV for the electrode is characterized by the one cathodic peak at around 0.8 V which could be due to the reduction of hydrogen. The other electrode composite (GC/PANI and GC/PANI/Ag NPs) exhibit the same voltammetric behaviour similar to their Pt based counterparts despite that the GC based films evidently show significant increase in current. The overall conductivity order then is: Pt < GC < Pt/PANI < Pt/PANI/Ag NPs < GC/PANI < GC/PANI/Ag NPs.

3.3.4.4 Effect of scan rate

The effect of the rate of sweep potential scan was studied by the variation of the sweep rate of the potential applied on the modified electrodes in a MF electrolyte solution and the current response was noted.

(a) PANI modified electrodes

Fig 3.10 illustrates the current response of Pt/PANI electrode as a result of increasing the scan rates as shown. The current increased in magnitude with the increasing scan rate. At lower scan rates, (10 - 20 mV/s) three pairs of redox peaks were observed. With increase in scan rate, the first anodic peak shifts while the middle peak disappears resulting in a shift of the third anodic peak to the lower potential which further disappears until only one anodic peak prevails. On the other hand, the first cathodic peak disappears with increasing scan rate as the third cathodic peak shifts to the lower potential until only one cathodic peak remains. This observable potential shift with increase in scan rate, consequently increasing the peak separation (ΔEp), is linked to the electron delocalization along the polymer backbone and repulsive interactions between redox centres (Larsson & Sharp, 1995) and small differences in the local environments of different redox centres, resulting in rise to range of redox potentials (Abruna, 1988).

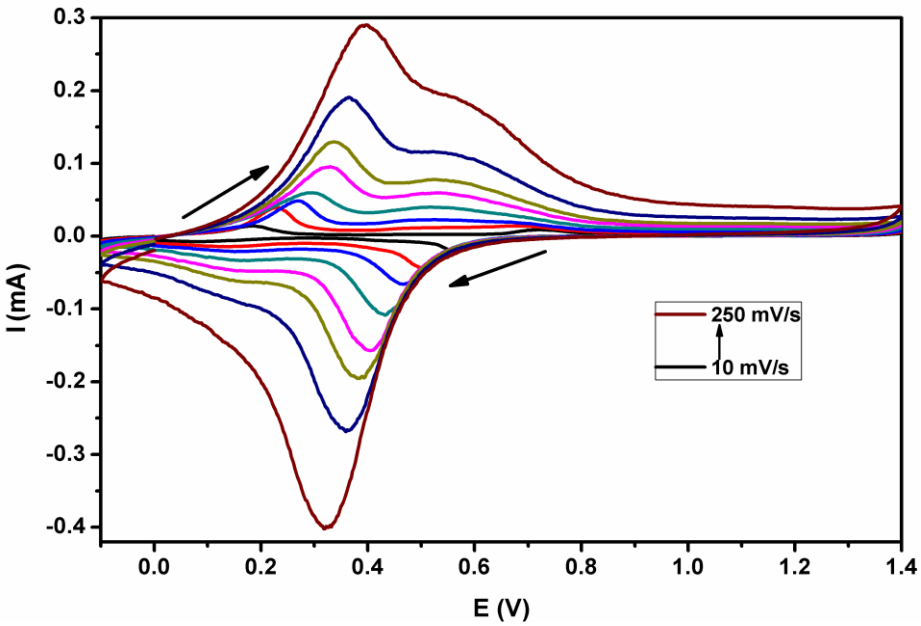

Figure 3.10: CVs at various scan rates for Pt/PANI in aniline-free 1 M HCl

The increase in ΔEp with scan rate is associated with kinetic limitations of charge transfer between the redox centres within the polymer film (Brown & Gray, 2010). This behaviour was observed with HCl as a supporting electrolyte in the study conducted by Hassan *et al.*, (2012) on dopant effect in electropolymerization of aniline. Pa_1 and pc_3 have higher current magnitudes than the rest of the peaks and are maintained up to the last highest scan rate. This proves the auto-catalytic electropolymerization of aniline (Inzelt, 2008; Wallace *et al.*, 2009). It also confirms that the peaks represent the formation of doped EM, the conducting form of PANI. The same current response behaviour was observed with GC/PANI except that it had higher current magnitudes.

(b) PANI/Ag NPs modified electrodes

The voltammograms obtained by incorporation of AgNPs in PANI have more defined and long-lived peaks as shown in Fig 3.11 (for Pt substrate). The peaks are maintained longer with increase in scan rate as compared to those of the sole PANI which disappear faster. The peaks still shift positions in the same manner as in PANI. The first anodic peak shifts to the higher potentials with ΔEp ranging from 0.04 to 0.13 V while the second does not show significant shift. The third cathodic peak shifts negatively with ΔEp range -0.1 to -0.17 V. The peak current also increase in magnitude with scan rate. Exept the differences in magnutude of ΔEp and peak currents, the Ag NP-doped PANI based on GC exhibits the same behaviour change pattern.

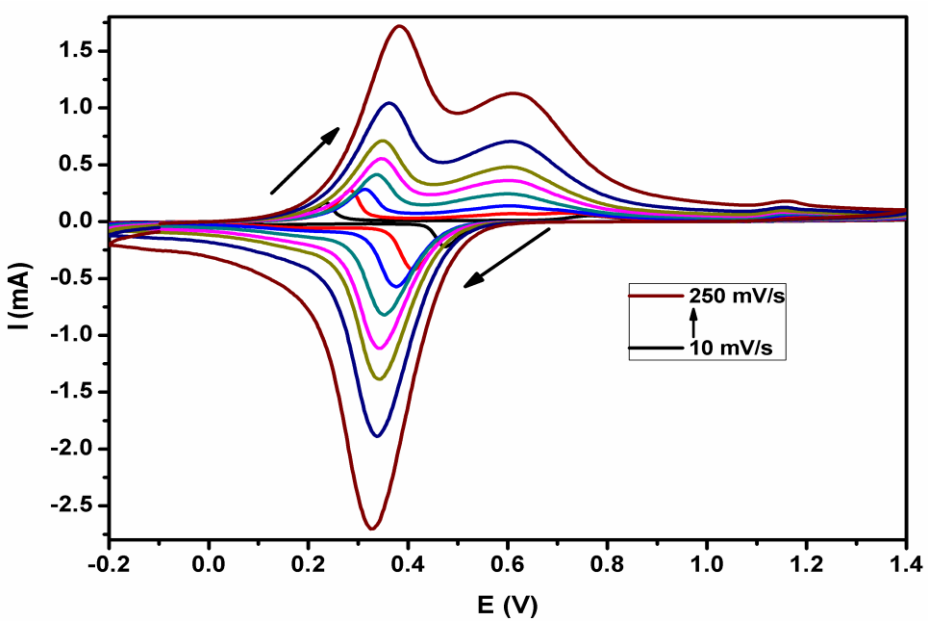

Figure 3.11: CVs at various scan rates for Pt/PANI/Ag NPs in aniline free 1 M HCl

3.3.4.5 Randles-Sevcik linear plots

For a quiescent solution that contains an electrolyte, diffusion is the sole means for an electroactive species to approach the electrode. This implies that the reaction at the electrode surface is diffusion controlled, which is the mass transport mechanism of aniline monomer to the surface of the electrode across the concentration gradient during polymerization. Doping of PANI occurs at nitrogen positions and depends on the protonation by hydrogen ion (H^+) (Motheo *et al.,* 1998). The protonation results in formation of the nitrogen cation radicals. For EM doping, which occurs during the first anodic peak, when the first anodic peak current is plotted against the square root of the scan rate, the Randles-Sevcik linear plot is observed (Fig. 3.12). This means protonation of PANI chains by the supporting electrolyte in the absence and presence of Ag NPs is controlled by H^+ diffusion. The diffusion coefficients of H^+ were calculated from the slopes of Randle Sevcik plots using equation (3.5) for both PANI and PANI/Ag NPs modified electrodes. The values of diffusion coefficient were used to determine the thickness of diffusion layer according to equation (3.7). Their calculated values (with RSD range of 1.5 - 4%) are summarized in Table 3.4. The effect of diffusion coefficient, diffusion layer thickness and film thickness on the behaviour of the electrodes was expressed using a dimensionless variable: $\mathbf{Dt/d^2}$. It was found to be larger than 1 for all the electrode composites. This is ascribed to a thin-layer behaviour of diffusion and it is the ideal behaviour of cyclic voltammetry of redox polymers (Bott, 2001).

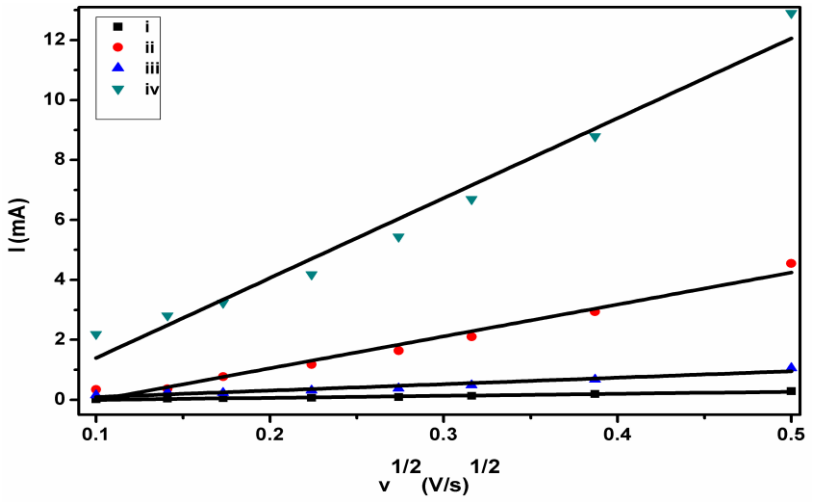

Figure 3.12: Randles-Sevcik linear plots for modified Pt and GC: (i) Pt/PANI, (ii) Pt/PANI/Ag NPs, (iii) GC/PANI, (iv) GC/PANI/Ag NPs

From both the effect of scan rate and Randle Sevcik studies for PANI and PANI/Ag NPs based electrodes for the first anodic peak, the ratios of the peak currents, I_{pa}/I_{pc}, are different from unity (1). Secondly, the peak potentials, E_p, are dependent on the scan rate, v, for example, E_{pa} increases with v and E_{pc} decreases with v, consequently shifting the position of current maxima. Lastly, the peak currents increase linearly with the scan rate, I_p α $V^{1/2}$. Based on these diagnostic tests according to Table 3.1, the electrochemical transformations of PANI based materials follow the transitional trend of electrochemical systems from reversible to quasi-reversible electron transfer reactions according to Brown and Gray, (2010). Additionally, the gradients of the Randles-Sevcik linear plots and diffusion coefficient for PANI/Ag NPs based elctrodes are much greater in magnitude than those based on PANI. This is indicative of high rate of diffusion and electron transfer within the polymer films in the presence of nanoparticles therefore, emphasizing the significance of Ag NPs in the polymer films.

Table 3.4: Diffusion parameters for the modified electrodes using pa_1 (n = 3)

Parameter	Pt		GC	
	PANI	PANI/Ag NPs	PANI	PANI/Ag NPs
Correlation coefficient, R^2	0.96	0.93	0.97	0.97
Slope, M x 10^{-4}	6.76	21.50	106.50	266.40
Diffusion coefficient, (D)10^{-15} cm^2 s^{-1}	1.57	16.30	3887.0	24320.0
Sweep potential time, (t) s	7.32	9.28	6.71	7.24
Diffusion layer thickness, (δ) x 10^{-7} cm	1.51	5.50	72.20	187.70
Dimensionless variable: **Dt/d^2**	4.00	4.30	23.00	24.70

In accordance with the findings above, GC based electrodes perform better than those based on Pt. This is evidenced by the high values of the surface concentrations, charge, the slopes of the electropolymerization process and Randles plots, the diffusion coefficients and lastly enhanced current response. These signify the high rates of polymer formation and electron transfer. These could be due to the fact that the surface area of the GC (0.071 cm^2) is much more than that of the Pt (0.0201 cm^2). The larger area contributes to high concentration of the polymer molecules being on/closer to the surface of the electrode thereby enhancing smoother surface for better performance. According to Valaski *et al.*, (2002), films exhibiting smooth morphology with ordered structures, demonstrate improved electrical behaviour due to increased charge carrier mobility. Therefore, GC/PANI/Ag NPs represents the best transducer for further applications.

3.3.4.6 Stability of PANI/Ag NPs

The stability of the fabricated transducer was assessed by measuring the current response with CV over a period of 15 days. The peak current for the first anodic peak (I_{pa1}) was used for the assessment and was used to determine the percentage current (I_R) relative to the initial first day peak current. The measurements were done in three replicates and the RSD ranged between 2 - 4.5% which implies good intra-measurements repeatability. Fig 3.13 shows the plot of I_R against the number of days for both PANI and PANI/Ag NPs. The peak current decreases gradually with increase in period for both the electrode composites at almost the same rate for the first 10 days. After 10 days, the rate of decrease in peak current obtained with PANI/Ag NPs is lower than that with PANI.

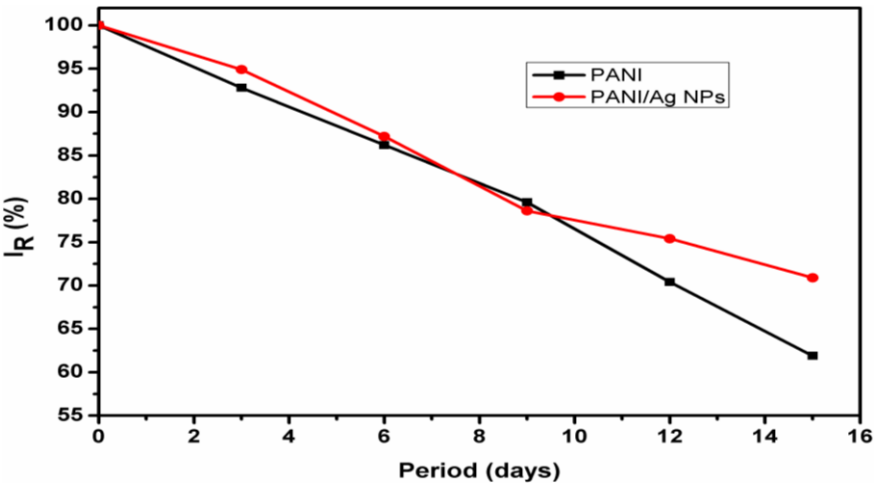

Figure 3.13: Stability of PANI and PANI/Ag NPs modified electrodes based on relative peak current (IR) over 15 days

It is further observed that after 15 days, PANI/Ag NPs modified electrode still recorded above 70% while the one modified with PANI recorded at least 60% of the initial current. The normal EM peak (I_{pa1}) and the dark-green colour of PANI were observed over the period of 15 days. The fact that the rate of decrease in current is the same for both composites could mean that Ag NPs do not have significant effect on the stability of the electrode composite, which is constituted mostly by PANI. In this case, the stability is dependent on PANI, which then degrades periodically. On the other hand, with effect from 10 days, as PANI continues to degrade, it could be understood that the conductivity of Ag NPs becomes predominant. For this reason, Ag NPs could adequately maintain the current resulting in the observed difference in peak current. This resulted with electrodes modified with PANI/Ag NPs and undoped PANI recording 70% and 60% respectively after 15 days. The maintenance of the green colour of the PANI composite throughout the entire period of 15 days was indicative that PANI in its conducting desired EM form was still present. This was evidenced by the exhibition of the EM anodic peak over the 15-day period despite the observed decrease in peak current.

Furthermore, stability was investigated by dissolution studies by dissolving the PANI and PANI/Ag NPs in some common organic solvents. The polymer did not dissolve in any of the solvents. This agrees with the reports that PANI in its emeraldine salt form is not soluble in aqueous solutions and most of the common organic solvents because of the presence of cationic charges present in the polymer backbone. The authors indicated that it is only the emeraldine base (EB) form of PANI that dissolves in the mentioned organic solvents because of the absence of the cationic charges (Molapo *et al.*, 2012). Additionally, Abdulla and Abbo, (2012) indicated that PANI resulting from electropolymerization, the method used in this study, is insoluble. These claims confirm that emeraldine salt form of PANI, the desired form, was successfully synthesized and expectedly environmentally stable.

3.4 Conclusion

In summary, the fabrication of electrochemical transducer has been successfully achieved through modifications made on the Pt and GC using undoped and AgNPs-doped PANI. The characteristic features borne by the polymer films on the electrode have proved the success of electrode modification. PANI based electrodes showed satisfactory electrochemical activity, reversibility, diffusion and electron transfer kinetics. The surface coverage and electrochemical band gap of the transducer, which have been rarely or not been reported before, have been clearly discussed with their influence on the effectiveness of the transducer.

This work has shown successful synthesis of the conducting emeraldine form of PANI. Ag NPs-based PANI thin films exhibit enhanced conductivity compared to bulk PANI counterpart. A comparison made amongst the three electrodes; Pt, Pt/PANI and Pt/PANI/Ag NPs showed that the conductivity of the three electrodes is in the order Pt < Pt/PANI < Pt/PANI/Ag NPs. A similar order was observed for GC based modification. The higher surface area of GC resulted in improved modification, accompanied by high conductivity, current and surface coverage. The effect of Ag NPs doping was evidenced by improved conductivity and higher currents. These improvements in Ag doped films are attributed to ordered arrangement of the polymer, layer-by-layer stacking with Ag NPs and the smooth surface of the modified film. The data obtained clearly indicates the potential applications of PANI/Ag NPs as a transducer material for electrochemical immunosensor construction since it exhibits electroreversibility and high conductivity that can amplify the response and, enhance the sensitivity and selectivity of the immunosensor. The transducer of choice is GC/PANI/Ag NPs because it showed superior qualities from the other studied transducers.

3.5 References

Abdulla, H.S. & Abbo, A.I. 2012. Optical and electrical properties of thin films of polyaniline and polypyrrole. *International Journal of Electrochemical Science*, 7: 10666–10678.

Abruna, H.D. 1988. Coordination chemistry in two dimensions: chemically modified electrodes. *Coordination Chemistry Reviews*, 86: 135–189.

Admassie, S., Inganäs, O., Mammo, W., Perzon, E. & Andersson, M.R. 2006. Electrochemical and optical studies of the band gaps of alternating polyfluorene copolymers. *Synthetic Metals*, 156(7-8): 614–623.

Almeida, N.F., Beckman, E.J. & Ataai, M.M. 1993. Immobilization of glucose oxidase in thin polypyrrole films: Influence of polymerization conditions and film thickness on the activity and stability of the immobilized enzyme. *Biotechnology and Bioengeneering*, 42: 1037–1045.

Andrade, B.W.D.Õ., Datta, S., Forrest, S.R., Djurovich, P., Polikarpov, E. & Thompson, M.E. 2005. Relationship between the ionization and oxidation potentials of molecular organic semiconductors. *Organic Electronics*, 6: 11–20.

Blecha, T., Hamáček, A. & Řeboun, J. 2007. Creating of thin film sensor layer by electropolymerization. *ElectroScope*, 1: 1–5.

Bott, A.W. 2001. Electrochemical techniques for the characterization of redox polymers. *Current Separations*, 19(3): 71–75.

Bott, A.W. 1996. Mass transport. *Current Separations*, 14(3-4): 104–109.

Brown, K. & Gray, S. 2010. Cyclic voltammetric studies of electropolymerized films based on ruthenium (II/III) bis (1, 10 phenanthroline) (4-methyl-4'vinyl-2,2'-bipyridine). *International Journal of Chemistry*, 2(2): 3–9.

Brown, K.L., Shaw, J., Ambrose, M. & Mottola, H.A. 2002. Voltammetric, chronocoulometric and spectroelectrochemical studies of electropolymerized films based on Co (III/II) - and Zn (II) -4 , 9 , 16 , 23-tetraaminophthalocyanine : effect of high pH. *Microchemical Journal*, 72: 285–298.

Brownson, D.A.C. & Banks, C.E. 2014. Interpreting electrochemistry. In Brownson, D.A.C. & Banks, C.E. *The Handbook of Graphene Electrochemistry*. London: Springer: 23–77.

Calvert, J.M., Schmehl, R.H., Sullivan, B.P., Facci, J.S., Meyer, T.J. & Murray, R.W. 1983. Synthetic and mechanistic investigations of the reductive electrochemical polymerization of vinyl-containing complexes of iron(II), ruthenium(II), and osmium(II). *Inorganic Chemistry*, 22(17): 2151–2162.

Cao, Y., Li, S., Xue, Z. & Guo, D. 1986. Spectroscopic and electrical characterization of some aniline oligomers and polyaniline. *Synthetic Metals*, 16(3): 305–315.

Cătrănescu, R., Bobîrnac, I., Crişan, M., Cojocaru, A. & Maior, I. 2012. Studies regarding electrochemical polymerization of aniline in ionic liquid and polymer properties. *UPB Scientific Bulletin, Series B: Chemistry and Materials Science*, 74(1): 1454–2331.

Chauhan, N.P.S., Ameta, R., Ameta, R. & Ameta, S.C. 2011. Thermal and conducting behaviour of emeraldine base (EB) form of polyaniline (PANI). *Indian Journal of Chemical Technology*, 18: 118–122.

Choudhury, A. 2009. Polyaniline/silver nanocomposites: dielectric properties and ethanol vapour sensitivity. *Sensors and Actuators B: Chemical*, 138(1): 318–325.

Daubinger, P., Kieninger, J., Unmüssig, T. & Urban, G.A. 2014. Electrochemical characteristics of nanostructured platinum electrodes - a cyclic voltammetry study. *Physical chemistry chemical physics : PCCP*, 16: 8392–8399.

Del Castillo-Castro, T., Larios-Rodriguez, E., Molina-Arenas, Z., Castillo-Ortega, M.M. & Tanori, J. 2007. Synthesis and characterization of metallic nanoparticles and their incorporation into electroconductive polymer composites. *Composites Part A: Applied Science and Manufacturing*, 38: 107–113.

Dhand, C., Das, M., Datta, M. & Malhotra, B.D. 2011. Recent advances in polyaniline based biosensors. *Biosensors and Bioelectronics*, 26(6): 2811–2821.

Furukawa, Y., Ueda, F., Hyodo, Y. & Harada, I. 1988. Vibrational spectra and structure of polyaniline. *Macromolecules*, 21: 1297–1305.

Gangopadhyay, R. & De, A. 2000. Conducting polymer nanocomposites: a brief overview. *Chemical Materials*, 12: 608–622.

Geniès, E.M., Lapkowski, M. & Penneau, J.F. 1988. Cyclic voltammetry of polyaniline: interpretation of the middle peak. *Journal of Electroanalytical Chemistry and Interfacial Electrochemistry*, 249(1-2): 97–107.

Ghadimi, F., Safa, K.D., Massoumi, B. & Entezami, A.A. 2002. Polyaniline doped with sulphosalicylic, salicylic and citric acid in solution and solid-state. *Iranian Polymer Journal*, 11(3): 159–166.

Gopalakrishnan, K., Elango, M. & Thamilselvan, M. 2012. Optical studies on nano-structured conducting polyaniline prepared by chemical oxidation method. *Archives of Physics Research*, 3(4): 315–319.

Harish, C., Sreeharsha, V.S., Santhosh, C., Ramachandran, R., Saranya, M., Mudaliar, T., Govardhan, K. & Grace, A.N. 2012. Synthesis of polyaniline/graphene nanocomposites and its optical, electrical and electrochemical properties. *Advanced Science, Engineering and Medicine*, 4: 1–9.

Hassan, H.K., Atta, N.F. & Galal, A. 2012. Electropolymerization of aniline over chemically converted graphene-systematic study and effect of dopant. *International Journal of Electrochemical Science*, 7: 11161–11181.

Heinze, J., Frontana-uribe, B.A. & Ludwigs, S. 2010. Electrochemistry of conducting polymers persistent models and new concepts. *Chemical Reviews*, 110(8): 4724–4771.

Inzelt, G. 2008. *Conducting polymers: a new era in electrochemistry*. *Berlin Heidelberg: Springer-Verlag.*

Joshi, G.P., Saxena, N.S., Sharma, T.P., Dixit, V. & Misra, S.K. 2003. Bandgap determination of chemically doped polyaniline materials from reflectance measurements. *Indian Journal of Pure & Applied Physics*, 41: 462–465.

Kulkarni, A.P., Tonzola, C.J., Babel, A. & Jenekhe, S.A. 2004. Electron transport materials for organic light-emitting diodes. *Chemical Materials*, 16(23): 4556–4573.

Kwon, O. & Mckee, M.L. 2000. Calculations of band gaps in polyaniline from theoretical studies of oligomers. *Journal of Physical Chemistry B*, 104: 1686–1694.

Larsson, H. & Sharp, M. 1995. Charge propagation in $[Os(bpy)_2(PVP)xCl]Cl$ polymers. An example of mean field behavior in a system with constrained diffusion of redox sites. *Journal of Electroanalytical Chemistry*, 381: 133–142.

Leonat, L., Sbârcea, G. & Brânzoi, I.V. 2013. Cyclic voltammetry for energy levels estimation of organic materials. *U.P.B. Scientific Bulletin Series B*, 75(3): 111–118.

Li, X. & Barron, A.R. 2014. Introduction to cyclic voltammetry measurements. In Barron, A.R. (Eds.). *Physical Methods in Chemistry and Nano* Science. OpenStax-CNX, http://cnx.org/content/col10699/1.20: 229–238.

Ling, X. 1998. Formation of Polymer Coatings by Electropolymerization. Unpublished PhD thesis. University of Waterloo, Waterloo, Ontario, Canada.

Molapo, K.M., Ndangili, P.M., Ajayi, R.F., Mbambisa, G., Mailu, S.M., Njomo, N., Masikini, M., Baker, P. & Iwuoha, E.I. 2012. Electronics of conjugated polymers (I): polyaniline. *International Journal of Electrochemical Science*, 7: 11859–11875.

Monk, P.M. 2001. *Fundamentals of electroanalytical chemistry*. Chichester, New York: John Wiley & Sons Ltd.

Motheo, A., Santos, J., Venancio, E. & Mattoso, L.H. 1998. Influence of different types of acidic dopant on the electrodeposition and properties of polyaniline films. *Polymer*, 39(26): 6977–6982.

Neelgund, G., Hrehorova, E., Joyce, M. & Bliznyuk, V. 2008. Synthesis and characterization of polyaniline derivative and silver nanoparticle composites. *Polymer international*, 57: 1083–1089.

Obaid, A.Y., El-Mossalamy, E.H., Al-Thabaiti, S.A., El-Hallag, I.S., Hermas, A.A. & Asiri, A.M. 2014. Electrodeposition and characterization of polyaniline on stainless steel surface via cyclic , convolutive voltammetry and SEM in aqueous acidic solutions. *International Journal of Electrochemical Science*, 9: 1003–1015.

Orata, D., Amir, Y., Nineza, C., Mbui, D. & Mukabi, M. 2014. Surface modified electrodes used in cyclic voltammetric profiling of quinine an anti-malarial drug. *IOSR Journal of Applied Chemistry*, 7(5): 81–89.

Orata, D. & Buttry, D.A. 1987. Determination of ion populations and solvent content as functions of redox state and pH in polyaniline. *Journal of the American Chemical Society*, 109: 3574–3581.

Park, S.Y., Cho, M.S. & Choi, H.J. 2004. Synthesis and electrical characteristics of polyaniline nanoparticles and their polymeric composite. *Current Applied Physics*, 4: 581–583.

Pharhad Hussain, A.M. & Kumar, A. 2003. Electrochemical synthesis and characterization of chloride doped polyaniline. *Bulletin of Material Science*, 26(3): 329–334.

Prodromidis, M.I., Florou, A.B., Tzouwara-Karayanni, S.M. & Karayanni, M. 2000. The importance of surface coverage in the electrochemical study of chemically modified electrodes. *Electroanalysis*, 12(18): 1498–1501.

Reda, S.M. & Al-ghannam,S.M. 2012. Synthesis and electrical properties of polyaniline composite with silver nanoparticles. *Advances in Materials Physics and Chemistry*, 2: 75–81.

Sapurina, I.Y. & Shishov, M.A. 2012. Oxidative polymerization of aniline : molecular synthesis of polyaniline and the formation of supramolecular structures. In Gomes, A.D. (Eds.). *New Polymers for Special Applications*. Philadelphia: InTech: 251-312.

Shinde, S.S. & Kher, J.A. 2014. A review on polyaniline and its noble metal composites. *International Journal of Innovative Research in Science, Engineering and Technology*, 3(9): 16570–16576.

Sun, Y. & Xia, Y. 2002. Large-scale synthesis of uniform silver nanowires through a soft, self-seeding, polyol process. *Advanced Materials*, 14(11): 833–837.

Tawde, S., Mukesh, D. & Yakhmi, J.V. 2002. Redox behavior of polyaniline as influenced by aromatic sulphonate anions: cyclic voltammetry and molecular modeling. *Synthetic Metals*, 125: 401–413.

Valaski, R., Ayoub, S., Micaroni, L. & Hummelgen, I.A. 2002. Influence of film thickness on charge transport of electrodeposited polypyrrole thin films. *Thin Solid Films*, 415: 206–210.

Van Dong, P., Ha, C., Binh, L. & Kasbohm, J. 2012. Chemical synthesis and antibacterial activity of novel-shaped silver nanoparticles. *International Nano Letters*, 2: 1–9.

Vijayanand, P., Vivekanandan, J., Ponnusamy, V. & Mahudeswaran, A. 2011. Synthesis, characterization and conductivity study of polyaniline prepared by chemical oxidative and electrochemical methods. *Archives of Applied Science Research*, 3(6): 147–153.

Wallace, G.G., Spinks, G.M., Kane-Maguire, P., L.A. & Teasdale, P.R. 2009. *Conductive electroactive polymers: Intelligent polymer systems*. Boca Raton, Florida, USA: CRC Press (Taylor & Francis Group).

Zhang, G., Li, X., Jia, H., Pang, X., Yang, H., Wang, Y. & Ding, K. 2012. Preparation and characterization of polyaniline (PANI) doped-$Li_3V_2(PO_4)_3$. *International Journal of Electrochemical Science*, 7: 830–843.

Zotti, G., Cattarin, S. & Comisso, N. 1988. Cyclic potential sweep electropolymerization of aniline: the role of anions in the polymerization mechanism. *Journal of Electroanalytical Chemistry*, 239(1-2): 387–396.

4. FABRICATION OF ELECTROCHEMICAL IMMUNOSENSOR AND DETECTION OF POLYCHLORINATED BIPHENYLS

4.1 Introduction

The focus of this chapter is on the systematic building of the label-free reagentless electrochemical immunosensor. It is based on the integration of the *Ab* with the transducer, GC/PANI/Ag NPs. As it has been objectively outlined, the immunosensor is designed for the analysis and monitoring of the worldwide life threatening PCBs, and its development is the core basis of this study in general. The GC/PANI/Ag NPs transducer, utilized here, has been successfully fabricated and thoroughly interrogated in chapter three for the feasibility of its application in the build-up of this analytical device. It exhibited satisfactory characteristics that made it fit for the use in electrochemical immunosensor fabrication. To the best of our knowledge, AgNPs - doped PANI coupled with electrochemical detection technique has not been used to design PCB immunosensors so far. Most reports for the immunosensor developed for PCBs represent competitive assays with labels. The integration of the *Ab* and transducer is achieved by immobilization through cross-linking as discussed below. The choice and use of solvent and electrolyte for PCBs and *Ab* solutions are also discussed.

Immobilization of an *Ab* plays a crucial role in fixation and insolubilization of the *Ab* on the transducer for its stability and functionality. Amongst the three methods possible for this procedure discussed earlier in this work (chapter two section 2.3.2.1) namely, adsorption, covalent attachment and electropolymerization, covalent attachment is given preference in the present study. It offers strong linkage that eludes loss of *Ab* and promotes its stability. It is achieved through use of bi-functional cross-linkers between the *Ab* and the transducer. Glutaraldehyde (GA) and N-succinimidyl-4-maleimido- butyrate (GMBS) are the most popular cross-linkers (Yu *et al.*, 2014). These researchers also reported adaptation of N-succinimidyl-4-(N-maleimido-methyl)-cyclohexane-1-carboxylate as a cross-linker for *Ab* immobilization in several studies.

GA however, has gained wide spread usage as a cross-linker for the formation of intra- and inter-molecular linkages especially in the fields of chemical sterilization, biomedical and pharmaceutical studies, histochemistry, cytochemistry, microscopy and enzyme technology (Migneault *et al.*, 2004). It is the linear di-aldehyde with five carbon chains. It has been reported that the reactivity in the series of aldehydes is maximum with the five carbon aldehyde, rendering GA the most reactive and favorable cross-linking substance. Its

successful application is further promoted by its commercial availability at low cost *(Okuda et al.*, 1991). Based on the conditions such as pH, concentration and temperature, GA can exist in at least 13 different forms, thereby broadening its reactivity (Migneault *et al.*, 2004), hence its wide-spread applicability. Previous studies have reported the successful application of GA as a cross-linker in fixation of *Ab* (Lopez-Gallego *et al.*, 2005; Arora *et al.*, 2007; Gunda *et al.*, 2014; Kang *et al.*, 2015) and it has been shown to enhance the stability of the biomolecule (Lopez-Gallego *et al.*, 2005; Betancor *et al.*, 2006). It is normally used in aqueous solutions at near neutral pH at which in its monomeric nature, it exists as a mixture of hydrated components at equilibrium and polymerizes into poly-glutaraldehyde (Hardy *et al.*, 1969).

GA polymer can have various concentrations of aldehyde, hydroxyl and carboxylic functional groups depending on pH and oxygen content. This implies that GA is commercially available in multi-component mixtures. It is said to react highly with proteins with minimal reversibility (Okuda *et al.*, 1991) forming stable complex. It has been previously purported that GA polymerization proceeds concurrently with protein linking reaction (Kawahara *et al.*, 1997). The concentration of *Ab* and GA is one factor that needs to be well and carefully considered in order to get water-insoluble *Ab* derivatives through cross-linking. This is achieved in this study by optimization of such concentration.

Choice of electrolyte and solvent

The choice of of these substances is important and needs a careful consideration for the best performance of *Abs* in immunosensor and solubility of PCBs. One of the vital properties of PCBs is their inertness to the external environment and it is this property that contributes to their persistent behaviour. Despite their inertness, they differently dissolve in a few organic solvents and organic - water solutions. Acetonitrile (ACN) has been found to be the best solvent for the dissolution of PCB 28 used in this study. It is this solvent that introduces the PCB into the electrolyte for the electrochemical measurement. In principle, the solvent should be compatible and miscible with the electrolyte. On the other hand, *Abs* are biological chemicals and are very sensitive to conditions under which they are manipulated outside their original environment. Such conditions include the pH, temperature and availability of essential ions. According to de Melo *et al.*, (1999), phosphate buffered saline (PBS) plays such a role of simulating the conditions for *Ab* fixation. It is a balanced salt solution that has been widely used in bio-laboratory researches because it maintains favourable and constant pH and osmotic balance. It provides biomolecules with water and essential ions. This then,

helps to keep and maintain biomolecules for some considerable time outside their original environment at optimal activity.

The immunosensor reported here was prepared by immobilizing the *Ab* on the GA activated GC/PANI/Ag NPs transducer. The prepared sensor coupled with electrochemical detection technique was used for detection of PCB 28. This PCB (Fig. 4.1) has been part of several studies because it is reportedly one of the seven persistent and prominent PCBs which are used as indicator congeners for environmental monitoring and analysis. Indicator PCBs form the basis of reference for evaluation and analysis of the entire PCB family due to their believed high potency of toxicity and adverse health effects (Date *et al.*, 2014; Net *et al.*, 2014). It has been implicated among the endocrine disrupting PCBs of global concern (Yurdakok *et al.*, 2015). It has been studied and determined mostly as total PCBs with other congeners using different methods. It was investigated by: Laschi *et al.*, (2003) using competitive electrochemical immunosensor, Date *et al.*, (2014) by label-free impedimetric immunoassay, Net *et al.*, (2014), Amdany *et al.*, (2014) and Lv *et al.*, (2015) using GC-MS. Therefore, these imply that the knowledge and information about PCB 28 is significant.

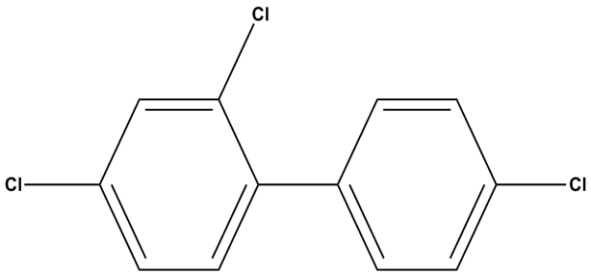

Figure 4.1: Structure of PCB 28

There are a number of conditions that have shown significant effect on the performance of the sensor on PCB analysis. Two or more of these conditions have been previously identified and optimized. Depending on the immunologists' interest, some of the factors include the pH of the solution, the concentration of *Ab*, the incubation time for *Ab-Ag* interaction, the incubation temperature, sweep potential range and scan rate. The pH of the solution can significantly affect the electrochemical behaviour of the immunosensor since acidity of the solution can influence the activity of the immobilized *Abs*. Also, the construction of the immunosensor is based on the use of *Abs* therefore, the amount of *Abs* immobilized can affect the electrochemical response of the sensor. The time taken by the antibody to interact with *Ag*, incubation time, is important on the efficiency of the developed analytical method. Higher or lower temperature can render denaturation or inactivity of the *Ab*. Lastly the sweep range can help identify the better response of the sensor to the analyte while the

rate of the sweep affects the charge/electron transfer during the electrochemical process (Katz & Willner, 2005; Chen *et al.*, 2014; Lu *et al.*, 2014). For the better performance of the proposed analytical tool, such conditions were optimized as outlined in the course of this chapter.

Furthermore, the success of the development of an immunoanalytical method is contributed by some important factors namely; precision, accuracy, stability, specificity and regeneration. Precision is the degree of closeness of the results obtained from repeat measurements under the same conditions. The important aspect of precision is reproducibility or repeatability which is referred to as the variation between the repeated measurements. Accuracy refers to the degree of closeness of the measurements of a quantity to the true value of the quantity. Both the precision and accuracy are important indicators of the method reliability and validity (Hopkins, 2000; Caruana *et al.*, 2005; Bartlett & Frost, 2008; Watanabe-Kanno *et al.*, 2009). For an immunosensor, repeated measurements can be done either by using one immunosensor for replicate analysis of the same analyte (intra-assay measurements) or by using multiple immunosensors fabricated in the same manner for analysis of the same analyte (inter-assay measurements). Then the coefficient of variation (COV) or standard deviation (SD) can be used to quantify the degree of closeness of the measurements (Chen *et al.*, 2014; Burcu Bahadır & Kemal Sezgintürk, 2015), hence the method reliability and validity. The stability of the immunosensor assesses the biocompatibility of the transducer with respect to the immobilized *Ab* molecules as to how long the *Abs* can stay immobilized with no significant change in the current signal. This aspect is useful for the assessment of the longevity of the applicability of the sensor.

Specificity is one other important parameter when it comes to the use of *Abs* as recognition materials in the development of immunosensors. *Abs* even though they are claimed to be specific to the intended measurand, it is important to evaluate and affirm their specificity. According to Chen *et al.*, (2014), the major threat for the specificity of label-free immunosensors is the nonspecific adsorption of some interferents. To prove the relative changes in current signal to be as a result of specific interaction between analyte and the immobilized *Abs*, the possible nonspecific interactions between the PCB and analogous substance(s) are evaluated to determine any possible cross reactivity. The analogues of PCBs are chlorophenols and chlorobenzenes (Bender & Sadik, 1998). The protocol of immunosensor development is also affected by another factor, interference. The working important definition of interference refers to it as any causal factor, other than the true cross-reactant, of the biased outcome of an assay. Many a times the manifestations of interference are considered as “matrix” effects. It has become a norm that the designed electrochemical

immunoassays are applied in in the analysis of real-life samples. These samples have varying compositions of different degrees and the materials present in the samples can constrain the performance of the immunosensor partially or completely. The mechanisms by which the performance hindrance can occur include: 1) changing of the effective concentration of the analyte by removal or blocking of the analyte, displacement of analyte from the physiological binding of *Abs* and de-conformation of *Ag*. 2) Interfering with *Ab* binding through physical masking of the *Ab* and de-conformation of the *Ab* binding site. The most common constituents of these materials include ionic compounds therefore, prompting the investigation of the matrix effects by testing the ionic interference (Bender & Sadik, 1998; Frank, 2002).

Regeneration is another key role in development and applications of immunosensors because many immunoanalysts desire to use the immunosensor again. It refers to breaking down of the attractive forces holding the *Abs* and analyte together resulting in reformation of the sensor that can be reused (Burcu Bahadır & Kemal Sezgintürk, 2015). Chemical regeneration has been reportedly possible using glycine-HCl, NaCl, NaOH or urea (Tang *et al*., 2006; Zhuo *et al.*, 2009). The following section outlines details of the procedural steps followed together with the materials, reagents and equipment used to accomplish the sensor development and its subsequent application on the PCB detection.

4.2 Experimental

4.2.1 Materials and reagents

The materials and chemicals for the fabrication of the transducer, GC/PANI/ Ag NPs were used as mentioned in the previous chapter. PCB 28 and 180 were obtained from Sigma Aldrich prepared by Dr Ehrenstorfer GmbH, Germany as 100 µg lyophilized in PBS. Glutaraldehyde (25% v/v) as a cross linker was also from Sigma. NaCl, KCl, $Na_2HPO_4{\cdot}12H_2O$, KH_2PO_4 and NaOH (analytical grades) were used for PBS preparation. Benzyl chloride ($C_6H_5CH_2Cl$) was used in analytical grade. Tap water and fruit juice were used without prior treatement as PCB-free matrices.

Phosphate buffered saline (PBS) (10x = 0.1M) solution

PBS solution, used as a supporting electrolyte and for preparation of solutions, was prepared using **Sambrook Fritsch & Maniatis preparation method**. 80 g NaCl and 2 g KCl

were dissolved into 800 mL distilled water. 14.4 g $Na_2HPO_4 \cdot 12H_2O$ and 2.4 g KH_2PO_4 were then dissolved into the solution. The pH was measured and adjusted to the desired value using 1 M HCl or 1 M NaOH solutions followed by making the solution up to 1000 mL with distilled water and stored at room temperature.

PCB standards

PCB 28 and 180 standard solutions were prepared in acetonitrile (ACN). Small volumes of the solvent were ensured to avoid and minimize the possible sacrifice of the signal due to solvent interaction.

4.2.2 Apparatus

Electrochemical measurements (CV, DPV and SWV) were carried out using Autolab and a three electrode compartment system as mentioned earlier. pH meter was used for measurement and adjustment of buffer pH.

4.2.3 Procedure

4.2.3.1 Preparation of PCB immunosensor

In preparing this analytical tool, the GC/PANI/Ag NPs transducer was prepared as illustrated in chapter three and air-dried. This was followed by activation of the transducer by coating with GA cross-linker. After coating, the electrode composite was dried and rinsed with distilled water. The last step was the immobilization of *Ab* on the GA activated platform, GC/PANI/Ag NPs/GA to yield GC/PANI/Ag NPs/GA/*Ab*. This was also dried and rinsed with distilled water and used or stored at 4 ^{0}C. As discussed earlier, *Ab* immobilization is one crucial step in development of immunosensor. It that regard, the factors that have influence on this step are considered and optimized. Such factors can affect the electrochemical performance of the immunosensor.

4.2.3.2 Optimization of immobilization parameters

The experimental factors that can influence *Ab* immobilization include method of coating (immersion or drop coating) on the transducer, the concentration of GA, incubation time in GA solution. To achieve maximum immunological performance, these parameters are optimized by SWV using PCB concentration of 1 µg/mL. The parameter features giving

maximum immunosensor performance render the optimum conditions suitable for immunological measurements.

Immersion or drop coating

Immersion and drop coating are the two possible ways GA and *Ab* can be coated on their respective platforms. The coating was done using both methods and compared in terms of which one would give the best results. Immersion was done by dipping the modified electrode in solutions of 1 % GA and 1 µg/mL *Ab* for 1 hour. On the other hand the modified electrodes were drop-coated with 5 µL of the GA and *Ab* solutions and left for an hour. The electrode were then rinsed with distilled water and dried prior to use.

GA concentration

The linker insolubilizes the *Ab* and fixes it on the support. The amount, stability and activity of the *Ab* depend greatly on the amount of this linker. In this case, the concentration of GA is optimized for maximum *Ab* loading and maintained activity. This exercise was done by GA concentrations of 1, 2 and 4 % prepared from 25 % GA stock solution in distilled water.

Incubation time in GA

The time needed for the activation of the GC/PANI/Ag NPs with GA can be important for GA to be adequately bonded to the platform. The optimum period was determined by variation of the time during immersion or after drop coating. 0.5, 1, and 2 hour periods were considered in this case.

4.2.3.3 Characterization of PCB immunosensor

Characteristic features of the present immunosensor are interrogated using CV. Characterization is done after each step in the building of the immunosensor. CV determines the electroactivity of the immunosensor and it is run in PCB free electrolyte, PBS (pH = 7.4)/ ACN (99.6:0.4 v/v %). The CV scans were done within the sweep range of -1 to +1 V at 20 mV/s.

4.2.3.4 Immunoanalysis and detection

Under the optimized conditions, the constructed label-free reagentless immunosensor was used for the detection of PCBs. The sensor was incubated with different concentrations of PCB (0.2 – 1.2 ng/mL) in an electrochemical cell containing 10 mL of PCB solution in PBS/CAN solution. The solution was deoxygenated using nitrogen gas for 10 min and allowed for incubation. SWV was used to measure the current response. The parameters for this technique were potential sweep of -1.0 to +1.0 V, scan rate of 20 mV/s, amplitude of 20 mV and frequency of 25 Hz. From the results, calibration studies were made.

4.2.3.5 Optimization of immunological parameters

The electrochemical performance of the developed immunosensor on the analysis of PCBs can be affected by a number of experimental factors. These factors include scan rate, sweep potential, detection method and incubation time of *Ab* and PCB. To achieve maximum immunological performance, these parameters were optimized using PCB concentration of 1 µg/mL. The parameters giving maximum immunosensor performance render the optimum conditions suitable for immunological measurements.

Sweep potential, scan rate and detection method

The stability and functionality of the electrode modifying materials (PANI, Ag or *Ab*) can be affected by the potential range within which the electrode is ramped. It is of great significance therefore, that the suitable range be determined for maintenance of the good and desirable characteristics of the modifiers for effective performance of the immunosensor. The suitable potential range was determined by ramping the modified electrode using CV at various potential ranges. These were within -1.5 to 1, the range covering the reductive PCBs dechlorination (-4 to 0) and immunoassays for PCBs (-0.6 to 0.6). The scan rate determines the rate at which the electrochemical process takes place. The rate was optimized from 5 to 100 mV/s while the methods of detection were optimized between CV, SWV and DPV since they were the available detection techniques.

Incubation time between Ab and PCB

The time taken by the *Ab* to interact with *Ag*, incubation time, is important on the efficiency of the developed analytical method. The optimum reaction time was investigated in the range 0.5, 1, 2, 4 hrs.

4.2.3.6 Reproducibility of the immunosensor

Reproducibility accounts for the ability of the immunosensor to reproduce the same signal on the repetitive measurements. For the fabricated immunosensor, reproducibility was evaluated by the intra- and inter-assay measurements and relative standard deviation (RSD) at 1 µg/mL PCB concentration using SWV. The intra-assay RSD was determined by running 5 replicate measurements using one immunosensor while inter-assay for the same PCB concentration was done using 5 individual immunosensors fabricated in the same manner.

4.2.3.7 Specificity, interference and validation

The prepared immunosensor was tested for cross-reactivity, matrix interference and then validated for the analysis of PCBs. Cross-reactivity was tested by spiking pure sample of the potential cross-reactants, benzyl chloride and PCB 180 (in the ratios 1:5, 1:10 and 1:20) to the PCB 28 solution followed by measuring the current response and determining the cross-reactivity. The test was done for the same concentration of PCB solution (1 ng/mL). Each measurement is completed through three replicates. The percentage cross reactivity, CR (%) is obtained as follows:

$$CR\ \% = \frac{(conc\ after\ spiking - conc\ before\ spiking)}{Concentration\ before\ spiking} x\ 100 \qquad (4.1)$$

The matrix ionic interference studies were done by spiking the PCB standard sample with the ionic compounds of Na and K at the concentration ratios as in the cross-reactivity above and determining the voltammetric current response. The extent (%) matrix effect was calculated the same way as the cross-reactivity. Method validation involves the use of the new method on analysis of samples in real life and testing the recoveries. It tests the feasibility of the future applications of the immunosensor and it is mostly used to assess the accuracy of the immunoassay whereby accurate amounts of the analyte are added to the samples to determine the possible increase in the concentration (Frank, 2002). It was done by spiking real water and fruit juice samples with 1.0 ng/mL PCB 28 standard. The analysis was made with three replications for each sample. Recovery is expressed as:

$$\%\ recovery\ = \frac{Measured\ \ concentration}{Expected\ concentration}\ x\ 100 \qquad (4.2)$$

4.3 Results and discussions

4.3.1 Optimization of immobilization parameters

4.3.1.1 Immersion and drop coating

Immobilization of *Ab* on the transducer was done by both methods for optimization. The electrode's CVs were obtained in electrolyte solution after modification of the electrode with *Ab* as in Fig. 4.2. The resultant electrode, GC/PANI/Ag NPs/GA/*Ab*, does not exhibit peaks for immersion while for drop-coating cathodic peak is observed with reduced intensity. In this context, the prevalence of peaks under drop coating suggests inadequate and inefficient modifications with GA and *Ab* while immersion offered better activation of the supporting transducer by the GA and ultimate success in the immobilization of the *Ab*. Immersion was therefore, opted over drop-coating for immunosensor fabrication.

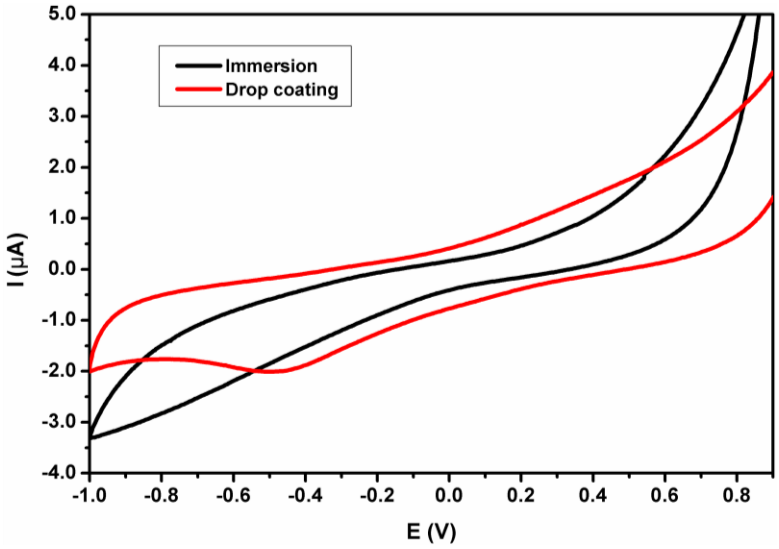

Figure 4.2: Immersion and drop coating CVs for GC/PANI/Ag NPs/GA/*Ab* in PBS/ACN (96.6: 0.4 v/v %) at 20 mV/s san rate

4.3.1.2 GA concentration

The effect of the amount of GA on the performance of the analytical immunosensor was assessed by insolubilizing the *Ab* using various GA concentrations of 1, 2 and 4%. The square wave voltammetric responses of the PCB 28 measurements showed significant effect as the concentration was varied. The current response was high for 1% and reduced with increased concentration (Fig 4.3). This influence could be explained as follows: the aim

of the use of GA was to fix the *Ab* in a specific confinement so as to restrict its movement. This happened by insolubilization of the *Ab* thereby making it rigid. Increasing GA concentration, for the constant *Ab* concentration, therefore, increased the rigidity which possibly destructed the *Ab*. Destruction of *Ab* led to ultimate underperformance of the immunosensor as evidenced by the low signal. This meant that the amount of *Ab* was not equivalent to that of the GA with respect to the increased GA concentration.

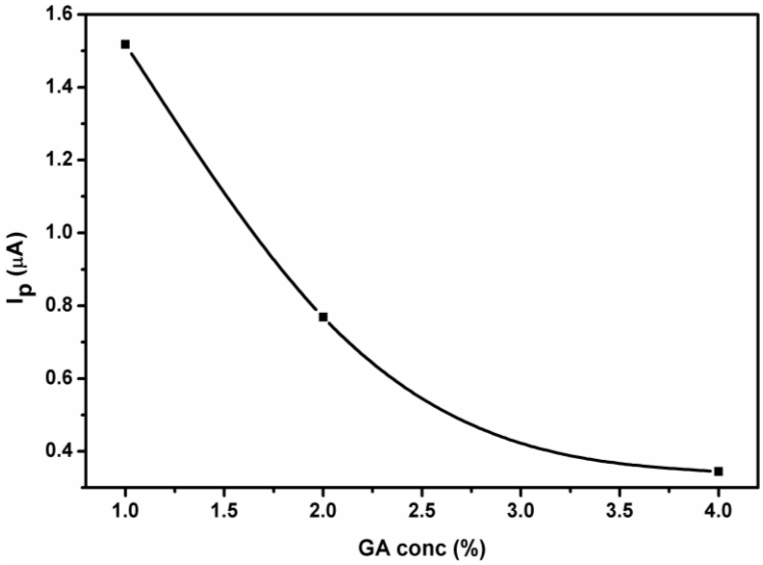

Figure 4.3: Effect of GA concentration on current response

In relation to other researches, variation of GA concentration showed no significance on the performance of the sensor (Sai *et al.*, 2006). Conversely, Broun, (1976) proclaimed that the concentration of the cross-linking material has an influence on the cross-linkage in that the strength and efficiency of the crosslinking are directly proportional to the concentration of the cross-linker. This means increased structural rigidity of the biomolecule. It is this structural stiffness that has negative impact on the activity of the *Ab*. This is supported by the indication by Chui & Wan, (1997) that the biomolecular activity has indirect proportion to the concentration of GA. On these bases, 1% GA represents the optimum concentration for the better performance of the device.

4.3.1.3 Immersion period in GA solution

The time needed to activate the transducer (GC/PANI/Ag NPs) with GA was optimized using 1% GA for periods of 0.5, 1 and 2 hrs. Their respective peak current responses were obtained at 1.487, 1.52 and 1.50 μA. These clearly demonstrate that the peak current reaches maximum when the period is 1 hr. However, the change in current is small and does not account for such waiting period of 0.5 hrs difference from 0.5 to 1 hr and from 1 to 2 hrs.

This indicates insignificant influence of the time needed to immerse the electrode in GA solution. As such 30 min was used for the rest of the analyses. The immobilization of *Ab* on the transducer was achieved under the optimal conditions; the immersion as a way of introducing GA and *Ab* on the transducer, 1 % GA concentration and 0.5 hr period in GA solution.

4.3.2 Immunosensor fabrication

The stepwise fabrication of an immunosensor followed as: firstly, the fabrication of transducer by modification of electrode with PANI/Ag NPs, secondly, activation of the transducer with the GA cross-linker and ended with the immobilization of *Ab* on the GA activated support. The first step has been thoroughly dealt with in chapter three. The second one results in the formation of enamines from combination of PANI and GA, while the last one forms imines from GA and *Ab*. These have been made possible by reportedly high rapid reaction of GA through its carbonyl functional groups with the amine groups of PANI in the transducer and those of *Ab* (Okuda *et al.*, 1991; de Melo *et al.*, 1999) and the high stability of the resultant bonds between GA and amine groups (Betancor *et al.*, 2006). This represents a well compatibility between the transducer and *Ab*. The fabrication protocol is believed to follow the mechanism presented in Fig. 4.4 (A).

During the immunosensor development process, each step was characterized and their CVs in PBS/ACN (99.6:0.4 v/v %) were obtained (Fig. 4.4 (B)). The resultant CV for GC/PANI/Ag NPs shows the displaced PANI anodic peak around 0.5 V and the cathodic one at -0.4 V. These represent the presence of the EM form of PANI as it has already been discussed previously. The CV for GC/PANI/Ag NPs/GA shows less intense cathodic PANI peak around -0.5 V. For GC/PANI/Ag NPs/GA/*Ab*, the peaks are not observed. The decrease in the original PANI peak is due to effective activation of the transducer platform by the GA which results in reduction of PANI. The disappearance of PANI peaks does not necessarily imply loss of the PANI conductivity because there is still a flow of charge since PANI is permeable to flow of ions.

This behaviour was explained by de Melo *et al.*, (1999). They indicated that in near neutral medium, GA reduces PANI but that has little effect on the loss of permeability of PANI for ions. This means PANI conductivity is retained even in the presence of GA. GA rather, activates the transducer thereby rendering it heterofunctionality for anion exchange. The disappearance of peaks with further electrode modification with *Ab* notes the successful immobilization of *Ab* and good compatibility of the biomolecule with the transducer. The CV

responses of each electrode modification during the immunosensor construction confirm the proposed mechanisms in Fig. 4.4 (A).

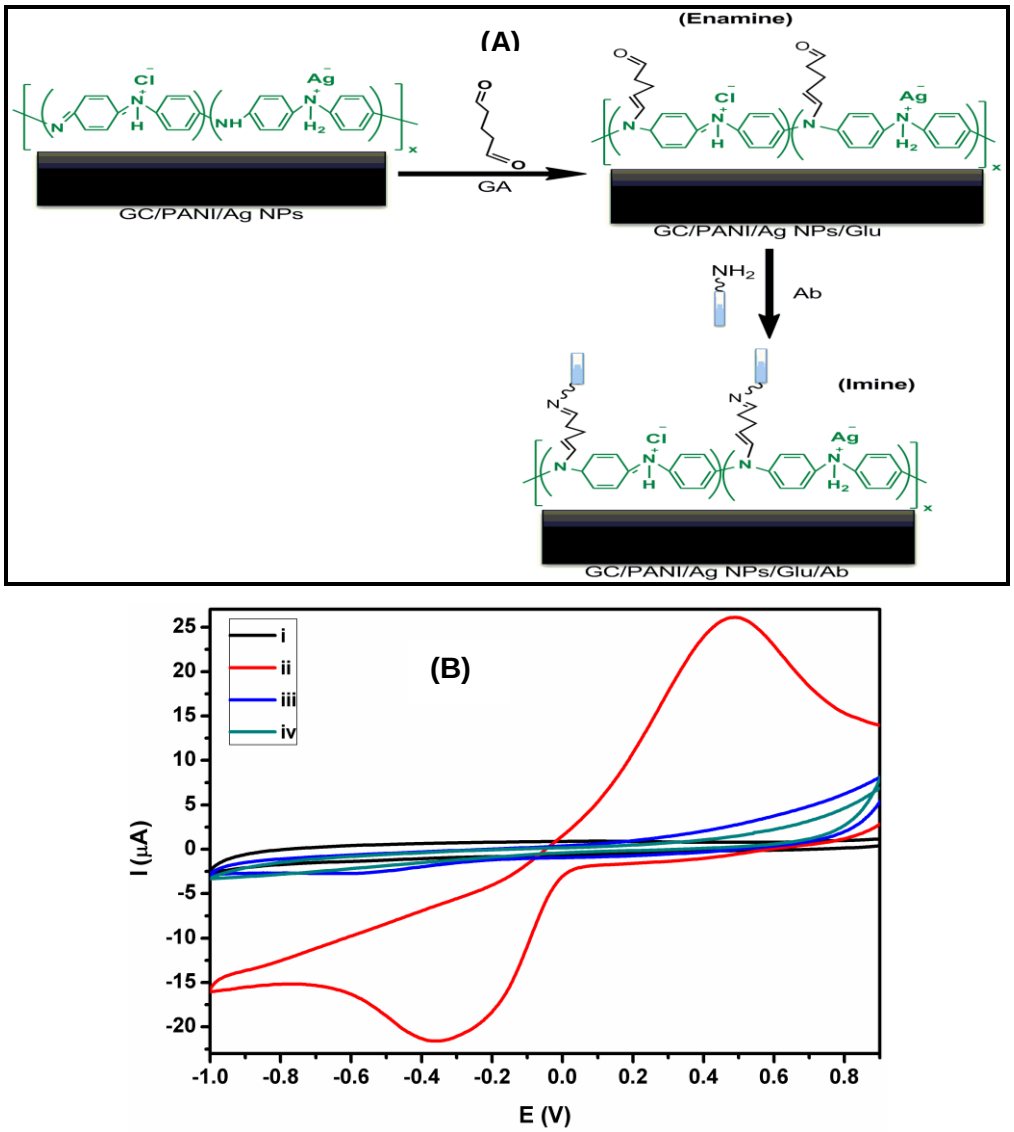

Figure 4.4: **Immunosensor fabrication steps; schematic steps mechanism (A) and CVs for each step (B): (i) GC, (ii) GC/PANI/ Ag NPs, (iii) GC/PANI/Ag NPs/GA, (iv) GC/PANI/Ag NPs/GA/*Ab***

4.3.3 Optimization of immunological detection conditions

4.3.3.1 Sweep potential, scan rate and detection method

The electrodes potential was screened from -4 to 1.4 V in PBS/ACN solution. Within -4 to -1.5, GC and Pt working electrodes show noise. Within the range -1 to 1.4, distorted and shifted PANI peaks prevail (first anodic and cathodic peaks) while between -1.5 and -1, PANI gets detached from the electrode surface as disgruntled layers falling into the solution. The

suitable range therefore was taken as -1 to 1 V. This was then used for the rest of the analysis. The scan rate of 20 mV/s was also found suitable for the assay since it offered adequately visible and resolved peaks than the others (not shown). The detection methods were optimized between CV, DPV and SWV and Fig. 4.4 shows their respective voltammetric responses. CV (Fig. 4.5 (A)) shows a very low-intensified broad peak at around -0.20 V and the current response does not show significance increase even when the PCB concentration is increased. DPV (Fig.4.5 (B)) shows a more intensified and resolved peak around -0.30 V accompanied by increase in current with respect to concentration.

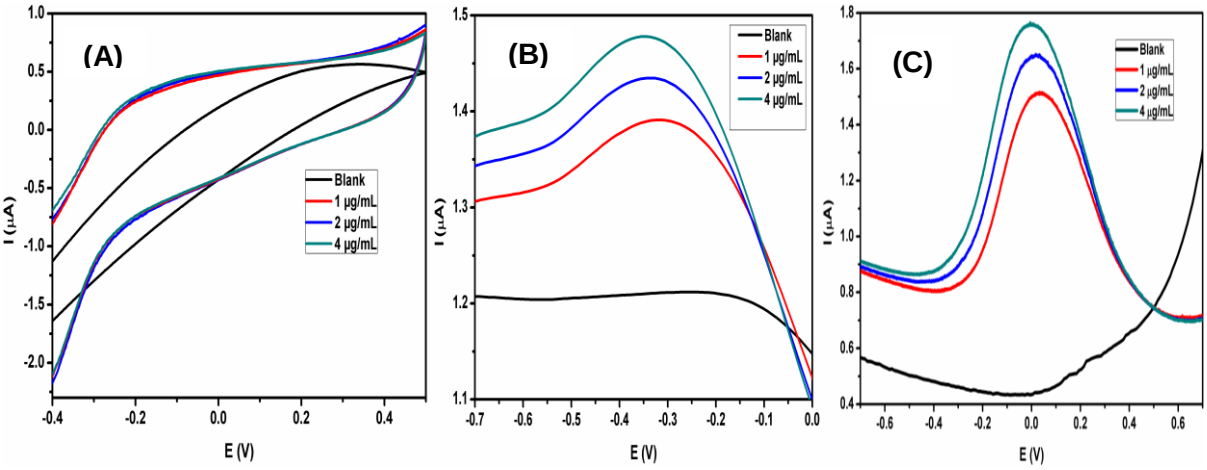

Figure 4.5: Effect of different electrochemical detection methods; CV (A), DPV (B) and SWV (C) on PCB 28 detection

However, the peaks are characterized by smaller peak height. These responses from CV and DPV are not representatively reliable and could lead to false interpretations. Contrarily, SWV (Fig. 4.5 (C)) shows a well resolved stable peak at around 0.0 V in response to PCB presence. Due to these promising results, reliance was put on SWV as the detection technique for the rest of the analysis.

4.3.3.2 Incubation time between *Ab* and PCB

The sufficient time needed to attain maximum interaction between the *Ab* and PCB 28 was determined by detection of 1 µg/mL PCB at varying *Ab*-PCB incubation periods of 0.5, 1, 2 and 4 hours. The measurements gave the resultant current with respect to time as shown in Fig. 4.6. The figure shows that the current response increased with the time from 0.5 to 2 hrs and then maintained constancy beyond 2 hrs. This could be due to saturation of the *Ab* binding sites with the PCB leaving no more room for more PCB molecules to bind to the *Ab* and be accompanied by increased peak current. This means that period of 2 hrs and more is

adequate for maximum *Ab*-PCB interaction. The 2 hrs period therefore, was considered optimum for PCB's detection with the developed analytical tool.

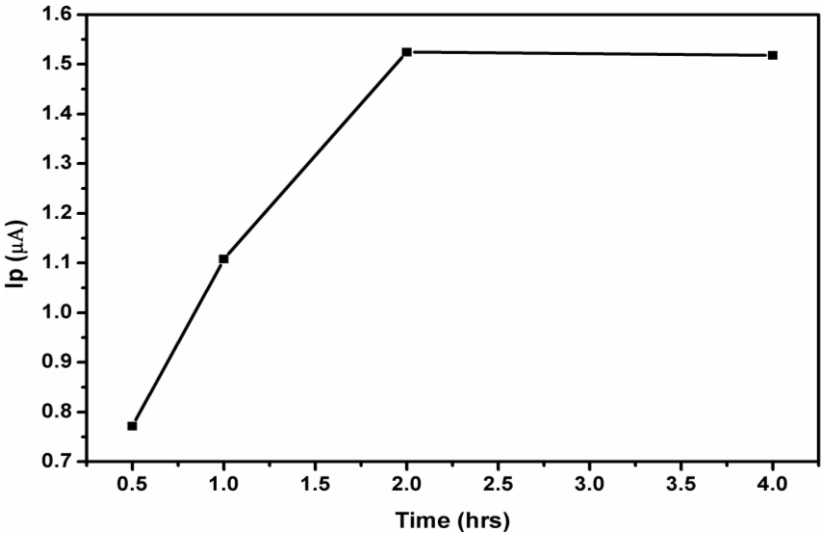

Figure 4.6: Effect of incubation period between Ab and PCB 28

4.3.4 Immunological detection and calibration studies of PCB 28

Immunoanalysis of the PCB was done using the optimized conditions (-1.0 to 1.0 V potential sweep, 20 mV/s scan rate, 2 hrs incubation period and using SWV as detection technique. The analysis was done for PCB concentrations of 0.2, 0.6, 0.8, 1.0 and 1.2 ng/mL. The voltammograms (Fig. 4.7 (A)) show the peak due to PCB at around 0.020 V for the lower concentration and shift to the lower potential with increasing concentration.

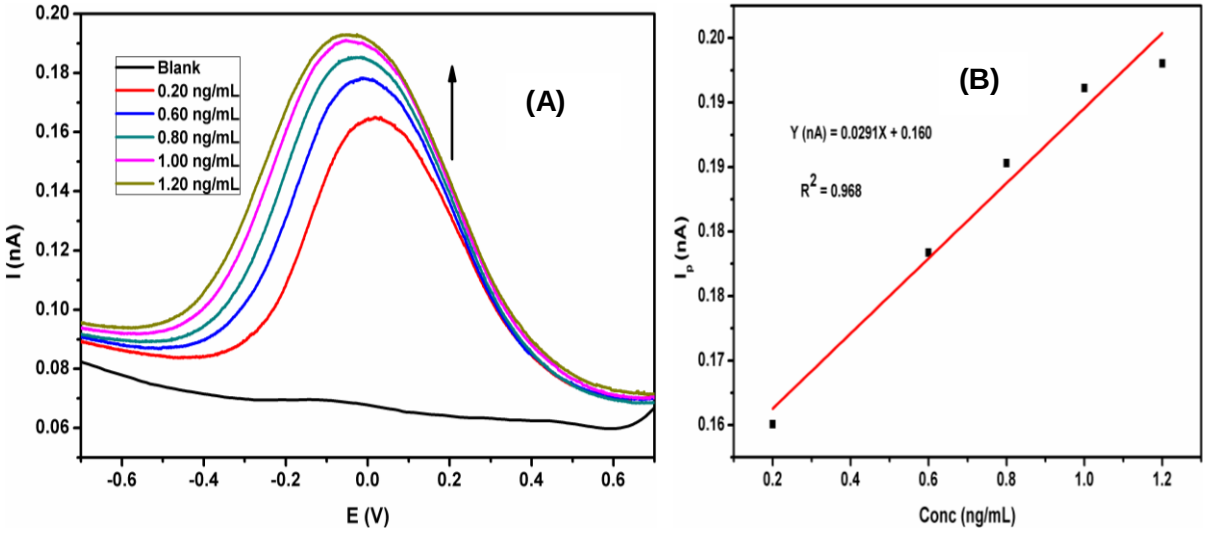

Figure 4.7: Current response with increasing concentration (A), calibration graph of PCB 28 (B)

According to Fig. 4.7 (A), the peak current increases with increasing PCB concentration. This is evident that the response in current was as a result of PCB detection by the immunosensor. This can be explained as follows: According to Bender and Sadik, (1998), the change in peak current is influenced mainly by the extent of chlorination or chlorine content in the electro-immunological system and further, the peak current increases with increasing chlorine content distinctly in **direct electrochemical immuno-detections of PCBs**. There is no evident clarity on the chemical changes accompanying these claims though. The claims suggested that there are changes in the conductivity of the mediating polymer due to the changes in the levels of chlorination. They clearly indicated that the current response due to PCB detection increased with increasing PCB concentration.

The concentrations and peak currents from the voltammograms were further used to construct the calibration graph (Fig. 4.7 B) for PCB 28. The figure represents a linear relationship between the peak current and the concentration in the range 0.2 - 10 ng/mL. The linear regression equation is Y (nA) = 0.0291X + 0.160, with a linear correlation coefficient (R^2) of 0.968, and the detection limit (LOD) was estimated to be 0.269 ng/mL. The limit of quantitation (LOQ) was determined to be 0.898 ng/mL. Therefore, the proposed electrochemical immunosensor has a good analytical performance for the detection of PCB 28. Recently, PCBs were determined at levels of 0.150 ng/mL in South Africa (Amdany *et al.*, 2014). The levels are normally higher in countries where PCBs were manufactured and found great application; 0.250 ng/mL in France (Net *et al.*, 2014), and 5.45 - 9.55 ng/mL in Turkey (Yurdakok *et al.*, 2014). Therefore, based on the analytical parameters exhibited by the proposed electrochemical immunosensor, a good analytical performance for the detection of PCB 28 can be anticipated.

4.3.5 Reproducibility

The reproducibility of the method was evaluated by calculation of RSD for the intra- and inter- assay measurements for 1 µg/mL PCB 28. The values were determined as 0.933 and 3.12 % respectively for intra- and inter-assays. These represent acceptable repeatability exhibited by the developed analytical immunosensor.

4.3.6 Specificity/cross-reactivity

Antibody specificity toward PCB 28 and the possible cross reactivity with benzyl chloride (BCl) and PCB 180 were investigated and Fig 4.8 depicts the results. The impact of BCl is observed in Fig 4.8 (A) whereby the peak current increases with the amount of BCl present

in the solution from 1:5 to 1:20 PCB 28/BCl. The respective % cross-reactivity ranges from 4 to 22 (Table 4.1). This clearly indicates that the presence of BCl affects the specificity of *Ab* toward PCB thereby cross-reacting with some of the *Ab* binding sites. This possibility is encouraged by the structural similarity between the PCB and BCl as they both bear the phenyl and chloride groups.

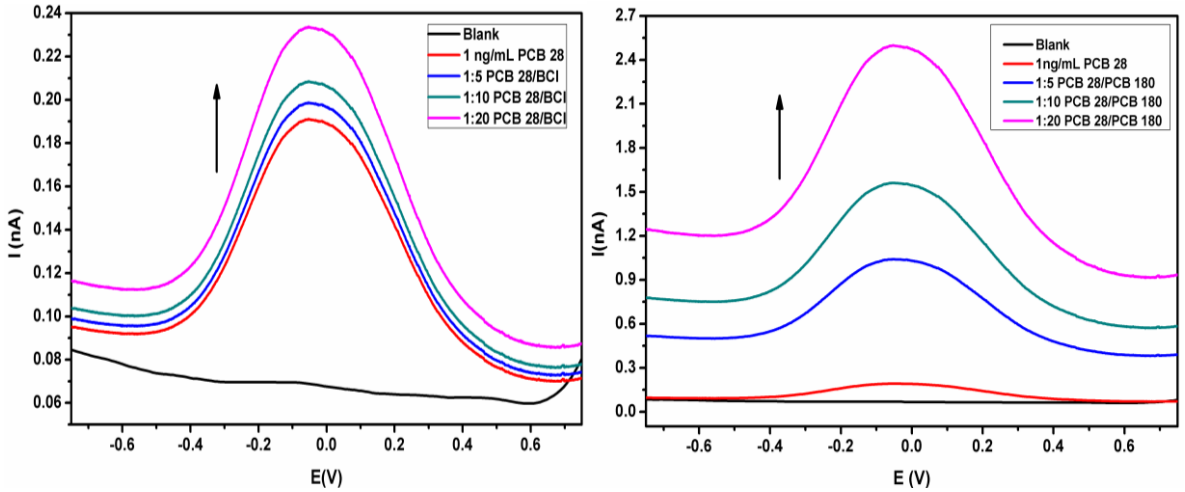

Figure 4.8: Current response for cross-reactivity due to BCl (A) and PCB 180 (B)

On the other hand, the presence of PCB 180 resulted in much more increased peak currents with increasing ratio (Fig 4.8 B). This demonstrates a high cross-reactivity which ranges from 475 to 1281% (Table 4.1). In essence, the acceptable cross-reactivity level is 5% (Garcia II *et al.*, 2007), and the high level of cross-reactivity of the *Ab* tested against PCB 28 implies that in this case, the designed immunosensor measures the total PCB. This is an indication that the immunosensor can generally be applicable for the entire PCB family as in an individual and total PCB levels. RSD ranges between 2.4 to 6%.

Table 4.1: Cross-reactivity studies (n = 3)

Analyte	Current response (nA)	% cross-reactivity
PCB 28 alone	0.191	
1:5 PCB 28/BCl	0.199	4.19
1:10 PCB 28/BCl	0.207	8.38
1:20 PCB 28/BCl	0.233	21.99
PCB 28 alone	0.181	
1:5 PCB 28/PCB 180	1.040	474.59
1:10 PCB 28/PCB 180	1.565	764.64
1:20 PCB 28/PCB 180	2.500	1281.22

4.3.7 Interference

The effect of matrix interference was tested using the Na and K salts of chloride and phosphate respectively and and their impact on the PCB 28 immunoanalysis is demonstrated in Fig 4.9. The current magnitudes with respect to the ratios are in the order: PCB 28 alone < 1:10 PCB 28/KH_2PO_4 < 1:20 PCB 28/NaCl < 1:10 PCB 28/NaCl < 1:20 PCB 28/ KH_2PO_4. The % interference (Table 4.2) ranges between 0.6 and 3.5. The increasing peak current order observed above does not show any proportionality or trend with respect to the increase in interferent concentration. Additionally the % interference is below the highest acceptable value (5%). Therefore, it is reasonable to believe that NaCl and KH_2PO_4 have no (or have insignificant) effect on the analysis of PCB. RSD ranges between 2 to 5%.

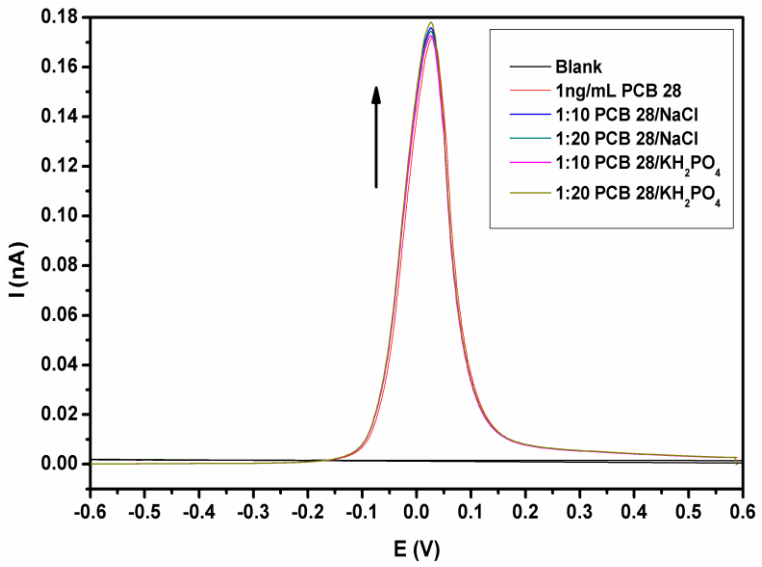

Figure 4.9: CVs for matrix effect

Table 4.2: Matrix effect studies (n = 3)

Analyte	Current response (nA)	% Interference
PCB 28 alone	0.172	
1:10 PCB 28/NaCl	0.176	2.33
1:20 PCB 28/NaCl	0.174	1.16
1:10 PCB 28/KH_2PO_4	0.173	0.58
1:20 PCB 28/ KH_2PO_4	0.178	3.49

4.3.8 Validation

The developed method was successfully validated through spiking and recoveries of the PCB 28 into tap water and juice. Fig 4.10 and Table 4.2 show the current response and % recoveries respectively. The recovered amounts range from 90 to 102%. This values are within the acceptable spike and recovery range of 80-120% (Garcia II *et al.*, 2007). This validates the applicability and accuracy of the developed immunosensor for measurement and monitoring of PCBs. RSD ranges between 3 to 5.4%.

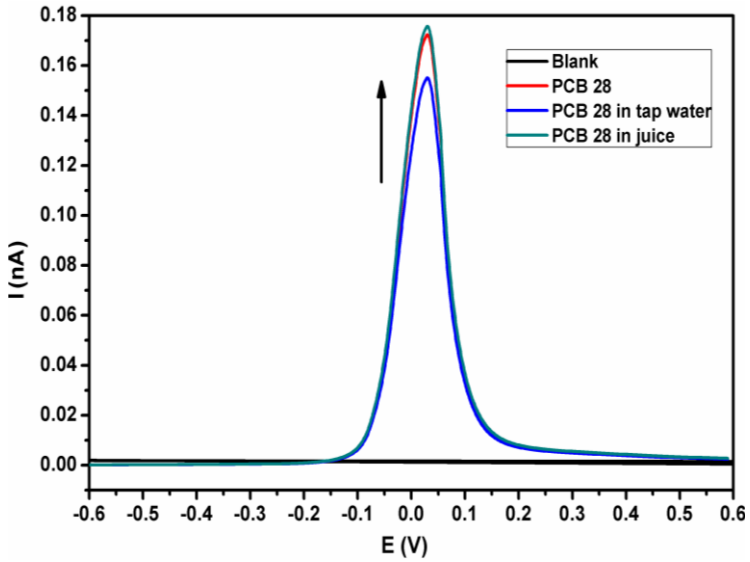

Figure 4.10: CVs responses for spiking and recoveries

Table 4.3: Recovery studies (n = 3)

Analyte	Current response (nA)	% recovery
PCB 28 alone	0.172	
PCB 28 in tap water	0.155	90.1
PCB 28 in juice	0.176	102.3

4.4 Conclusion

The main objective of the study was to develop an electrochemical immunosensor as a unique method for PCBs analysis. This was successfully achieved through immobilization of *Ab* on the Pt/PANI/ Ag NPs using covalent attachment approach. The development protocol demonstrated a good biocompatibility of the transducer with *Ab* as enhanced by the GA cross-linker. Electrochemical activity changes of the film were used to monitor step by step

fabrication of the immunosensor. The immunosensor fabricated was tested against PCB 28. The method exhibited good analytical parameters with limit of detection (LOD) and limit of quantitation (LOQ) being respectively 0.269 ng/mL and 0.898 ng/mL. The linear range was obtained within 0.2 to 1.2 ng/mL. The method is also characterized by acceptable repeatability with error of less than 5%. It also has good specificity with interference less than the highest accepted level of 5%. The method again showed the potential of wide application in the analysis and monitoring of the entire PCB family at total PCB.

4.5 References

Amdany, R., Chimuka, L., Cukrowska, E., Kukučka, P., Kohoutek, J. & Vrana, B. 2014. Investigating the temporal trends in PAH, PCB and OCP concentrations in Hartbeespoort Dam, South Africa, using semipermeable membrane devices (SPMDs). *Water SA*, 40(3): 425–436.

Arora, K., Sumana, G., Saxena, V., Gupta, R.K., Gupta, S.K., Yakhmi, J.V, Pandey, M.K., Chand, S. & Malhotra, B.D. 2007. Improved performance of polyaniline-uricase biosensor. *Analytica Chimica Acta*, 594: 17–23.

Bender, S. & Sadik, O.A. 1998. Direct electrochemical immunosensor for polychlorinated biphenyls. *Environmental Science and Technology*, 32(6): 788–797.

Betancor, L., Lopez-Gallego, F., Hidalgo, A., Alonso-morales, N., Mateo, G.D.C., Fernandez-Lafuente, R. & Guisan, J.M. 2006. Different mechanisms of protein immobilization on glutaraldehyde activated supports : effect of support activation and immobilization conditions. *Enzyme and Microbial Technology*, 39: 877–882.

Broun, G.B. 1976. Chemically aggregated enzymes. In *Mosbach, K. Methods in Enzymology. (Eds.), New York: Academic Pres,*: 263–280.

Chen, X., Qin, P., Li, J., Yang, Z., Wen, Z., Jian, Z., Zhao, J., Hu, X. & Jiao, X. 2014. Impedance immunosensor for bovine interleukin-4 using an electrode modified with reduced graphene oxide and chitosan. *Microchimica Acta*, 182(1-2): 369–376.

Chui, W. K. & Wan, L.S.C. 1997. Prolonged retention of cross-linked trypsin in calcium alginate microspheres. *Journal of Microencapsulation*, 14(1): 51–61.

De Melo, J.V, Bello, M.E., de Azevedo, W.M., de Souza, J.M. & Diniz, F.B. 1999. The effect of glutaraldehyde on the electrochemical behavior of polyaniline. *Electrochimica Acta*, 44: 2405–2412.

Frank, S.A. 2002. *Immunology and Evolution of Infectious Disease*. Princeton, New Jersey: Princeton University Press, 41 William Street.

Garcia II, B.H., Hargrave, A., Morgan, A., Kilmer, G., Hommema, E., Nahrahari, J., Webb, B. & Wiese, R. 2007. Antibody microarray analysis of inflammatory mediator release by human Leukemia T-Cells and human non–small cell lung cancer cells. *Journal of Biomolecular Techniques*, 18(4): 245–251.

Gunda, N.S.K., Singh, M., Norman, L., Kaur, K. & Mitra, S.K. 2014. Optimization and characterization of biomolecule immobilization on silicon substrates using (3-aminopropyl)triethoxysilane (APTES) and glutaraldehyde linker. *Applied Surface Science*, 305: 522–530.

Hardy, P.M., Nicholls, A.C. & Rydon, H.N. 1969. The nature of glutaraldehyde in aqueous solution. *Journal of the Chemical Society D: Chemical Communications*, (10): 565–566.

Kang, H.J., Cha, E.J. & Park, H.D. 2015. Protein immobilization onto various surfaces using a polymer-bound isocyanate. *Applied Surface Science*, 324: 198–204.

Katz, E. & Willner, I. 2005. Switching of directions of bioelectrocatalytic currents and photocurrents at electrode surfaces by using hydrophobic magnetic nanoparticles. *Angewandte Chemie*, 117(30): 4869–4872.

Kawahara, J., Ishikawa, K., Uchimaru, T. & Takaya, H. 1997. Chemical cross-linking by glutaraldehyde between amino groups: its mechanism and effects. In Swift *et al.*, (Eds.). *Polymer Modification*. New York: Springer: 119–131.

Lopez-Gallego, F., Betancor, L., Mateo, C., Hidalgo, A., Alonso-morales, N., Dellamora-ortiz, G., Guisan, J.M. & Fern, R. 2005. Enzyme stabilization by glutaraldehyde crosslinking of adsorbed proteins on aminated supports. *Journal of Biotechnology*, 119: 70–75.

Lu, W., Ge, J., Tao, L., Cao, X., Dong, J. & Qian, W. 2014. Large-scale synthesis of ultrathin Au-Pt nanowires assembled on thionine/graphene with high conductivity and sensitivity for electrochemical immunosensor. *Electrochimica Acta*, 130: 335–343.

Migneault, I., Dartiguenave, C., Bertrand, M.J. & Waldron, K.C. 2004. Glutaraldehyde : behavior in aqueous solution, reaction with proteins and application to enzyme crosslinking. *BioTechniques*, 37(5): 790–802.

Net, S., Dumoulin, D., El-Osmani, R., Rabodonirina, S. & Ouddane, B. 2014. Case study of PAHs , Me-PAHs , PCBs , phthalates and pesticides contamination in the Somme River water, France. *International Journal of Environmental Research*, 8(4): 1159–1170.

Okuda, K., Urabe, I., Yamada, Y. & Okada, H. 1991. Reaction of glutaraldehyde with amino and thiol compounds. *Journal of Fermentation and Bioengineering*, 71(2): 100–105.

Sai, V.V.R., Mahajan, S., Contractor, A.Q. & Mukherji, S. 2006. Immobilization of antibodies on polyaniline films and its application in a piezoelectric immunosensor. *Analytical Chemistry*, 78(24): 8368–8373.

Yu, Q., Wang, Q., Li, B., Lin, Q. & Duan, Y. 2014. Technological development of antibody immobilization for optical immunoassays: progress and prospects. *Critical Reviews in Analytical Chemistry*, 45(1): 62–75.

Yurdakok, B., Tekin, K., Daskin, A. & Filazi, A. 2014. Effects of polychlorinated biphenyls 28, 30 and 118 on bovine spermatozoa in vitro. *Reproduction in Domestic Animals*: 1–6.

5. CONCLUSIONS AND RECOMMENDATIONS

The chapter reports the conclusions based on the initial aim and objectives of the study. It also gives the recommendations and suggestions on the future work to be considered for further studies on the present field.

5.1 Conclusions

In this study the comparative interrogation has been made for the suitability and potency of PANI and Ag NPs-doped PANI as an electrochemical transducer material for the development of immunosensor for PCBs analysis. This was achieved by electrochemical formation and deposition of the polymer composites on the Pt and GC electrodes followed by characterization of the material using electrochemical (CV), spectroscopic (FTIR) and microscopic techniques (TEM). The increase in peak current as shown in CV analysis, confirmed the formation of the conducting form of PANI (EM form) films on the electrodes' surfaces. The cyclic voltammograms exhibited characteristic PANI peaks which are due to different PANI redox forms. The formation of EM was also affirmed by the FTIR spectra that showed the bands confirming the EM characteristic functional groups. Presence of PANI functional groups in all polymers including the Ag NPs containing one is indicative of the retention of the PANI structure strongly suggesting layer by layer arrangement. All PANIs were nanofibric tubes. However, the appearance of the PANI and PANI/Ag NPs was different, with the latter being bigger and smoother than the former, which is in agreement with the physical and electrochemical properties observed. Comparison of the GC and Pt based transducers clearly indicates the superior electrical quality of GC based electrode which is a result of better physical and chemical properties; such as larger surface area, smoothness and band gap. The elemental composition from TEM analysis highlighted the constituents of the PANI/Ag NPs that was synthesized in the present work.

Suitability of the successfully synthesized PANI/Ag NPs composite based transducer for electrochemical detection was evaluated. The most desired property for the composite is its electroactivity. This property comprises of conductivity and electroreversibility which are directly or indirectly influenced by its physical and chemical properties. The physical properties of the composite that have a direct influence on the electroactivity are the band gap, surface coverage and film thickness. Therefore, these were determined as part of the evaluation of the composite. The band gap determined for PANI/Ag NPs is lower than that for PANI alone and the values for surface coverage and film thickness are higher than those

for PANI. This clearly signifies the role of Ag NPs incorporated in PANI. Its effect on reducing the band gap and increasing the surface coverage and film thickness resulted in enhancement of the electroactivity. This is evidenced by the fact that currents from the CV measurements with PANI/Ag NPs coated electrode were some orders of magnitude higher than those of sole PANI coated electrode. For these reasons, the composite, PANI/Ag NPs was found to be reliably fit as potential modifying material for the fabrication of the electrochemical transducer for the development of PCBs immunosensor.

The immunosensor was then developed from this transducer. The successful construction of the immunosensor from the PANI/Ag NPs based transducer demonstrated good compatibility of the *Ab* and PANI/Ag NPs by the help of GA cross-linker. The developed sensor was tested against the standard PCB 28 samples at varied concentrations and gave satisfactory response and analytical parameters. The method's linear range was found is 0.2 - 1.2 ng/mL. LOD and LOQ were determined respectively to be 0.269 and 0.898 ng/mL. The immunosensor was 3.12 % reproducible and gave repetitive measurements to the extent of 0.933 %. These demonstrate reliability of the device and feasibility for application in the real samples. The specificity of the sensor was found to be less than the highest acceptable level (5%) of interference and was successfully validated for the analysis and monitoring of the entire PCB family in real life samples.

5.2 Recommendations and future work

Fabrication of the transducer and immunosensor can be characterized using other techniques which were not at our disposal thus enhancing chemical understanding of the materials involved. The transducer chemical composition elucidation using PXRD and EIS studies could help in understanding the chemical interactions. Step by step immunosensor fabrication studies with other techniques such as EIS and SEM can assist in understanding the chemistry involved in the detection of the PCB. Other parameters can be considered in optimization of fabrication of the immunosensor such as temperature, solvent, pH, *Ab* concentration and incubation time. These parameters could improve the method performance. Regeneration studies can be considered in future. Regeneration is about the use of certain chemicals and methods to break the contact between the *Ab* and *Ag* with the aim of regenerating the sensor for multiple uses.